Mathematical Modelling and Analysis on Male Urine Flow Rate

Rui Li

A thesis submitted in partially fulfilment of the requirements of the University of the West of England, Bristol for the degree of Doctor of Philosophy.

This research programme was carried out in collaboration with the Bristol Urological Institute

Faculty of Environment and Technology
University of the West of England, Bristol

March 2019

Abstract

Troublesome voiding lower urinary tract symptoms (LUTS) are a common problem in men, particularly with ageing. Management of voiding LUTS can be guided by accurate determination of underlying mechanisms, distinguishing men with voiding symptoms caused by outlet obstruction from those with reduced bladder contractility. The aim of this study is by analysing measured data to establish proper characteristic vector and model sets to provide quantitative interpretation of the male urine flow rate (UFR) in order to assist medical diagnosis and prediction non-invasively. The methods we propose have not been described before, so this work is clearly novel.

This study initially demonstrates a critical review of urine flow shape and current non-invasive urodynamic methods on diagnosing Bladder outlet obstruction (BOO) and Detrusor underactivity (DU), along with diagnosing accuracy and limitations of each method. Furthermore, a urodynamic model using first order discrete transfer function has been designed initially to lay down a fundamental assessment of whole urine flow shape. However, in follow up research this model shows limited diagnosing power for differentiation. To view the possible frequency difference between two groups, a simple Butterworth filter with two different cut-off values is designed and adapted to separate the frequency components caused by abdominal straining and detrusor contraction. Continuously to quantify the difference of frequency range in BOO and DU flow curve, an elliptic filter has been developed and adapted for UFR curve and fast Fourier transform is employed to derive median power frequency. Additionally, the diagnosing utility of flow template is assessed and mathematical criteria of intermittent shape is proposed.

This thesis employs three statistical models, multivariate analysis of variance (MANOVA), classification and regression tree, and artificial neural network to optimise the diagnosing accuracy. The MANOVA model is consider as the most robust statistical model and achieve 79.5% discrimination accuracy.

Acknowledgement

Firstly, I wish to express my gratitude to my girlfriend Chen Chen for her constant supports and love, and to my parents for their encouragement and finial supports.

I would like to take this opportunity to express my sincere gratitude to my supervisors, Professors Quanmin Zhu, Mr Andrew Gammie and Dr Mokhtar Nibouche, for their encouragement and guidance during the past years of my studies not only to my research but also to my English, and I also give my thanks to staff and PhD colleagues from the Faculty of Environment and Technology of UWE with whom I share the excellent and comfortable research environment.

I also would like to thank Professor Yufeng Yao who is critical review my research progresses every year and providing useful suggestions for my research. Special thanks to my colleagues and friends, Ji Qiu, Liwei Xu, Bo Ouyang and Dr Xin Liu for their help and useful discussions on many occasions.

List of Publications

Conference presentations

Li, R., Gammie, A., Zhu Q., Nibouche, M. and Kiely, J. (2015), A new procedure for analysis and modelling of male urine flow rate. In: *Chinese Control Conference (CCC) 34th*, Hangzhou, China, 27-28 July 2015.

Li, R., Gammie, A., Zhu Q. and Nibouche, M. (2016), Mathematical Modelling Analysis of Male Urine Flow Trace. In: *International Continence Society 2016 conference*, Tokyo, Japan, 15-17 September 2016.

Gammie, A., Rosier, P., Li, R. and Harding, C. (2017), How can we maximize the diagnostic utility of uroflow?: ICI—RS 2017. In: *International Consultation on Incontinence Research Society 7th conference*, Bristol, UK, 8-10 June 2017.

Li, R., Gammie, A., Zhu, Q. and Nibouche, M. (2017), Mathematical analysis on Urine Flow Traces for Non-invasive Diagnosis of Detrusor Underactivity in Men. In: *International Continence Society 2017 conference*, Florence, Italy, 13-15 September 2017.

Li, R., Gammie, A., Zhu, Q. and Nibouche, M. (2017), Non-invasive Parameter for Assessing Urine Flow Rate in Frequency Domain to Differentiate Detrusor Underactivity with Bladder Outlet Obstruction in Male. In: *Incontinence: The Engineering Challenge XI*, London, UK, 29 November 2017.

Li, R., Gammie, A., Zhu, Q. and Nibouche, M. (2018), Multivariance Analysis on non-invasive urodynamic parameters for Differentiating DU with BOO in Male. In: *UKCS 2018/The First UK Pelvic Floor Summit*, Telford, UK, 19 April 2018.

Li, R., Gammie, A., Zhu, Q. and Nibouche, M. (2018), Median frequency and sum of amplitude changes in rising slope: two potential non-invasive indicators for differentiating DU with BOO in male. In: *International Continence Society 2018 conference*, Philadelphia, US, 29-31 August 2018.

Li, R., Gammie, A., Zhu, Q. and Nibouche, M. (2018), Multivariate analysis of variance for maximising the diagnosing accuracy in differentiating DU with BOO in male, In: *International Continence Society 2018 conference*, Philadelphia, US, 29-31 August 2018.

Li, R., Gammie, A., Zhu, Q. and Nibouche, M. (2018), Urine flow rate shape template and intermittent flow in males, In: *International Continence Society 2018 conference*, Philadelphia, US, 29-31 August 2018.

Journal articles:

Li, R., Gammie, A., Zhu, Q. and Nibouche, M. (2017) Mathematical analysis on Urine Flow Traces for Non-invasive Diagnosis of Detrusor Underactivity in Men, *Neurourology and Urodynamics*. 36 (supplement 3), pp. 87-88.

Gammie, A., Rosier, P., Li, R. & Harding, C. (2017) How can we maximize the diagnostic utility of uroflow?: ICI—RS 2017, *Neurourology and Urodynamics*. 37 (supplement 4). pp. 20-24.

Li, R., Gammie, A., Zhu, Q. and Nibouche, M. (2018) Urine flow rate curve shapes and their descriptors, *Neurourology and Urodynamics*. 37(8). pp. 2938-2944

Li, R., Gammie, A., Zhu, Q. and Nibouche, M. (2018) Median frequency and sum of amplitude changes in rising slope: two potential non-invasive indicators for differentiating DU with BOO in male, *Neurourology and Urodynamics*. 37 (supplement 5), pp. 248-249

Li, R., Gammie, A., Zhu, Q. and Nibouche, M. (2018) Multivariate analysis of variance for maximising the diagnosing accuracy in differentiating DU with BOO in male, *Neurourology and Urodynamics*. 37 (supplement 5), pp. 327-328.

Li, R., Gammie, A., Zhu, Q. and Nibouche, M. (2018) Urine flow rate shape template and intermittent flow in males, *Neurourology and Urodynamics*. 37 (supplement 5), pp. 128-129

Table of Content

Abbreviations and Nomenclature

Abbreviations:

BOO	Bladder outlet obstruction
DU	Detrusor underactivity
DO	Detrusor overactivity
PFS	Pressure-flow studies
MPF	Median power frequency
FFT	Fast Fourier transform
OAB	Overactive bladder
UFR	Urine flow rate
CWT	Continuous wavelet transforms
DWT	Discrete wavelet transforms
WPT	Wavelet packet transforms
CART	Classification and regression tree
ICS	International continence society
GUP	Good Urodynamics Practice
OR	Odds ratio
MANOVA	Multivariate analysis of variance
ANN	Artificial Neural Network
RES	Ratio of sum squared errors
PPV	Positive predict value
NPV	Negative predict value
UFA	Urine flow acceleration
HSG	Hand grip strength
VR	Velocity ratio
IPP	Intravesical prostatic protrusion
QoL	Quality of life
PVR	Post void residual
LUT	Lower urinary tract

Nomenclatures:

Q_{max}	Maximum flow rate (ml/s)
$Q_{max2sec}$	Maximum flow rate in 2 seconds window filtered curve (ml/s)
Q_{ave}	Average flow rate (ml/s)
$P_{detQmax}$	Detrusor pressure at maximum flow rate (cm H_2O)
$Q_{max2sec}$	Maximum flow rate in 2 second window filtered curve (ml/s)
T_v	Voiding time (s)
T_f	Flow time (s)
T_r	Ratio of time to Q_{max} to flow time
Q_r	Ratio of Q_{ave} to Q_{max}
DeltaQ	Q_{max}-Q_{ave} (ml/s)
AG number	$P_{detQmax}$-2*Q_{max}
$G(\omega)$	frequency response
ω	Angular frequency (rad/s)
Q_i	Model output sequence
P_i	Model input sequence

$\varphi(t)$	Regression variable sequence
θ	Parameter vector sequence
$e(t)$	Error variable sequence
Y	Matrix of dependent variable *y(1)* to *y(N)*
Φ	Matrix of regression variable *φ(1)* to *φ(t)*
$\hat{\theta}$	Matrix of estimated parameters
$F(s)$	Continuous transfer function
$F(z)$	Discrete time transfer function
T_s	Normalised sampling period

List of Figures

List of Tables

Chapter 1 Introduction

1.1 Overview

With worldwide population growing, the proportion of ageing population is rising continuously. There is an increased number of patients with lower urinary tract symptoms (LUTS), especially in older males. Urodynamic tests have been predominantly used to check the function of the bladder and help to investigate the cause of urinary dysfunctions or incontinence.

In the older man it is generally accepted that the outcome of outlet tract surgery is improved if patients with bladder outlet obstruction (BOO) are selected by urodynamic studies (Abrams, 1999). Some urodynamic investigations are non-invasive, such as urine flow studies, while the majority used in the diagnosis of urinary symptoms are invasive, involving urethral catheterisation and placement of an abdominal pressure catheter.

The standard for diagnosing BOO is pressure-flow studies (PFS) that offer information regarding the degree of BOO through measuring the BOO index (BOOI). A report produced at the request of International Continence Society by Griffiths *et al*. (1997) has derived a provisional diagnostic classification as:

- If ($P_{det.Qmax} - 2 * Q_{max}$)>40, the patient is obstructed;
- If ($P_{det.Qmax} - 2 * Q_{max}$)<20, the patient is unobstructed;
- Otherwise, the study is equivocal.

where $P_{det.Qmax}$ stands for detrusor pressure at maximum flow and Q_{max} stands for maximum flow rate. Although the PFS remain the gold standard for diagnosing BOO, this invasive diagnostic method may not only lead patients to feel stress and uncomfortable and have a risk of infection, but there is also a 38% mean reduction of the Q_{max} when men using standard measuring catheters are compared with free uroflowmetry. Specifically, the Q_{max} reductions for normal, BOO and detrusor underactivity (DU) patients are 47%, 30% and 37% respectively (Harding *et al.*, 2012).

Meanwhile, non-invasive diagnosing methods for BOO cannot challenge the gold standard of PFS studies, but they are a reliable adjunct for physicians in planning the management of patients with LUTS. However almost all non-invasive diagnosing methods will need extra urodynamic equipment, such as ultrasound or penile cuff equipment, and also have a less reliable result. More detailed review on different non-invasive methods is included in chapter 2.

Compare to other LUTS such as detrusor overactivity (DO), DU is still largely under researched and there is no consensus regarding which of the available formulae should be used for quantification. Abrams *et al.* (2002) has defined DU as 'contraction of reduced strength and/or duration, resulting in prolonged bladder emptying and/or a failure to achieve complete bladder emptying'. A research conducted in Korean on male patients aged over 65 to identify the prevalence of DU, and found out as much as 40.2% of patients gone through evaluation for LUTS come with evidence of DU (Jeong, 2012). However, there is still a lack of agreed terminology and detailed definition, and it is widely accepted that it cannot be differentiated from BOO without PFS studies (Chancellor et al., 1991). There is, moreover, no simple effective treatment.

The urine flow rate shape analysis has been carried out a few decades ago but has only been qualitatively proposed. Abrams (2006) proposed four archetypes for urine flow shape as presented in the figure 1.1 to 1.4, in which y-axis is flow rate.

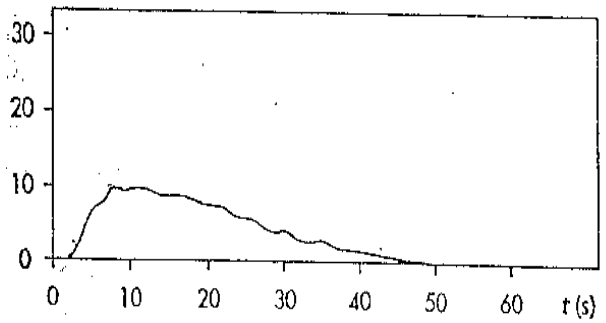

Figure 1.1 Bladder outlet obstruction (Abrams, 2006) [Used with permission of the publisher]

In which he defines a disease-free urine flow rate curve should present a bell curve and the maximum of flow rate of approximately 30ml/s appearing around 10 seconds from flow commencing, while a classical BOO curve shape has a large reduced maximum flow rate of less than 10ml/s (Figure 1.1).

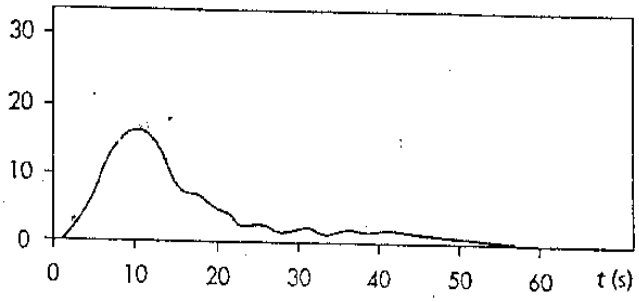

Figure 1.2 BOO with terminal dribble (Abrams, 2006) [Used with permission of the publisher]

However, when maximum flow rate is more than 15ml/s there is still one-third chance of BOO if a terminal dribble appears (Figure 1.2).

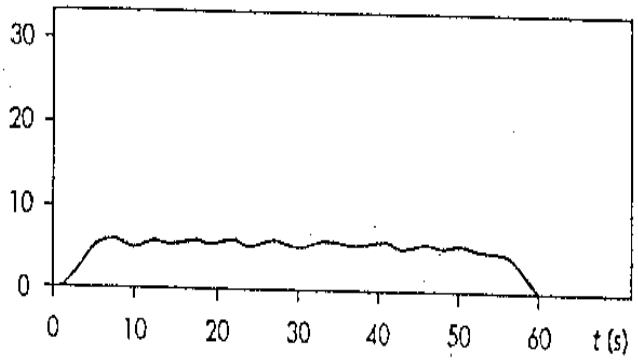

Figure 1.3 Plateau (Abrams, 2006) [Used with permission of the publisher]

The plateau can be defined as when the maximum flow rate is almost the same as the mean flow rate, with maximum flow rate less than 10ml/s (Figure 1.3) and is suggestive of a urethral stricture.

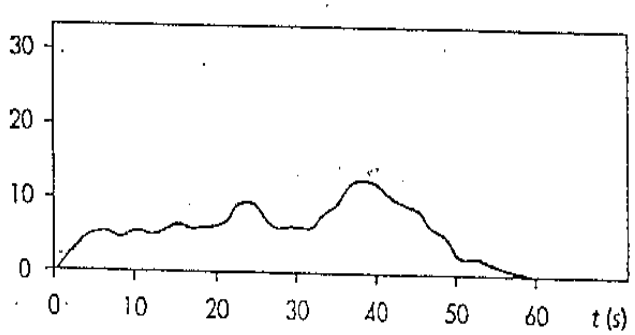

Figure 1.4 Detrusor underactivity (Abrams, 2006) [Used with permission of the publisher]

Often with detrusor underactivity, a plateau shows in the first half of the flow rate curve and the relatively lower maximum flow rate appears in the second half (Figure 1.4).

Nevertheless, in the real urodynamic test procedure, the flow curve could take many forms and the shape is affected by multiple muscle activities. Moreover, the flow curve contains a large number of fluctuations which occur during the whole micturition, and

results in it being impossible to diagnose LUTS by qualitative analysis of flow shape. Therefore, a simple and effective diagnostic method to quantitatively analyse the urine flow rate shape for non-invasively differentiating or diagnosing LUTS has been suggested in research and clinical practice.

1.2 Research Motivation

There have already been some sophisticated methods for possible non-invasive diagnosis proposed, such as VBN model (Valentini et al., 2014). However, the reliability and robustness of these models has not been validated yet and the diagnosing accuracy cannot challenge the PFS. There are many reasons to explain the importance and necessity of non-invasively diagnosing LUTS, which have three essential aspects: the potential benefit for patients and health care system, the simplicity of the diagnosing procedures and strong robustness of the diagnosis result.

For diagnosing urinary dysfunction, the pressure flow studies are the only gold standard. However, patients undergoing this invasive test may experience unpleasant sensation and anxiety during the filling and voiding phase, and have a potential risk of urinary bleeding or infection. Therefore a simple and effective non-invasive diagnosing method has been in high demand over the last half century (Gammie et al., 2017). However, most of these non-invasive methods either require additional urodynamic equipment apart from flowmetry, or have poor diagnosing accuracy especially when tested with data from a larger cohort. Some non-invasive diagnostic methods, for instance the penile cuff test (Harding et al., 2004), may cause an extra burden for national health service (NHS) for training the clinician to operate and for purchasing the penile cuff equipment.

The PFS involves urethral catheterisation and placement of an abdominal pressure catheter, which are not only a physical and mental burden for patients, but also requires urologists and nurses to be well trained to perform the whole urodynamic test precisely. Additionally, a number of artefacts in the flow rate curve and pressure curve need to be identified and removed if possible. The International Continence Society (ICS) good urodynamic practice (GUP) also recommends the urine flow curve should be smoothed either visually by an experienced urologist or by a two seconds window filter. However

the majority of urodynamic equipment currently in use does not support the filter, thus the smoothing of curve is mostly processed visually by urologists, which could incur inaccurate Q_{max} reading and potentially further misdiagnosis. A simple, low cost and non-invasive diagnostic method of urinary dysfunction is desired, with high robustness of the diagnostic accuracy. A number of non-invasive diagnosing methods have been proposed, for instance the flow index for diagnosing overactive bladder in female (Futyma et al., 2015), which has been discussed on its limitations (Schaefer, 2015) and the accuracy varies when trialled in different database.

Overall, Researchers are continuously attempting mechanical, geometric, statistical or engineering approaches to non-invasively diagnose LUT dysfunctions with promising accuracy. Therefore, a synthesised analytical method combining geometric, statistical and engineering approaches can be established to provide non-invasive diagnosis with simplified operational procedure and robust diagnostic result.

1.3 Research Questions

From the above information, research questions of this project can be listed as followings:

1.3.1 Urodynamic model: would shape analysis have promising diagnostic utility?

A simple model of urine flow rate with low cost is in high demand to diagnose urodynamic dysfunction. However the complexity of the biological mechanism in the whole micturition procedure and the non-reproducibility of flow curve limit the possibility of developing a UFR global model to differentiate possible dysfunctions. Therefore, to date the only gold standard for diagnosing urodynamic dysfunction is PFS, although it is relatively expensive and may cause urinary tract infection. This study initially proposes a urodynamic model using discrete transfer function to represent the global shape, but it shows limited utility when applied on large number of patient data. To overcome this limitation, an alternative simple method of peak counting is developed to explore the frequency difference between BOO and DU groups urine flow curves.

1.3.2 Would frequency analysis be suitable for urodynamic diagnosis?

The peak counting method could only indicate the potential difference of frequency between BOO and DU groups, and due to its global counting, intermittency and artefact in the UFR curve may limit its utility. Therefore a quantitative method is required to investigate on the detail of frequency content. According to the hypothesis proposed by Gammie et al. (2014), the frequencies of detrusor muscle activity and abdominal straining may have ten times of difference, which could be used as an indicator for differentiating DU from BOO group. This study uses peak counting method and median power frequency (MPF) to verify the hypothesis and further develops diagnosing utility based on verification results.

1.3.3 Would mathematical and statistical models improve overall diagnostic accuracy?

Apart from the most researched non-invasive parameter Q_{max}, there are also a number of non-invasive parameters proposed in this study by analysing UFR in both time domain and frequency domain, with similar diagnosing accuracy to differentiate DU from BOO. However, including Q_{max}, the diagnosing accuracy of proposed parameters is individually limited for diagnosing DU patients from a mixed symptomatic group. Therefore the research question arises – would it be possible to develop mathematical and/or statistical models for maximising the diagnostic utility by combining the proposed non-invasive indicators?

1.4 The Aims and Objectives of the Project

The aim of this PhD research is to non-invasively differentiate DU from BOO in male by analysing urine flow rate curve shape. This requires a number of non-invasive parameters derived that have statistical difference between two groups, and explores possible methods to combine the derived parameters for optimising the diagnostic power.

To achieve this aim the following major objectives have been outlined:

- To analyse the urine flow rate in time domain and investigate the possibility of potential frequency difference between two groups.

- To design suitable low-pass and band-pass filters for precisely analysing UFR in frequency domain.
- To optimise the diagnostic power by combining proposed non-invasive parameters.
- To establish prototypes of UFR shape in two groups to assess the diagnostic utility of flow shape alone.

1.5 Structure of Thesis

This thesis is divided into seven chapters. It starts with an overview and introduction to the research in Chapter 1, and ends with conclusions drawn from this research in chapter 7. Chapter 2 provides the background, methodology and literature review for the research. Chapters 3 and 4 present the analysis of the UFR curve in time domain and frequency domain respectively. Chapter 5 addresses the mathematical and statistical approach for optimising the diagnostic power. Chapter 6 interprets the analytical result and diagnostic utility of each parameter derived and validates the robustness of mathematical/statistical models.

The outline of the thesis is as follows:

Chapter 1 Introduction to the research background, motivation, project aims and objectives, as well as the outline of the thesis.

Chapter 2 The literature review covers a survey of UFR shape and a summary of other non-invasive methods, including diagnosing BOO and DU, or differentiating one from others.

Chapter 3 Analysing UFR curve in time domain is presented with a discrete transfer function for modelling the curve, and a Butterworth filter is designed for peak counting analysis.

Chapter 4 To further explore the frequency content in two groups, a bandpass filter is designed and applied, median power frequency and sum of amplitude changes is derived.

Chapter 5 Introducing three mathematical and statistical models for optimising diagnostic power, which are multivariate analysis, neural network application and classification and regression tree analysis.

Chapter 6 Interpretation of the analytical result, with diagnostic power of each derived parameters and all models, validation tests are conducted for testing the robustness of multivariate analysis and CART analysis.

Chapter 7 Conclusions are drawn to summarise the study and propose future research to follow up this study.

Chapter 2 Research Background and Literature Review

2.1Urodynamics and lower urinary tract dysfunctions

2.1.1 Urodynamics

Urodynamics provides assessment of patients possible lower urinary tract (LUT) function by measuring physiological status, which allows urologists to assess patient LUT functionality by comparing normal and pathological function. For a full urodynamics study recommended by ICS standardisation community, a questionnaire containing physical and clinical history is initially surveyed, then the non-invasive free flowmetry measurement including post void residual volume is conducted to provide objective information prior to invasive urodynamics such as pressure flow studies (Schaefer et al., 2002).

The quality of life (QoL) questionnaire normally includes bladder dairy and symptoms such as urgency, pain, day/night voiding frequency, nocturia and incontinence frequency. This information verifies the patient's symptoms and provides a baseline for the following urodynamic tests.

The non-invasive and inexpensive features make uroflowmetry an easy preliminary screening test prior to the invasive pressure flow studies. The urine flow rate data is recorded and post void residual (PVR) volume is measured by ultrasound equipment. Urine flow rate and PVR help the physician to understand storage and voiding symptoms, the maximum flow rate (Q_{max}) is also reported to serve as an indicator to select symptomatic men with a high likelihood of BOO. However, the LUT dysfunction cannot be accurately predicted if the pressure-flow data is not provided.

Following the uroflowmetry test, the invasive pressure flow studies (PFS) measures intravesical pressure by inserting a narrow catheter into the bladder, while the abdominal pressure is simultaneously monitored by inserting a similar catheter with a balloon attached into the rectum. Combined with flow rate data, the PFS provides information on the bladder's functionality and gives the urologist enough evidence to diagnose the cause of the LUTS.

2.1.2 Two Lower urinary tract dysfunctions: Detrusor underactivity and bladder outlet obstruction

ICS standardisation report (Abrams et al., 2002) defines LUTS as 'the subjective indicator of a disease or change in condition as perceived by the patient, caregiver or partner and may lead him/her to seek help from health care professions. It can be divided into storage, voiding or post-micturition symptoms when they appear during the filling phase, voiding phase or after voiding. LUTS, especially storage symptoms, could be troublesome for male patients and decrease their quality of life. However, it is suggested that LUTS are insufficient to definitively diagnose (Abrams et al., 2002).

Bladder outlet obstruction is a pressure-flow studies observation which has been defined by the ICS as obstruction during voiding and is characterised by increased detrusor pressure and decreased urinary flow rate, which is normally diagnosed by studying the synchronous values of flowrate and detrusor pressure (Abrams et al., 2002). It is suggestive of BOO in male when patient complain of voiding symptoms, while in females voiding symptoms reported are rather more often suggestive of DU instead of BOO. The obstruction between the bladder and the tip of the urethra, such as urethral stricture and bladder neck stenosis, can be a cause of BOO, but in men it is normally a result of benign prostatic hyperplasia (Patel and Parsons, 2014).

Compare to BOO, DU is still relatively under researched, with a lack of unified terminologies and of diagnostic criteria. It is defined by ICS (Abrams et al., 2002) as 'a contraction of reduced strength and/or duration, resulting in prolonged bladder emptying and/or a failure to achieve complete bladder empty within a normal time spam'. Gammie et al. (2016) investigate possible signs and symptoms associated with DU and a number of signs and symptoms are reported having statistical difference between DU and BOO-DU-free groups, including urinary stream decreased/interrupted, hesitancy, feeling of incomplete bladder emptying, palpable bladder, absent or decreased sensation, always straining to void, any retention, surgery with possible denervation, chronic retention, antibiotics in use and antidepressants in use. Though it is well reported that the of signs and symptoms have statistical difference between DU and BOO patients, it is widely accepted that DU cannot be differentiated from BOO non-invasively.

2.2 Urine flow rate shape and its descriptors

Uroflowmetry serves as a preliminary urodynamic test for physicians to indicate the possible cause of LUTS. Alongside the most researched parameter maximum flow rate (Qmax), the shape of urine flow rate curve is also suggested to associate with one or more voiding abnormalities (Abrams, 2006).

To review the descriptor and definitions of urine flow rate curve shape, a literature search has been made in Pubmed and ICS standardisation documents dated to 5 January 2018, in which 22 articles were included in the survey. The detailed summary of shape definition is presented as in table 2.1.

Table 2.1 Summary table of flow shape descriptors (Li et al., 2018) [Used with permission of the publisher]

	Normal	Constrictive	Compressive	Fluctuating	Intermittent	Tower-shaped
ICS (Schaefer et al., 2002; Abrams et al., 2002; Haylen et al., 2010)	smooth arc-shaped, high amplitude, no rapid amplitude changes	smooth flat, plateau-like, lower flow rate	flattened asymmetric low curve with a slowly declining end part	multiple peaks during a period of continuous urine flow	flow stops and starts during single void	
ICCS (Austin et al., 2014)	'"bell-shaped': regardless of volume voided	'plateau': Flattened, prolonged pattern with low amplitude		'staccato': irregular, fluctuating curve without reaching zero. Fluctuations > square root of Q_{max}	'interrupted': segments with cessation, discrete peaks	sudden, high-amplitude flow with short duration
Fantl, 1983	fast crescendo and relatively slow diminuendo, minimal fluctuations			'multiple peak': 2nd peak >= 20% of Q_{max}	'interrupted'; flow rate < 2 ml/s between repetitive peaks	
Jensen et al., 1983	'adult'	'plateau': flow rate variation<1ml/s for at least 4 seconds		'intermittent': wavy curve not reaching the baseline with a duration of at least 15 seconds	'fractionated': wavy curve reaching baseline several times, for at least 15 seconds	
van der VIS-MELSEN et al., 1989	'single sharp peak'		'low flat': flat pattern with low average and maximum Index of Urine Transport value	'sawtooth': low average, and normal maximum, Index of Urine Transport		
Boothroyd et al., 1990	bell-shaped and approximately symmetrical	'plateau': prolonged voiding time and reduced Q_{max}			'sawtooth'	
Jorgensen et al., 1990	unbroken, bell-shaped with slight to moderate asymmetry	'plateau': unbroken, flattened, large part of voided volume is voided by a constant Q_{max}	'prostatic': unbroken, pronounced asymmetry, elongated and flattened curve from Q_{max} to zero	unbroken, greater fluctuations without reaching baseline	'fractioned': discontinuous, flow reaches baseline one or several times	
Kinahan et al., 1992		'prolonged': low, steady Q_{max}	'approximately normal': normal initiation and Q_{max}, end void prolongation		'intermittent'	
Mattsson et al., 1994	bell-shaped			'intermittent': variations in flow rate of at least 5 ml/s	'fractionated': at least one total interruption	
Gutierrez	'bell shape'	'plateau-shaped': constant flow with				high Q_{max} achieved rapidly, followed by a slight plateau

1997		variations<1ml/s				and sudden decreased flow
Jorgensen et al., 1998	bell-shaped, unbroken, steep rise to Q_{max} and steep fall	'plateau': flattened with a steep acceleration toward Q_{max}, relatively large volume under a constant Q_{max}	'low flow': unbroken, bell-shaped flattened with a low Q_{max}	unbroken flow, less steep rise and fall, without reaching baseline	'fractionated': discontinuous flow reaches baseline one or several times	'high flow': very high Q_{max} with short voiding time
Wyndaele, 1999	symmetrical, uninterrupted, Q_{max}>15ml/s	'long flow+low max flow'	'slow start': slow rises to Q_{max}	'undulating': flow moving up and down	'void 2x': voiding 2 times with complete stopping of flow between	
Chou et al., 2000	bell-shaped and rapid rise to Q_{max} and rapid fall.	'plateau': flattened with a steep acceleration toward Qmax, relatively large volume under a constant Q_{max}	'flattened': flattened with a low Q_{max}	flow fluctuates but does not reach baseline	'intermittent': flow reaches baseline at least once	'tall and peaked'
Ghobish, 2000	'bell-shaped': Q_r 25%-75% and T_r 25-60%	'box-shaped': Q_r>80% and T_r<10%	'long-tail': 30%<Q_r<60% and 10%<T_r<25%		'interrupted': subdivided with interruption duration threhold of 2s	
Babu et al., 2004	'bell-shaped': bell shape, smooth pattern	'plateau-shaped': constant flow with variations<1ml/s				
Pauwels, 2005	continuous, bell-shaped, steep slope and short flow time	'long and low Q_{max}': long flow time, relatively constant low flow rate		'undulating': asymmetric, steep slope, long and flattened foothill	'fractionated': discontinuous, repetitive flow peaks reaching zero in between	
Abrams, 2006	'bell shape': Q_{max} in first 30% of curve and within 5 seconds from start	'plateau': Q_{ave} almost same as Q_{max}			flow stops and starts on one or more occasions	'supranormal': sharply increased flow to a very high Q_{max} in 1-3 second, followed by a sudden reduction
Mostafavi et al.[13] 2012	'bell': symmetric, continuous curve between 5% and 90% of Iranian nomogram	'plateau': Q_{max}/flow time<0.5		'staccato': fluctuations > square root of Q_{max}	'interrupted': curve reaches baseline	'tower': Q_{max}>95% on Iranian nomogram

The table 1 provides an overview of flow shape descriptors and their definitions, which are not consistent, and it is much more difficult to uncover pathophysiology when terms are not consistently used. It is suggested that only 'normal', 'fluctuating', 'intermittent' and 'plateau' descriptions, with additional comment on symmetry and Q_{max}, be used to describe urine flow rate curve shape, but this has not become standard (Li et al., 2018).

2.3 Non-invasive diagnosing methods for BOO

Although the PFS are the standard for diagnosing BOO, due to its invasive nature and side effect include haematuria and urinary tract infection, there are variety of non-invasive method and techniques that have been used to evaluate LUTS and hold great promise.

2.3.1 Ultrasound and Ultrasonography

Several novel ultrasound methods were developed to address the need for a reliable non-invasive method for diagnosing BOO. Researches indicate intravesical prostatic

protrusion (IPP), velocity ratio (VR), post void residual (PVR), detrusor wall thickness (DWT) and bladder wall thickness (BWT) have promising diagnosing power and good correlation with BOO, which is summarised in following section. Moreover, bladder weight can be also measured by ultrasound but there are still arguments on its weak correlation and diagnosing power for BOO. Prostate volume and post void residual (PVR), two predictors that can be also measured by ultrasound method, are found have weak correlations with BOO and cannot be used in isolation as a diagnostic test.

Post Void Residual (PVR) is defined as the volume of urine left in the bladder at the end of micturition (Abrams, 2002), which is another screening test for assessing voiding dysfunction and could be measured by ultrasonography non-invasively. Measuring PVR is widely performed during or after the initial uroflowmetry test due to its non-invasive features, and it provides evidences for physicians to identify if further evaluation or treatment is needed. Although it is agreed a larger PVR could be associated with LUT dysfunction and a threshold used in defining an abnormal residual volume, there is lack of quantitative definition of normal and abnormal PVR volume. Kolman et al. (1999) measure PVR in 477 random men and described the distribution of PVR volume with a median of 9.5 ml, with 2.5 ml to 35.4 ml in 25% to 75% interval. PVR volume is significantly increased in elder male patients. An analysis based on 1763 male participants aged 50 to 80 reveals that a significant rise of mean PVR volume of 52 ml in 75 or older males comparing with mean PVR volume of 23.5 ml in 50 to 54 year old men (Berges and Oelke, 2011). It is demonstrated in a study that only 24% of male BOO patients have PVR less than 50ml (Griffiths and Castro, 1970), though another study finds 30% of men who have PVR greater than 50ml do not suffer from BOO (Leblanc et al., 1995). The PVR volume considerably varies by age and time of voiding, therefore it could not serve as an effective indicator for BOO. Furthermore, poor detrusor contractility could also result a high PVR volume and could not be distinguished from outlet obstruction by PVR volume.

Intravesical Prostatic Protrusion (IPP) measures the vertical distance from the tip of the prostatic protrusion to the circumference of the bladder at the base of the prostate gland in the mid-sagittal line. There are three grades of IPP: grade I less than 5mm, grade II from 5mm to 10mm and grade III more than 10mm. Abdel-Aal et al. (2011) demonstrate in total of 135 patients undertook PFS and IPP analysis, IPP shows best

diagnostic accuracy 80% better than combined DWT and IPP 77.6%. The sensitivity, specificity, positive predictive value (PPV) and negative predictive value (NPV) are 80%, 80%, 73.7% and 85.1% respectively. In 2006, in research (Lim et al., 2006) containing as database of 95 patient data, IPP was compared with prostate specific antigen (PSA) and prostate volume (PV). The result shows IPP has the best correlation with BOO and diagnosing power of these three predictors, in which sensitivity, specificity, PPV and NPV are 46%, 65%, 72% and 46% respectively. Another research (Chia et al., 2006) on the relationship between IPP and BOO has conducted in an earlier research work in 2003, in which the result shows the third grade IPP has the best correlation with BOO with a 94% sensitivity, 70% specificity, 94% PPV and 79% NPV. In conclusion, this measure requires further validation and it is not significantly better than PVR alone for diagnosing BOO, and there are multiple of thresholds of IPP values proposed in several analytical methods which make diagnosing results difficult to interpret.

Detrusor Wall Thickness (DWT) can be visualised with ultrasound technology very clearly, and measurements of DWT have been used lately to diagnose BOO in male patients. The diagnostic accuracy of DWT measurement has been evaluated (Oelke et al., 2007), comparing with free uroflowmetry and postvoid residual urine in one group of patients defined as having BOO by PFS analysis. The result shows DWT is the most accurate test to determine BOO with an 83% sensitivity, 95% specificity, 94% PPV and 86% NPV. Another recent research (Elsaied et al., 2013) compares the diagnostic accuracy of DWT to other non-invasive diagnosing method for BOO, with database of 50 patients with PFS used as reference. Compare to PVR, Qmax and prostate volume, DWT shows the most reliable diagnosing accuracy with 90.5% PPV, 86.2 NPV, 82.7% sensitivity and 92.6% specificity. Although DWT has been recognised wildly as a reliable ultrasound measured diagnostic method for BOO, the measurements and techniques still need to be standardised and a larger study need to be designed.

Velocity Ratio (VR) is equal to the maximum flow velocity in the distal prostatic urethra just proximal to the external urethral sphincter divided by the maximum flow velocity in the membranous urethra, which represents the change in velocity from distal prostatic urethra to the membranous urethra, and is found to be the a good parameter for diagnosing BOO. Ozawa et al. (2000) indicate by using combined VR and AG

number ($P_{detQmax}$-2*Q_{max}) can achieve 100% sensitivity and 97.5% specificity in a database of 22 patient data (unobstructed or equivocal). Although the result shows promising diagnosing accuracy, this method still needs to be verified in further clinical trials.

Bladder wall thickness (BWT) is measured by transabdominal ultrasound, and could be a potential diagnostic tool for BOO. Compared to DWT, these two methods use the same urodynamic equipment to measure the bladder status, but have different diagnosing power and diagnostic threshold values since the bladder wall is thicker than the detrusor wall. In recent research (Guzel et al., 2015) of 236 male patients, the relationship between BWT and uroflowmetric parameters is investigated. The result shows BWT combined with specified urodynamic parameters (IPSS, Q_{max} and PVR) has the accuracy in diagnosing BOO of 78.9% sensitivity, 68.1% specificity, 57.6% PPV and 85.5% NPV. Although overall diagnosing accuracy of 71.9% shows promise to diagnose BOO, this method still needs to be validated and shows relatively poor diagnosing accuracy compare to other methods.

2.3.2 Free Uroflowmetry and Flow Shape Analysis

It is widely accepted that the flow curve in men with BOO has a lower Qmax than normal flow curve. However, uroflowmetry cannot distinguish BOO from DU, since reduced flow occurs in both. Furthermore, some patients with BOO and high detrusor pressures can still retain normal flow rates.

Qmax indicates the maximum flow rate and it is a widely used parameter for physicians to assess BOO. Abrams (2006) concludes in his book that 90% patients with BOO have Qmax<10ml/s and 48% with Qmax>15ml/s. Another research (Guzel et al., 2015) shows when Qmax<15ml/s, this single predictor holds the highest NPV of 97%, with 59% PPV, 99% sensitivity and 39% specificity. When using predictor Qmax<10ml/s, PPV and specificity raise to 69% and 73%, however NPV and sensitivity drop to 72% and 68% respectively.

Flow curve analysis of voiding symptoms often find poor correlations with BOO. Furthermore, a research (Reynard, Lim and Abrams, 1996) on intermittence and terminal dribble indicated these two predictors were not observed to be associated with BOO. Despite the high specificity and PPV, the weak sensitivity and NPV suggest these

two predictors cannot be widely used in non-invasively diagnosing BOO. Kuo (1999) analyses 324 male data and concludes a constrictive flow curve shape could serve as an indicator for BOO with 87.2% sensitivity, though this terminology is poorly defined by ICS without a quantitative definition. Rollema (1981) analysed urine flow rate curve and derived three novel parameters for serving as non-invasive indicator of BOO, T90 (voiding time for central 90% of volume voided), T_{desc} (time of descending leg) and QM90 (mean flow rate for the central 90% of volume voided), for which sensitivity range from 90% to 95%.

Urine flow acceleration (UFA) is proposed by Wen et al. (2013) and defined as the increased uroflow rate in a period of time from start the micturition to the Q_{max}, which is reported could has better diagnosing accuracy than Q_{max} with 88% sensitivity and 75% specificity.

Uroflowmetry could be the easiest and economical way to analyse urinary symptoms, however wide thresholds across studies make diagnosing accuracy uncertain. The sensitivity raises up when the cut-off value of Q_{max} increased, with lowering the specificity, and vice versa. Furthermore, the relatively poor diagnosing power for BOO and its undifferentiability from low detrusor contractility limit further clinical application of this method.

2.3.3 Other Non-invasive Methods

Abdominal straining is included in various symptom scores which are used for assessment of patients with BOO. The objective evidence of straining is assessed by rectal pressure measurement. In a clinical study (Reynard et al., 1995), 56 patients with BOO underwent the abdominal straining test four times and specificity for patients who strain on 4 flows is 87%, along with 36% specificity, 80% PPV and 51% NPV. Although abdominal strain does not have a great effect on flow rate in men, it is still an unreliable and insufficient predictor for diagnosing BOO.

Penile cuff test is a choice of non-invasive test method for assessing BOO. In the test, a cuff is placed around the penis before voiding, and automatically inflated and deflated for several times during the voiding process to stop urine flow (Griffiths et al., 2002). Recent research (Finazzi Agrò et al., 2012) investigated penile cuff test in diagnosing with a database of 48 patients, which shows a remarkable result of 100% sensitivity,

63% specificity, 66.7% PPV and 100% NPV. An earlier research conducted by Harding et al. (2014) show penile urethral compression release (PCR) index, which relies on penile cuff test, provides 78% sensitivity, 84% specificity and a PPV of 69%. In conclusion, a penile cuff test has some ability to diagnose BOO, but the extra equipment requirement may result in high charge for diagnosis and treatment. Furthermore, the limited research with varied threshold values make this method not yet unreliable for clinical use.

Condom Catheter method is used to measure isovolumetric bladder pressure by replacing an external catheter connected with penis (Pel and Mastrigt, 1999), and aims at assessing BOO non-invasively by combining this with Q_{max}. The minimum of discomfort and leakage occurred is confirmed in a follow up research, and a mathematical equation is derived to estimate isovolumetric pressure with measured data and Q_{max} (Pel and Van mastrigt, 2001). This method also been tested to confirm the reproducibility and reliability of isovolumetric bladder pressure measurement (Rikken et al., 1999; Huang Foen Chung et al., 2004). Its diagnostic utility has been tested, in which 12 out of 13 non-obstructed and 30 out of 33 obstructed patients are tested correctly according to their pressure flow test result (Pel et al., 2002). The promising diagnostic accuracy is also confirmed in an another follow up research with larger number of patients involved, with 94% successful measurement in 618 participants and 84% of two successful measurement in 555 subjects (Huang Foen Chung et al., 2003).

2.3.4 Combined Parameters

The drawback of individual parameters for non-invasively diagnosing BOO have led researchers to investigate the diagnostic potential of different parameters combined.

IPP and DWT, Prando (2010) has investigated baseline parameters including International Prostate Symptom Score, prostate volume, urinary flow rate, intravesical prostatic protrusion, detrusor wall thickness, Schaefer obstruction class, minimal urethral opening pressure and the urethral resistance algorithm bladder outlet obstruction index. He indicates the association of IPP and DWT produced the best diagnostic accuracy for BOO (87%) when the 2 tests were done consecutively.

IPP grade and Doppler ultrasound, Shin et al. (2013) assessed the accuracy of two noninvasive, ultrasound method and combined method of diagnosing bladder outlet

obstruction with 57 male outpatients. The sensitivity and specificity of the intravesical prostatic protrusion (IPP) grading system are 90% (grade 3) and 60% (grade 1 and 2). The sensitivity of the ultrasound Doppler system for a BOOI more than 40 is 100%, and the specificity is 68%. When these two methods were combined, the sensitivity for grade 3 patients is 100% and specificity for grade 1 and 2 patients is 91% .

Causal Bayesian Networks have emerged as an advanced alternative to conventional statistical models in the medical field. Kim et al. (2014) investigate multiple non-invasive clinical parameters and selected total prostate volume, Q_{max} and post-void residual volume as predictors in causal Bayesian networks model. The sensitivity, specificity and diagnosing accuracy are 51.4%, 85.2% and 73.5% respectively.

However, there remains a majority of patients presenting with LUTS who are not assigned to a diagnostic group with any certainty. To date there is little evidence show these combining parameters methods decrease the number of men who require PFS.

2.3.5 Non-invasive Diagnosing Methods for DU

As DU is still largely under researched and as there is a lack of quantitative definition, the non-invasive diagnosing methods are still small in number. Furthermore, each method is still in need of larger clinical trial to make the diagnosing power reliable.

Hand grip strength (HSG) has been researched (Paick et al., 2014) as a predictor of DU in male patients with LUTS. 64 men are included in this study, in which 36 patients had DU. All patients were asked to preform hand grip test before urodynamic study, and HGS was compared between DU group and non-DU group. The results show DU patients had lower HGS than non-DU patients. By using cut off HGS of 25kg, the sensitivity, specificity, PPV and NPV are 30.6%, 89.3%, 78.6% and 50% respectively. When cut off HGS increases to 35kg, this single predictor has 83.3% sensitivity, 39.3% specificity, 63.8% PPV and 64.7% NPV.

HGS method may be an economical and easy way to diagnose DU, however two thresholds result in either poor sensitivity or specificity, which makes the diagnosing accuracy appears to be relatively limited compare to current invasive PFS.

DWT and bladder capacity are analysed by classification and regression tree (CART)

for diagnosing DU with non-invasive clinical tests in the recent research (Rademakers, van Koeveringe and Oeleke, 2016). This study consists of 143 consecutive men with 33 patients with DU. The result shows that all men with DWT<1.23mm plus bladder capacity >445ml have DU. The classification and regression tree model shows a sensitivity of 42%, specificity of 100%, PPV of 100% and NPV of 85%.

DeltaQ is defined as Q_{max} minus Q_{ave}, which is reported could serve as a predictor to differentiate DU from BOO non-invasively (Lee et al., 2016). In an analysis of 240 male free flow data, DeltaQ and PVR are reported having significantly statistical difference between two diagnostic groups, in which DeltaQ is reported of 71.3% sensitivity and 70.3% specificity, and PVR is reported of 70.3% sensitivity and 75.2% specificity.

There are a large variety of non-invasive techniques and methods has been proposed for diagnosing BOO, and a combination of non-invasive urodynamic measures and ultrasound measures holds promise for decent diagnosing accuracy. However, each type is currently insufficient to challenge the gold standard of PFS. Furthermore, DU was largely under researched till lately, but as a bladder condition it shows an important cause of LUTS in men, and it can only be diagnosed and differentiated from BOO by PFS.

2.4 Summary

In this chapter, the up to date literature review on non-invasively diagnosing BOO and DU has been summarised and presented. Various methods hold the promise to non-invasively diagnose BOO, with or without extra urodynamic equipment. However, DU is still largely under researched and only a few researchers propose non-invasive diagnostic method, though with limited accuracy. The similarity of relatively lower Q_{max} and flow curve shape make PFS the only effective method to differentiate DU from BOO.

Though the shape of urine flow is reported to associate with one or more voiding abnormalities, it has not been done quantitatively apart from Q_{max} and Q_{ave}. Therefore, this study starts by analysing urine flow shape in the time domain.

Chapter 3 Analysing Urine Flow Rate Data in Time Domain

3.1 Overview

Urine flow rate is one of the most significant parameters for assisting physicians to assess urinary system status/symptoms, such as normal, underactive and obstructive. In this research all the urine free flow rate data were measured by uroflowmetry equipment in Bristol Urological Institute and anonymously sent to researcher. The diagnostic results were determined by PFS and totally blind to researcher in model design stage. According to Gammie's suggestion, the start and end micturition points are reselected by the threshold value of 0.5ml/s to avoid erroneous classification of urine flow shape (Gammie et al., 2016).

The hypothesis of peak counting analysis is based on the hypothesis that DU patients may perform more abdominal straining than BOO patients due to their underactive detrusor muscle, which would be reflected in the shape of their urine flow rate curve. Rollema (1981) compares peak number in BOO and disease-free data, and finds this parameter has statistical difference between two groups. The latest symptomatic definition of DU proposed by a working group set up by ICS is 'Underactive bladder is characterised by a slow urinary stream, hesitancy and straining to void, with or without a feeling of incomplete bladder emptying and dribbling, often with storage symptoms' (Wein and Chapple, 2017), and straining in DU and BOO groups with significant statistical difference has been verified in a large database analysis (Gammie et al., 2016). Therefore it might be possible to analyse DU with peak counting method and compare with BOO group to assess if the straining difference could be reflected by this parameter.

The hypothesis of UFR modelling analysis is based on UFR curve shape may vary in different diagnostic groups, in which BOO curve is relatively lower in Q_{max} with plateau or asymmetry shape while DU curve may have its Q_{max} in the second half of the flow time and a prolonged falling descent (Abrams, 2002). Hence, a non-invasive parameter based on curve shape could serve as an indicator for differentiating DU from BOO if it could reflect the shape difference between two groups.

To understand this, consider a measured typical normal male urine flow rate curve in figure 3.1. It can be observed the shape is like a bell shape with slight added fluctuations. Deviation from this normal shape could suggest some problems in urine flow process.

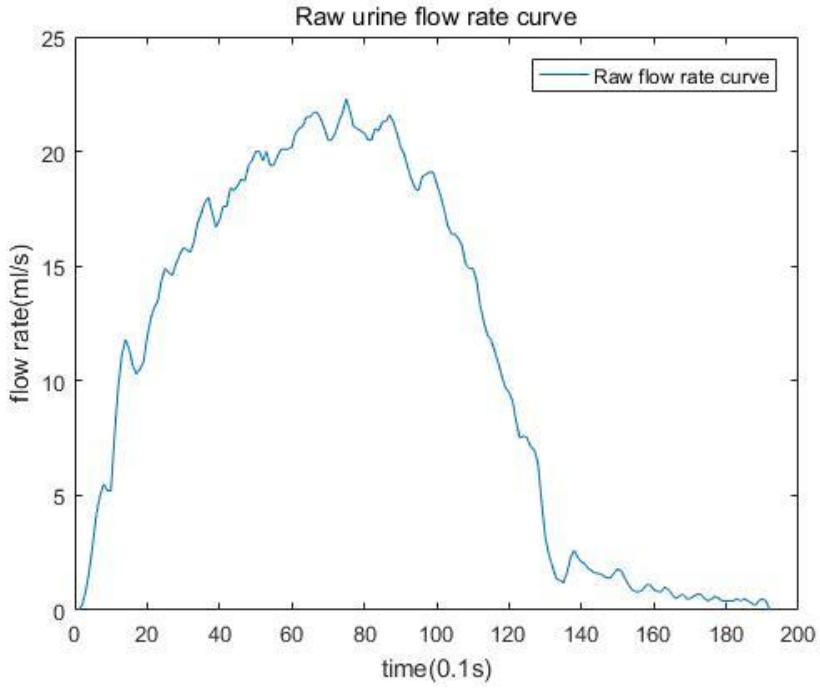

Figure 3.1 Measured normal urine flow rate curve

These observations give guidance in determining a model structure with the following characteristics 1) it is a dynamic that could be represented by first order dynamic principle, 2) it is piecewise linear, meaning it could be separated into upward rate flow session and downward rate flow session from the peak value (that is the top of the bell shape), in which the time of the peak value is defined as the 'ridge point' in the following descriptions.

To analyse urine flow rate data in time domain, two analytical methods have been proposed: peak counting analysis and time constant analysis. These two methods would be the easiest to implement in future and use the existing qualitative information available (Abrams, 2002). They are therefore a valid starting point for this quantitative study.

All analyses have been developed in MATLAB version 2018b and earlier version with pre-code script. 158 BOO and 135 DU free flow data from male patients who underwent PFS, studied in a single specialist centre between 2012 and 2018 were randomly

selected for analysis in this study. Free flowmetry was performed before each PFS which was carried out according to ICS guidelines current at the time of testing, with a sampling rate of 10Hz by Laborie weight transducer type uroflowmeters. The diagnostic criteria for DU is bladder contractility index (BCI) less than 100 and bladder outlet obstruction index (BOOI) less than 20, and for BOO is BCI greater or equal to 100 and BOOI greater or equal to 40. The urine flow rate data was transferred to an Excel file and pre-processed with a threshold value of 0.5ml/s for defining the starting and end point.

For a clearer view on the urine flow rate shape, DU and BOO UFR 2 seconds window filtered curve plots are presented in the appendix VII and VIII respectively, in which each plot contains maximum of 20 UFR curves.

3.2 Filter Design and Peak Counting Analysis

3.2.1 Introduction of peak counting analysis

In the uroflowmetry test, during micturition process there are normally a number of fluctuations, caused by abdominal straining and involuntary bladder contraction. It is reported that straining is an uncommon complaint in men with BOO (Reynard et al., 1995), while it happens more frequent in DU patients (Wein and Chapple, 2017). Abdominal straining might last a short period compared with involuntary or voluntary bladder contraction, and peaks generated by abdominal straining is hypothesised to have statistical difference between DU and BOO groups, which is our goal to count in this analysis. However there are a large amount of fluctuations caused by coughs, changing voiding position, accidentally knocking or kicking the uroflowmetry which may affect UFR's estimated characteristics, and consequently produce incorrect result of peak counting analysis. These fluctuations are normally called artefacts and need to be removed from UFR curve. ICS GUP suggests manually removing artefacts by an experienced urologist or automatically removing by a two seconds window filter for a clearer observation of Q_{max} and flow shape (Schaefer et al., 2002). However, the two seconds window filter could smooth the curve in the time domain which indeed provides better observation on Q_{max} and curve shape, but with a relatively slow roll off between passband to the stopband, it may result in missing some meaningful high frequency components, such as a part of peaks caused by straining.

In the ICS guideline on urodynamic equipment performance, it states the clinical requirements for a standard urodynamic system lead to technical recommendations, which also specified the minimum equipment frequency to measure abdominal and detrusor muscle activities (Gammie et al., 2014). As a matter of fact, the specified frequencies provide guidance on selection of cut-off frequency in filter design to reduce noise effect. According to this, we make a proposal for the peak counting analysis, that three frequency bands and components are defined:

- Fluctuations frequency less than or equal to 0.1Hz – major involuntary detrusor contractions
- Fluctuations frequency between 0.1Hz to 1Hz – relatively small detrusor contractions, abdominal straining, some artefacts
- Fluctuations frequency equal or greater than 1Hz – pure artefacts

It should be noted, that some artefact fluctuations are ranged between 0.5Hz to 1Hz, which are not filtered out in peak counting analysis as the fluctuations caused by abdominal straining may perform fast and in this range as well.

3.2.2 Filter design and verification

There are several types of digital filters that can be used to reduce signal noise. For an easier start, only Finite Impulse Response (FIR) filters are considered in the initial stage of this project. Compared to the other digital filters, the Butterworth filter rolls off slower around the cut-off frequency than Chebyshev filter or the Elliptic filter, but without ripple on both passband and stopband. As the artefact peaks generated by the filter have to be avoided for the accuracy of analytical result, the Butterworth filter can effectively reduce the artificial noise but does not add peaks to the original peak characteristics in the raw data. The frequency responses and group delay response of four filters are shown in figure 3.2 and figure 3.3 respectively.

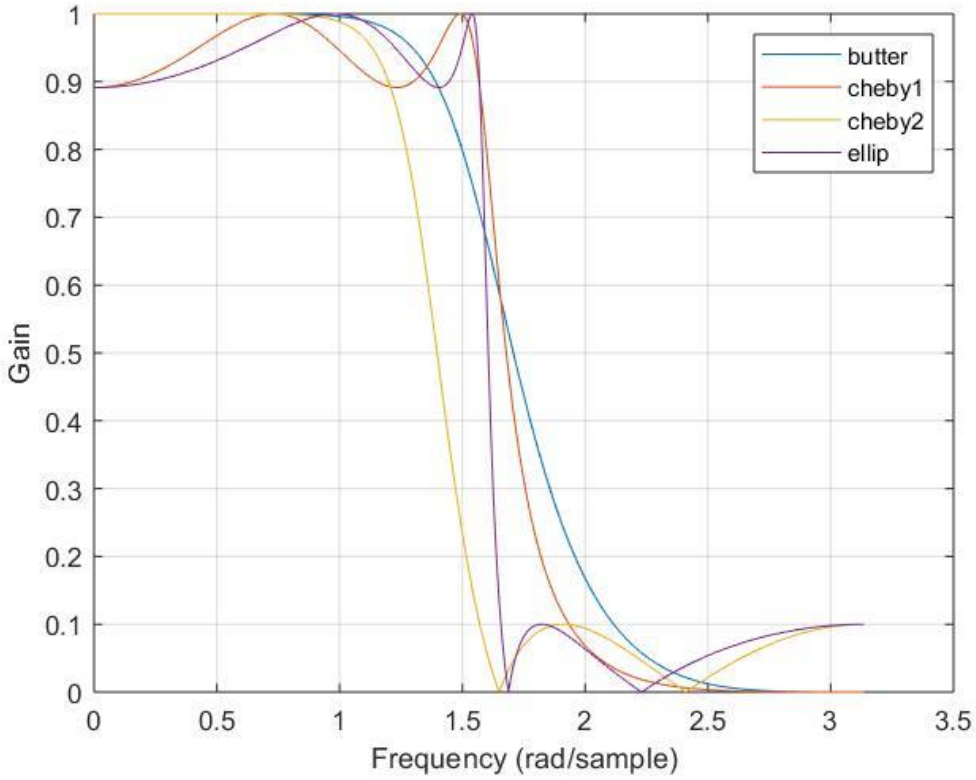

Figure 3.2 Butterworth comparison with other FIR filters

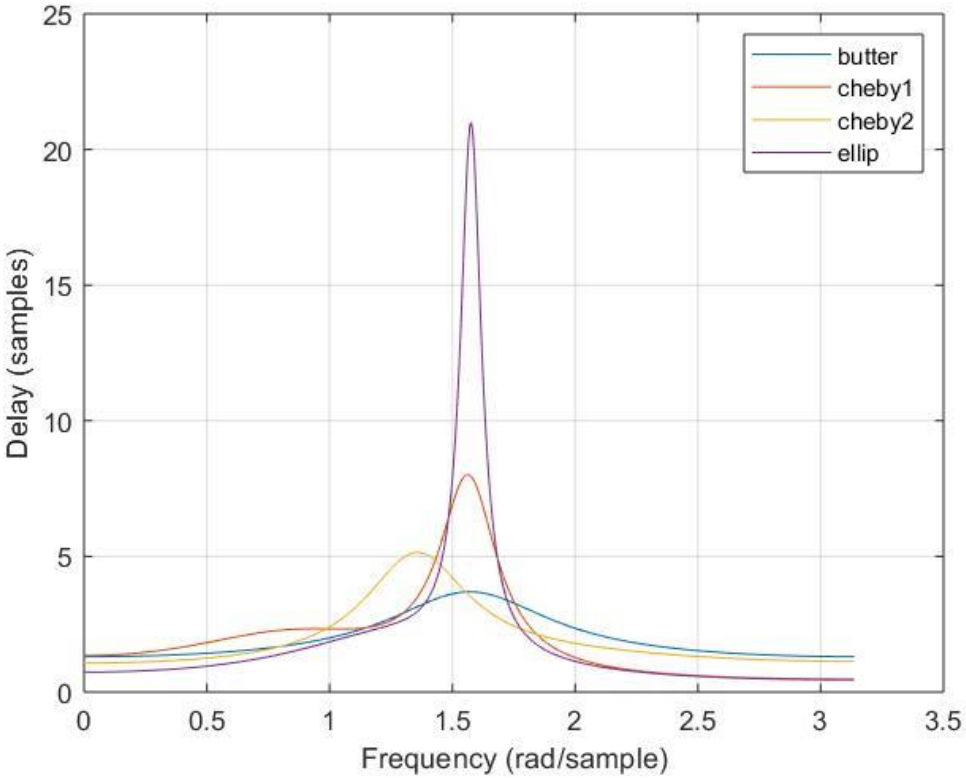

Figure 3.3 Frequency delay response

Therefore, Butterworth filter can be considered as a suitable candidate for reducing the artefacts, which shows that a low pass filter could be designed whose cut-off frequency is normalised to 1 radian per second and whose frequency response (gain) is

$$G(\omega) = \sqrt{\frac{1}{1+\omega^{2n}}} \tag{3.1}$$

Where ω is the angular frequency in radians per second and n is the number of poles in the filter — equals to the number of reactive elements in a passive filter.

When used in forms of digital filter, a Z transfer function of an n-order Butterworth low pass filter can be expressed as

$$H(z) = \frac{B(z)}{A(z)} = \frac{b_1+b_2z^{-1}+\cdots+b_{n+1}z^{-1}}{a_1+a_2z^{-1}+\cdots+a_{n+1}z^{-n}} \tag{3.2}$$

where n is the order of the filter (Williams, 2006).

The FIR filters have non-constant group delay response, so the filtered data could not be shifted back according to the group delay. Therefore the order of designed filter needs to be considered carefully, as greater group delay response value may result in a risk of loss of a part of information in the very end of falling part. The group delay response for Butterworth order 1, 3, 5 and 10 with stopband of 0.2 sample rate are presented as in figure 3.4.

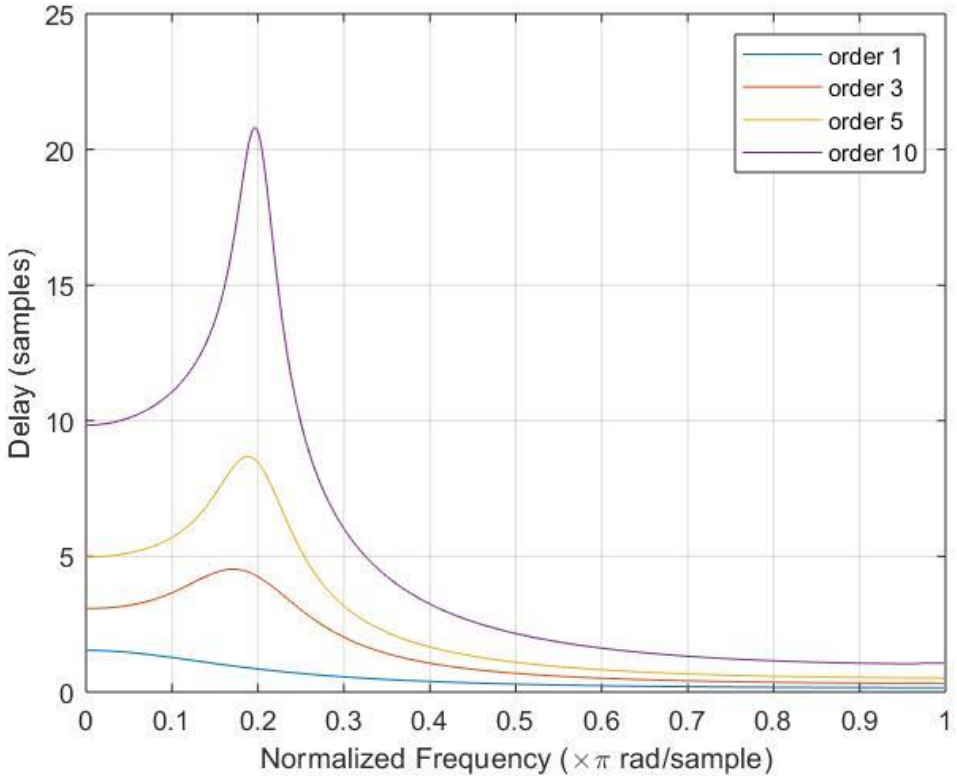

Figure 3.4 Group delay response for Butterworth filter

Though the group delay response is small in value and almost constant in order 1 Butterworth filter, the performance on frequency response is poor. Figure 3.5 presents the frequency response for Butterworth filter with order 1, 3, 5, 10 and stopband of 0.2 sampling rate. It can be witnessed that the start of roll off in order 1 is much earlier than other three, which will reduce the amplitude of fluctuations generated by detrusor contraction. To optimise the filter performance and group delay value, Butterworth third order filter is chosen for the peak counting analysis.

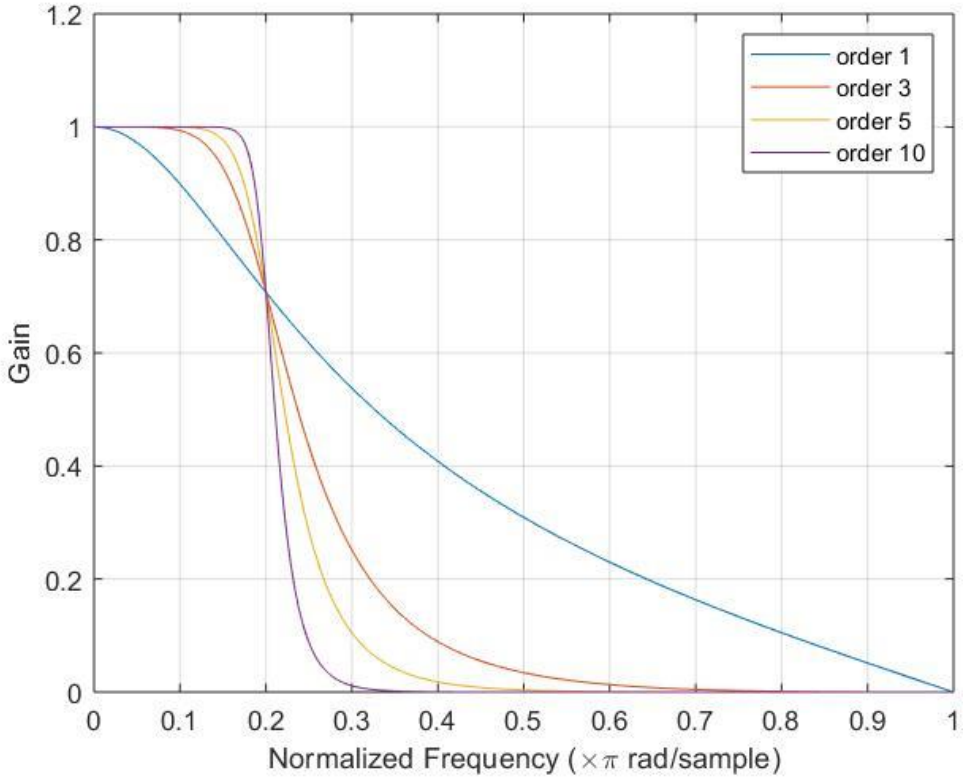

Figure 3.5 Frequency response of Butterworth filter in different orders

In MATLAB code design, the cut-off frequency ω_n must be $0.0 < \omega_n < 1.0$, with 1.0 corresponding to half the sampling rate. The sampling rate of the uroflowmetry is 10Hz, thus the coefficients in MATLAB filter design have inputted as 0.2 for 1Hz filter to reduce fluctuations caused by artefacts and 0.02 for 0.1Hz filter to reduce fluctuations caused abdominal straining. The digital filter transfer functions for two sessions have been identified below.

$$H(z)_{1Hz} = \frac{0.2452+0.2452z^{-1}}{1-0.5095z^{-1}} \tag{3.3}$$

$$H(z)_{0.1Hz} = \frac{0.0305+0.0305z^{-1}}{1-0.9391z^{-1}} \tag{3.4}$$

The frequency and phase response plots for 1Hz and 0.1Hz designed filters are shown in figure 3.6 and figure 3.7 respectively.

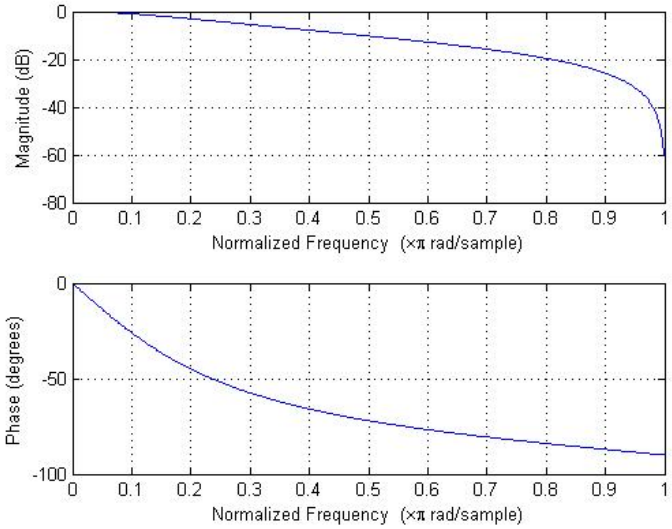

Figure 3.6 Frequency and phase response plots for 1Hz filter

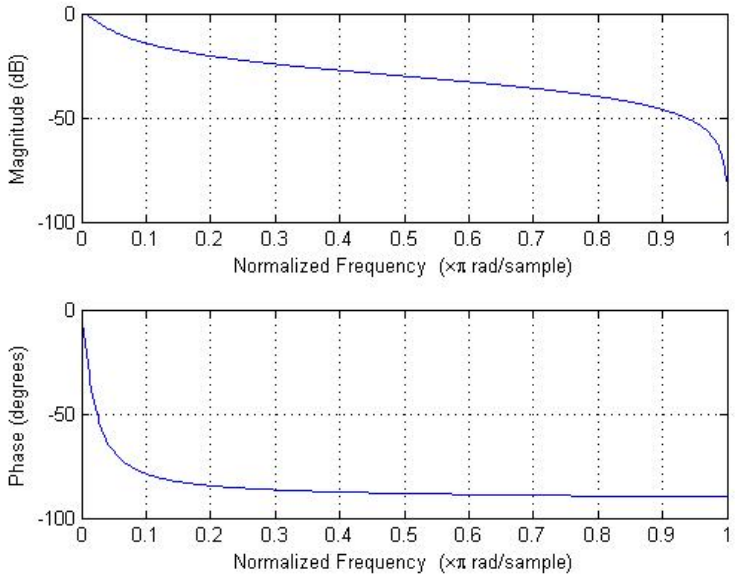

Figure 3.7 Frequency and phase response plots for 0.1Hz filter

In the peak counting analysis, 1 Hz and 0.1 Hz third order filters act on the raw flow curve to maximum reduce peaks caused by abdominal squeezing and bladder squeezing respectively. The selection of cut-off frequency is referred by ICS guideline (Gammie et al., 2014). The peak is defined as a data sequence point is greater than its before and after points, and have minimum amplitude of 1 for the flow data with Q_{max} greater or equal to 5ml/s or minimum amplitude of 0.5 for the flow data with Q_{max} less than 5ml/s.

An example plot for filter applied on raw flow curve shows in figure 3.8. It can be counted automatically in MATLAB that there are 104 peaks in raw curve, 48 peaks in

1 Hz filtered curve and 5 peaks in 0.1 Hz filtered curve. The peak number may have a linear correlation with volume voided, therefore the peak numbers per 100 ml in both raw flow and 0.1 Hz filtered curve are counted separately for peak counting analysis. The derived parameters include peak numbers in raw curve, 1Hz filtered curve and 0.1Hz filtered data. Ratios of peak number in raw curve against 1Hz filtered curve and raw curve against 0.1Hz filtered curve are also included for statistical analysis.

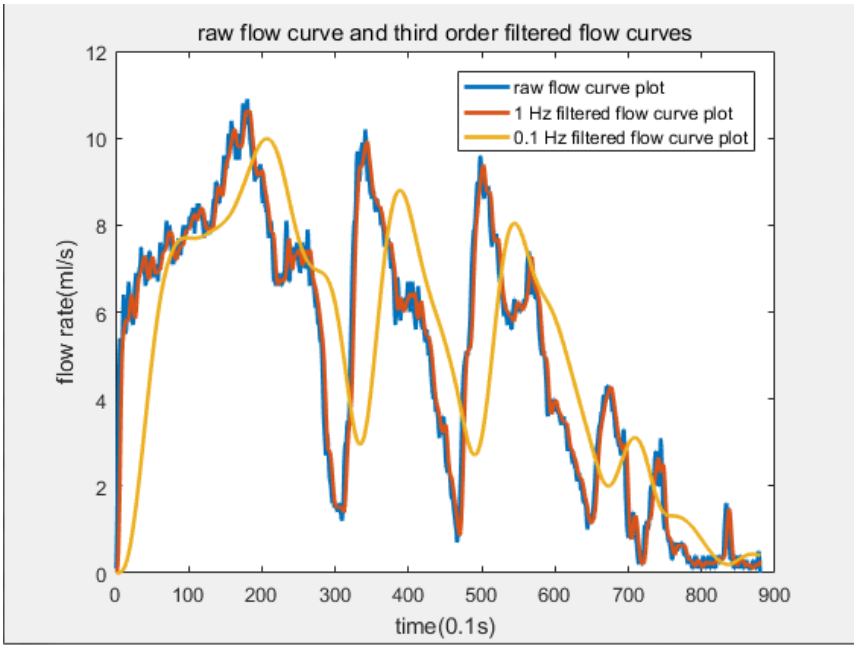

Figure 3.8 Raw flow curve and third order filtered flow curves

3.2.3 Filter cut off frequency verification

In the peak counting analysis, the cut-off frequency adopted is 0.1Hz and 1Hz which are assumed to indicate detrusor contraction and abdominal straining respectively, which is a hypothesis inspired from the ICS urodynamic equipment guideline paper (Gammie et al., 2014). However, there are no such precise definition for detrusor contraction and abdominal straining frequencies in ICS guideline or terminology documents. Therefore, a robust analytical result for these two frequencies is needed for laying down a reliable foundation of further research.

Cut-off frequencies were selected for 1Hz, 0.8Hz, 0.6Hz, 0.5Hz, 0.3Hz, 0.1Hz and 0.08Hz, with third order Butterworth filter. Each filter with different cut-off frequencies was applied on raw UFR curve, then peak numbers was counted in each filtered curve and raw curve as well. Furthermore, ratios of peak number comparing in pairwise

filtered curve and original curve were calculated, and summarised in an excel file for further statistical analysis.

All statistical analysis was performed using SPSS version 23, Mann-Whitney U test and T-student test were performed as appropriate depending on normality. The results of statistical analysis are as presented in Table 3.1 with only significantly statistical difference are shown. Statistically significant was considered as a $P<0.05$.

Table 3.1 Statistical analysis result on ratio of peak numbers in different filtered curves

Ratio	R/0.5	R/0.1	R/0.08	1/0.6	1/0.5	1/0.3	1/0.1	1/0.08	0.8/0.5	0.8/0.1
P	0.024	0.002	0.001	0.032	0.019	0.033	0.002	0.001	0.019	0.002

Abbreviations: R=peak numbers in raw curve; 0.5=peak numbers in 0.5Hz filtered curve; 0.1=peak numbers in 0.1Hz filtered curve; 0.08=peak numbers in 0.08Hz filtered curve; 0.6=peak numbers in 0.6Hz filtered curve; 0.5=peak numbers in 0.5Hz filtered curve; 0.3=peak numbers in 0.3Hz filtered curve.

Further area under curve (AUC) analysis was performed for those having greater significantly statistical difference ($P<0.01$), with best sensitivity/specificity and cut-off ratio are presented in Table 3.2.

Table 3.2 AUC analysis results on median power analysis

Ratio	R/0.1Hz	R/0.08Hz	1Hz/0.1Hz	1Hz/0.08Hz	0.8Hz/0.1Hz
Area under curve	0.671	0.59	0.608	0.597	0.617
Sensitivity	59.1%	50%	68.2%	65.9%	59.1%
Specificity	58.7%	69.6%	60.9%	54.3%	67.4%
Cut-off value	16.1	15.3	8.4	7.1	8.6

Abbreviations: R=peak numbers in raw curve; 0.1Hz=peak numbers in 0.1Hz filtered curve; 0.08Hz=peak numbers in 0.08Hz filtered curve; 0.8=peak numbers in 0.8Hz filtered curve.

From table 3, the optimised sensitivity and specificity for differentiating DU with BOO is comparing peak numbers in 1Hz filtered curve with 0.1Hz filtered curve. This result also verifies the hypothesis that the average frequency for detrusor contractions is 0.1Hz and 1Hz filter have reduce the artefacts successfully.

3.3 Urine Flow Rate Model for Time Constant Analysis

The modelling analysis of urine flow rate aims at to quantify the flow shape and to assess if the shape of the UFR curve could serve as a indicator for differentiate DU from BOO. In this analysis, the UFR curve is separated into rising and falling parts by the Q_{max} point and each part is estimated as a first order transfer function. The Least

Squares method is adopted for the curve approximation and the time constant value in each part is calculated to assess its diagnostic utility.

3.3.1 Urine Flow Rate Model

The urine flow rate model is proposed as

$$Q(t) = \begin{cases} Q_1(t) = a_1 Q_1(t-1) + b_1 P_1(t) & t \le n_r \quad upward \\ Q_2(t) = a_2 Q_2(t-1) + b_2 P_2(t) & t \succ n_r \quad downward \end{cases} \tag{3.5}$$

where t (1, 2, …) is the discrete time index, model output$Q_i(i = 1,2)$ and model input $P_i(i = 1,2)$ are the observed urine flow rate value and the virtual input value respectively, parameter$a_i(i = 1,2)$ are linked to the corresponding time constants of the associated dynamic models and parameters $b_i(i = 1,2)$ are the gain associated with the inputs, the coordinate (n_r, Q_r) is the ridge point time index and the value. It should be explained that the model parameters have physical meanings and can be estimated from measured data. In dynamic principle, the time constant value determines how quickly a urine process moves toward to steady state, the greater of time constant value, the lower speed urine flow rate can be observed. It has been observed that even when two patients have different urine flow rate curves and the maximum values, the time constant value still can be the same. Also, the time constant value can be related with the pressure of the detrusor, and possibly links with the pressure in the bladder.

3.3.2 Model Parameter Estimation

The work of model parameter estimation is to obtain the parameters $a_i(i = 1,2)$ and $b_i(i = 1,2)$ in model of (3.5) by using a statistical algorithm with measured data. For this research, a classical Least Squares (LS) algorithm (Soderstrom and Stoica, 1989) is tailored to implement the data driven computations.

Consider a general linear in parameters regression model

$$y(t) = \varphi^T(t)\theta + e(t) \quad t = 1,2,\dots,N \tag{3.6}$$

where *t* is a discrete time index, N is the length of measured data sequence, dependent variable $y(t)$ is a measurable quantity, regression variable $\varphi^T(t) =$

$[\varphi_1(t) \quad \varphi_2(t) \quad \cdots \quad \varphi_L(t)]$is a measurable L-vector, and error variable$e(t)$ is an unmeasurable quantity to represent modelling error caused from various factors such as measurement noise and external disturbance, and parameter vector $\theta = [\theta_1 \quad \theta_2 \quad \cdots \quad \theta_L]^T$ is a L-vector to be estimated from measured $y(t)$ and $\varphi(t)$ in terms of the least squares errors, the difference between measured dependent variable $y(t)$ and model output variable θ.

In the computation algorithm, to find an estimate $\hat{\theta}$ of the parameter vector θ from measurements$y(1) \quad \varphi(1) \quad \cdots \quad y(N) \quad \varphi(N)$, a set of linear equations are formed, namely,

$$\begin{aligned} y(1) &= \varphi^T(1)\theta \\ y(2) &= \varphi^T(2)\theta \\ &\vdots \\ y(N) &= \varphi^T(N)\theta \end{aligned} \tag{3.7}$$

This can be written in matrix notation as

$$Y(N) = \Phi(N)\hat{\theta} \tag{3.8}$$

Where

$$Y = \begin{bmatrix} y(1) \\ \vdots \\ y(N) \end{bmatrix} \quad \Phi = \begin{bmatrix} \varphi^T(1) \\ \vdots \\ \varphi^T(N) \end{bmatrix} \tag{3.9}$$

The normal equations take the form

$$[\Phi^T\Phi]\theta = \Phi^T Y \tag{3.10}$$

Therefore, the estimation for the parameters can be determined by

$$\hat{\theta} = [\Phi^T\Phi]^{-1}\Phi^T Y \tag{3.11}$$

In this research, the parameter estimation work includes 1) by inspecting measured urine flow rate data sequence, identify the ridge point coordinate (n_r, Q_r), which split the sequence into upward and downward sub-sequences, 2) with reference to (n_r, Q_r), setup virtual stimulate inputs for each sub-sequence, 3) form the associated matrices

and vectors from each of the sub-sequences, 4) use equation (3.9) to calculate the parameter vectors. The step by step procedure is illustrated below.

1) Let N be the measured data sequence, determine ridge point coordinate (n_r, Q_r)

2) Setup virtual step stimulate inputs

For rising part $(t = 1 \cdots n_r)$, setup $P_1(t)$ as a step input n_r*1 vector with amplitude of Q_r and zero initial, which represents a urine flow process driven by an internal force from the bladder. Accordingly, the sub-data sequence is formed as

$$P_1(t)^T = [1 \quad \cdots \quad 1] \tag{3.12}$$

3) Form normal matrices $\Phi_i(i = 1,2)$ and output vectors $Y_i(i = 1,2)$

$$\Phi_1 = \begin{bmatrix} q(1) & p(2) \\ \vdots & \vdots \\ q(n_r - 1) & p(n_r) \end{bmatrix} \quad \Phi_2 = \begin{bmatrix} q(n_r - 1) & p(n_r) \\ \vdots & \vdots \\ q(N-1) & p(N) \end{bmatrix} \tag{3.13}$$

and

$$Y_1 = \begin{bmatrix} q(1) \\ \vdots \\ q(n_r - 1) \end{bmatrix} \quad Y_2 = \begin{bmatrix} q(n_r) \\ \vdots \\ q(N) \end{bmatrix} \tag{3.14}$$

Let the parameter vectors be expressed as

$$\theta_1 = \begin{bmatrix} a_1 \\ b_1 \end{bmatrix} \quad \theta_2 = \begin{bmatrix} a_2 \\ b_2 \end{bmatrix} \tag{3.15}$$

4) Then substitute the formed matrices and vectors into equation (3.9) to obtain the parameter estimates.

3.3.3 Calculation of Time Constant Values

Time constant is defined by a first order Laplace transfer function (Soderstrom and stoica, 1989), as represented by a first order linear differential equation which is presented as in equation 3.16.

$$\frac{Q_i(s)}{P_i(s)} = \frac{k_i}{T_i s+1} \quad i = 1,2 \tag{3.16}$$

where s is the Laplace operator, $Q_i(s)$ and $P_i(s)$ are the Laplace transforms of the observed urine flow rate value and the virtual input value in terms of continuous time, respectively. T_i is defined as time constant.

The proposed model (3.5) is in form of discrete time description and it corresponding Z transform (a representative to a first order linear difference equation) can be expressed as

$$\frac{Q_i(z)}{P_i(z)} = \frac{b_i}{1+a_i z^{-1}} \quad i = 1,2 \tag{3.17}$$

With reference to residue theorem to convert to continuous transfer function $F(s)$ from discrete time transfer function $F(z)$

$$F(s) = \sum Re\, s\left[F(z)\frac{z^{-1}}{s-\frac{1}{T_s}ln\, z}\right]$$
$$= \sum\left\{\frac{1}{(m-1)!}\frac{d^{m-1}}{dz^{m-1}}\left[(z-z_i)^m F(z)\frac{z^{-1}}{s-\frac{1}{T_s}ln\, z}\right]\right\}_{z=z_i} \tag{3.18}$$

where normalised sampling period $T_s = 1$. For the proposed discrete time first order urine flow rate model, $\sum \quad = 1$, $m = 1$, $z_i = a_i (i = 1,2)$ and then the time constant values of the continuous time model can be obtained by

$$T_i = -\frac{1}{ln\, a_i} \quad i = 1,2 \tag{3.19}$$

Therefore, from the above analysis, the procedure to obtain the time constants of model (3.5) is consist of two steps 1) estimate $a_i (i = 1,2)$ of model (3.5) from measured data and 2) calculate T_i from the relationship of (3.19).

The plot for an example of 0.1Hz first order filtered data and urine flow rate model is presented in figure 3.9.

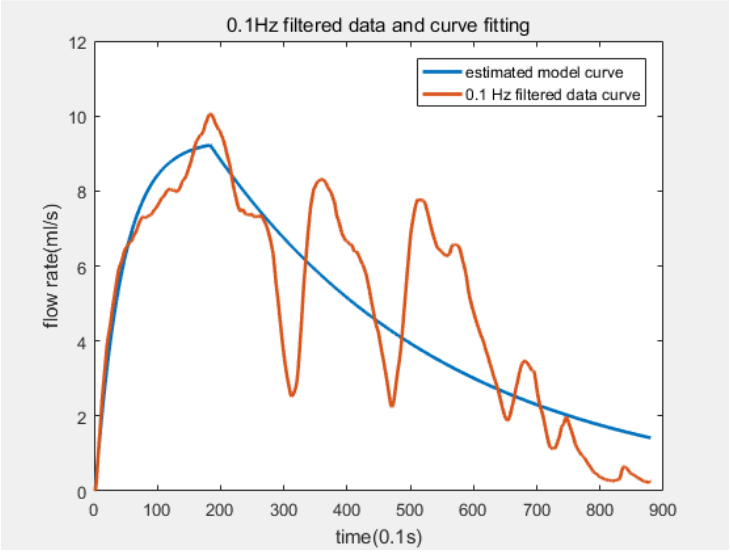

Figure 3.9 0.1 Hz filtered data and urine flow rate model

In the analytical procedure, the time constant value could be negative, as the flow curve is manually separated which potentially results in raising part showing an infinite trend. Also it should be noted, the time constant analysis may not work properly on analysing intermittent traces as the first order transfer function is not sufficient for describing a multi-peak curve.

3.4 Urine Flow Rate Curve Normalization and shape archetype

The shape of urine flow rate curve is suggested to associate with one or more voiding abnormalities (Abrams, 2017). In this UFR shape normalization analysis, two shape archetypes, BOO and DU, are generated from each diagnostic group data and it is proposed to assess their capacity to non-invasively differentiate DU from BOO. The time constant value analysis is re-conducted on normalised flow rate curve to isolate shape from time and flow rate, for assessing the diagnostic utility on modelling UFR pure shape.

3.4.1 Quantitative detection of intermittent shape

To generate the shape template for each diagnostic group, intermittency shape data need to be excluded. However the intermittency terminology from ICS is not a quantitative definition, and describes a flow stopping and starting during a single void (Abrams et al., 2002). The early dribble (figure 3.10) and terminal tribble (figure 3.11) are normally included in the urine flow rate curve as they are produced as a part of micturition, but dribbles will critically influence the accuracy of shape template generated from each

diagnostic group. Especially terminal dribble is reported as happening in 39% of DU male patients (Uren et al., 2017). Early dribble could happen in less urine flow volumes, but either early or terminal dribble should be avoided when detecting intermittency from a UFR data input. A quantitative definition of the early and terminal dribble which could be used in intermittency detection is needed for the urine flow curve normalisation and template analysis.

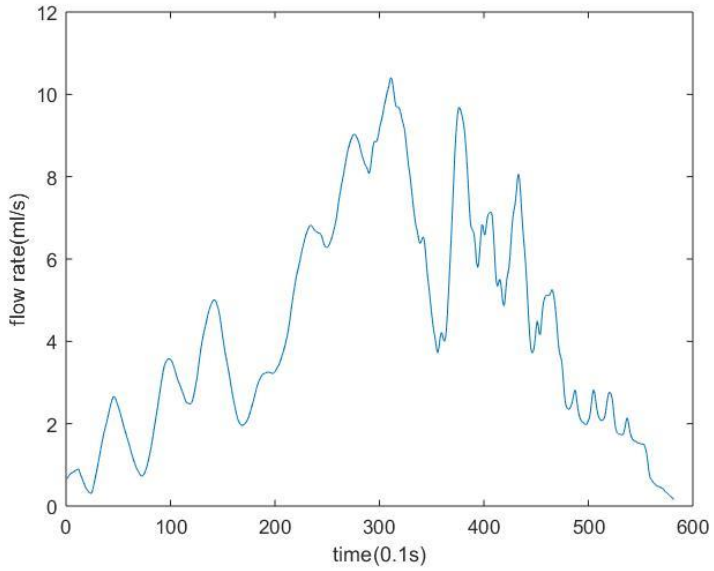

Figure 3.10 A UFR curve plot shows a 'hump' at the very beginning of curve. The data is filtered by 2 seconds window filter to remove artefacts.

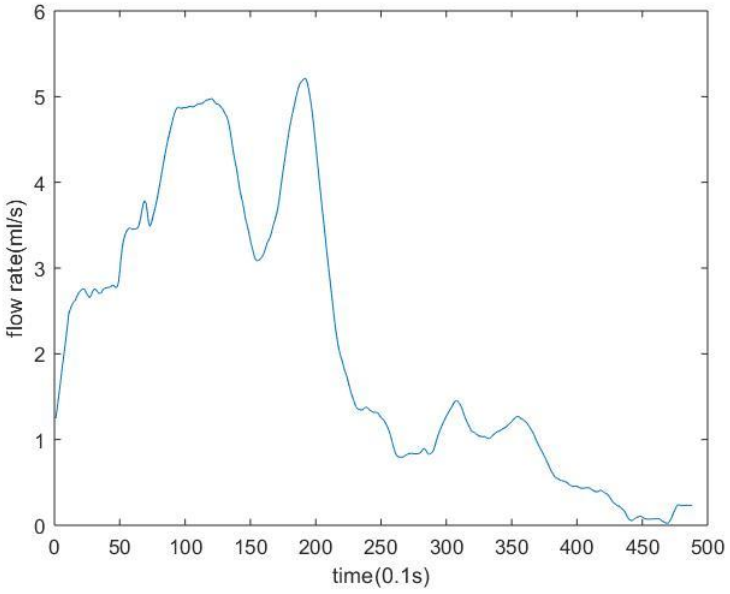

Figure 3.11 A UFR curve plot shows a 'hump' at the very end of curve. The data is filtered by 2 seconds window filter to remove artefacts.

In the literature, Fantl (1983) gives the additional definition of flow rate falling below 2ml/s, instead of ICS terminology of completely stopping for intermittency shape, which could increase the risk of mis-classifying a curve with large fluctuations appearing in the micturition as a intermittency shape. This would especially be the case for those with lower maximum flow rate, for instance a patient with Q_{max} of less than 5ml/s possibly has a major part of the flow rate in the curve under 2ml/s. Another research defines intermittent flow as lasting for at least 15 seconds of flow time with one or more interruptions (Jensen et al., 1983). In conclusion, none of these two additional definition will help to quantitatively exclude early or end terminal dribble when detecting intermittency shape.

After observation of all urine flow rate data and discussing with the supervisory team, intermittency curve will only be detected in the 0.5% to 98% of volume voided part under a baseline of 0.5ml/s flow rate. The early dribble followed by a non-intermittent curve only happens very rarely and with a short duration, while a non-intermittent curve with terminal dribble happens more often, especially in DU group, and could have a relatively longer duration. Therefore the excluded volume voided part for intermittent detection is asymmetric, with smaller area in the starting and larger area in the ending.

3.4.2 Study design of flow normalisation analysis

Free-flow data of 293 adult male patients who had also undergone PFS were analysed in this research. Based on their PFS record, these patients are divided into two groups: 158 DU and 135 BOO. For each flow data, the starting and ending point has been selected by the threshold value of 0.5ml/s, then 2 seconds averaging window filter has been applied as suggested by ICS good urodynamic practice. Intermittency detection, filtered application and template generation are automatically calculated with pre-code programme in MATLAB 2018b. Flow shape template are normalised on non-intermittency data in the same area following the steps listed below:

1. Port in the DU and BOO data to MATLAB separately and apply 2 seconds window filter on each data.
2. Locate volume voided 0.5% and 98% point, and detect intermittency in this area with criteria of flow rate under 0.5ml/s.
3. normalise each non-intermittent flow data in VV 0.5% to 98% area into

amplitude of 1 and samples of 1000 by dividing whole flow curve by Q_{max} and resampling of 1000 samples.

4. Calculate the mean value on each sample point of normalised curve in both diagnostic groups.
5. Divide the whole generated data sequence by the maximum value in both diagnostic groups.

Then the derived data sequences are the shape template for BOO and DU. In database of 293 free flow data, 90 flow curves are detected as intermittent, and 107 BOO and 76 DU non-intermittent data are employed to generate the flow template in each diagnostic group. The generated flow curve templates are presented as in figure 3.12.

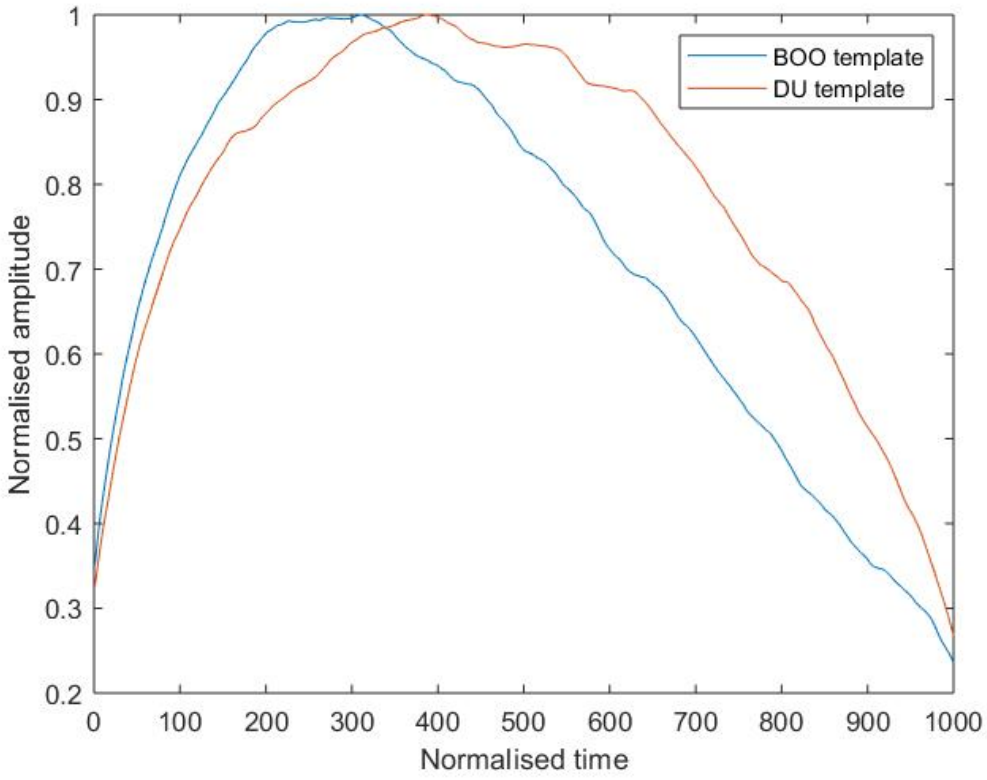

Figure 3.12 BOO and DU template

The maximum point located in BOO is at 30% of normalised time, with a flat roof ranged from 20% to 32% of normalised time. The BOO template shows an asymmetric shape that most of non-intermittent BOO data have Q_{max} appear around 25% voiding time. While DU template is a relatively symmetric shape, with the maximum point located at 40% of normalised time.

To assess the diagnostic usage of the template, all BOO and DU non-intermittent flow data in 0.5%-98% volume voided area are normalised and calculated the ratio of sum square errors (RES) on each re-sample point comparing with DU template and comparing with BOO template. The smaller RES value indicates the curve is more like a DU shape rather than a BOO shape, and vice versa.

From the figure 3.12, it can be witnessed that the rising slopes in two templates do not have much difference, but in the falling slope BOO template shows an almost linear fall to the baseline and DU template falls much slower. The shape difference in these normalised curves suggests we may be able to assess diagnostic utility of the modelling analysis of normalised urine flow data. Therefore, the raw UFR curve is normalised in three methods as following:

1. Normalise raw UFR curve into max value of 1 and 1000 samples
2. Normalise 2 seconds window filtered UFR curve into max value of 1 and 1000 samples
3. Normalise 2 seconds window filtered UFR curve with 0.5% to 98% volume voided part into value of 1 and 1000 samples

Then each normalised method data in BOO and DU group is assessed for their diagnostic utility by calculating the RES value, and this test is run again by excluding intermittency data in each group. In addition, a bell shape is generated by sine function which presented as in figure 3.13 and is employed to test the RES value with bell shape in 2 second window filtered curve. The statistically analytical results are addressed in the chapter 6.

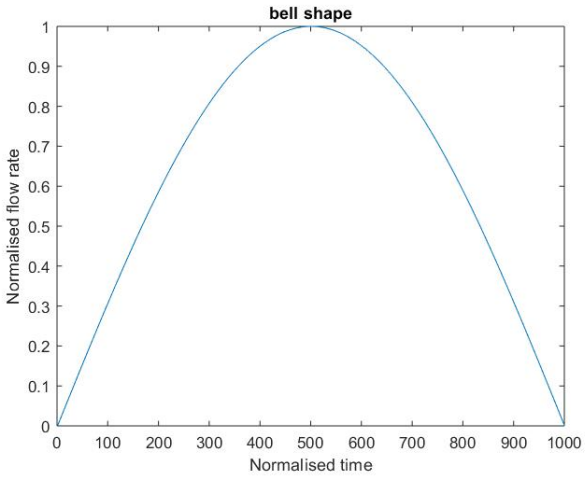

Figure 3.13 Generated bell shape by sine function

3.5 Summary

This chapter starts with introduction of the rationales for the peak counting analysis and time constant analysis, and the step by step design of each analytical methods. However there are some limitations discussed for the time constant analysis which could limit its diagnostic application. The peak counting analysis result shows promising frequency difference between two groups and prompts a quantitative analysis of UFR curve in its frequency domain.

The flow template is proposed to assess if the normalised shape of the urine flow rate curve could serve as an indicator to differentiate DU from BOO, and a quantitative method of detecting intermittent curve is developed. The modelling method is re-conducted and test on its diagnostic ability with normalised UFR curve.

Chapter 4 Analysing Urine Flow Rate Data in Frequency Domain

4.1 Overview

In chapter 3, urodynamic model and peak counting analysis have presented some mathematical analysis of urine flow curve, counting multiple peaks within filtered curves and considering the frequency content of the curve shape, but this has only limited diagnosing accuracy and the specificity does not yet exceed that of $Q_{max} < 10$ ml/s for detecting male bladder outlet obstruction (Gratzke et al., 2015). However a significant statistical difference is found on peak numbers between patients with DU and BOO, thus it is worthwhile to further quantitatively investigate the frequency difference between the two diagnostic groups. Therefore, in this chapter, two analytical methods are designed and developed for analysing UFR data in the frequency domain, which are median power frequency analysis and amplitude changes in rising slope analysis.

The hypothesis for these two studies is that the frequency difference may vary in DU and BOO groups, as underactive patients are reported to perform more abdominal straining for successfully passing of urine out of the bladder (Gammie et al., 2016). Specifically, DU patients may have higher average frequency and vary the fluctuations with higher sum of amplitude than BOO patients in their UFR curve (with fluctuations caused by detrusor contractions excluded), since abdominal straining normally lasts for a shorter time period than detrusor contractions. It may also be that since DU is linked to a poorly sustained contraction, the median frequency of these contractions may decrease over time (Uren and Drake, 2017).

All analytical procedures are conducted in the MALTAB version 2018b, reselection on the start and end point of urine flow rate curve by the threshold value of 0.5ml/s is pre-processed prior to frequency analysis in the Microsoft Excel 2016.

4.2 UFR Frequency Domain Analysis

To verify the hypothesis that there is the potential frequency difference between two diagnostic groups, a parameter is needed for representing the average frequency in the urine flow rate data excluding fluctuations generated by involuntary detrusor contraction. Therefore, the median power frequency (MPF) is introduced to serve as a parameter to assess the frequency difference.

MPF is defined as the frequency at which the power spectrum is divided into two regions with equal value, which is widely applied in EMG signals to assess the muscle fatigue (Angkoon et al., 2012). Compare to Mean power frequency, the MPF is less affected by artefacts (Stulen and De Luca, 1989). The mathematical definition of MPF is given by

$$\sum_{i=1}^{i_{MPF}} P_i = \frac{1}{2}\sum_{i=1}^{i=n} P_i \tag{4.1}$$

where P_i is the power spectrum at the frequency bin *i*, and *n* is the length of frequency bin.

In the frequency domain analysis, the component of urine flow curve is defined into three frequency ranges:

1. Frequency range less than 0.1Hz: fluctuations definitely generated by detrusor contractions which last longer than 10 seconds.
2. Frequency range greater than 1Hz: fluctuations most likely generated by artefacts which last shorter than 1 seconds.
3. Frequency range between 0.1Hz to 1Hz: containing a small amount of detrusor contraction which last short than 10 seconds, most likely all fluctuations caused by abdominal straining, and a small number of artefacts which last longer than 1 seconds.

The urine flow curve component in the frequency range 3 is the target to analyse in the frequency domain. To ensure a reliable result could be derived, the Butterworth filter is not suitable for the frequency analysis as it rolls off relatively slowly and its group delay response is not a constant value. Thus a new filter is needed to design for a precise cut off in the desired frequency band.

4.2.1 Filter design

As discussed, the new filter should be designed with additional requirements to the filter applied in the peak counting analysis. To start with, the baseline would be the same, which is that the filter stopband must be flat without any ripple to avoid artefactually adding any frequency component. Furthermore, the roll-off of the designed filter should be sharp to avoid components in the frequency range 1 or 2 being involved when generating the frequency spectrum. A 10% tolerance is accepted between passband and stopband for the frequency domain analysis, which is 0.1Hz to 1Hz for the passband then less to 0.09Hz and greater than 1.1Hz for the stopband. However, such high filter performance would result in a higher value of group delay, for instance the group delay response could be a few hundred samples and vary according to the frequency. Thus the group delay response must be a constant value for shifting the filtered curve back to the original position, otherwise the filtered flow curve will be stretched and delayed for an uncertain number of samples. The FIR filters do not deliver a constant value of group delay response, hence the designed filter needs to be considered in the infinite impulse response (IIR) filter family.

The attenuation on each stopband of designed filter is also needed to be specified. In this analysis, the maximum artefact amplitude and fluctuations caused by detrusor contraction are considered to possibly reach as high as 50ml/s, which is needed to be filtered down to 0.5ml/s as the baseline threshold. The attenuation equation is presented as in equation 4.2.

$$attenuation(dB) = 20\,log_{10}\left(\frac{a_{out}}{a_{in}}\right)(dB) \tag{4.2}$$

where a_{out} is the amplitude after filter and a_{in} is the original amplitude in the urine flow curve. Then the attenuation could be derived as -40dB for filtering a fluctuation with amplitude of 50ml/s down to 0.5ml/s.

In summary, the desired filter should be designed to fulfil the following requirements:

1. The passband must be flat without any ripple.
2. The group delay response must be a constant value.
3. The passband is 0.1Hz to 1Hz with 10% tolerance of sharp roll off to stopband.
4. The attenuation of designed filter is set to -40dB.

With such specifications, the Kaiser window filter in the IIR filter family is chosen to be employed for the frequency analysis. The magnitude response of designed Kaiser window filter is presented as in figure 4.1.

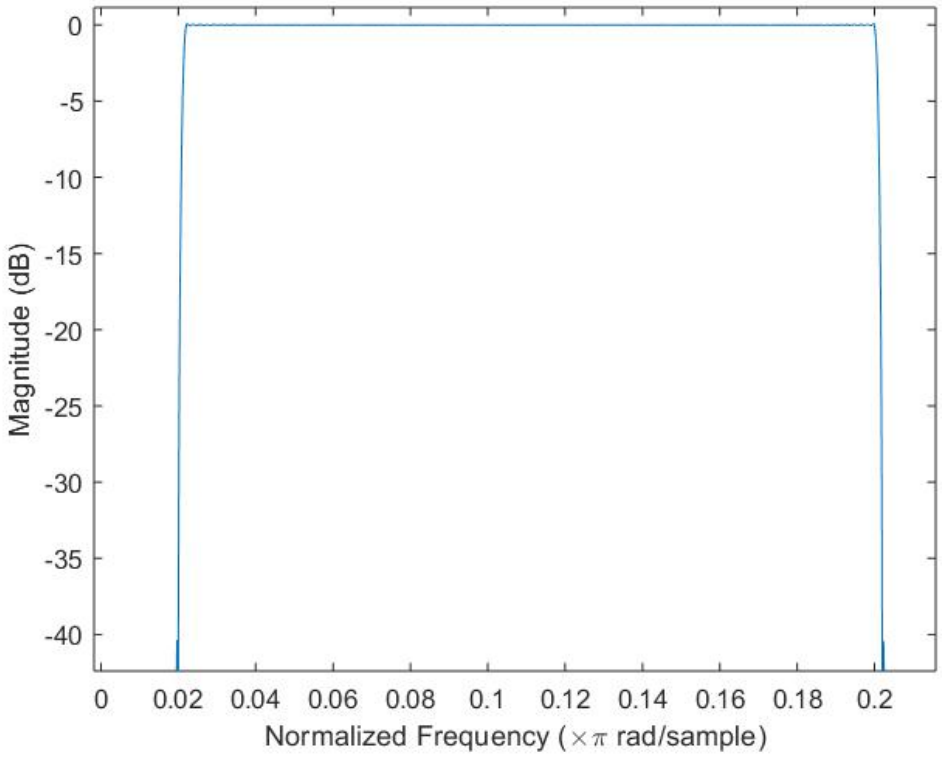

Figure 4.1 Magnitude response plot for designed Kaiser window filter

where the sampling rate is 10Hz thus 0.02 normalized frequency represents the start of passband of 0.1Hz and 0.2 normalized frequency represents the end of passband of 1Hz. The group delay response for designed Kaiser window filter is presented as in figure 4.2.

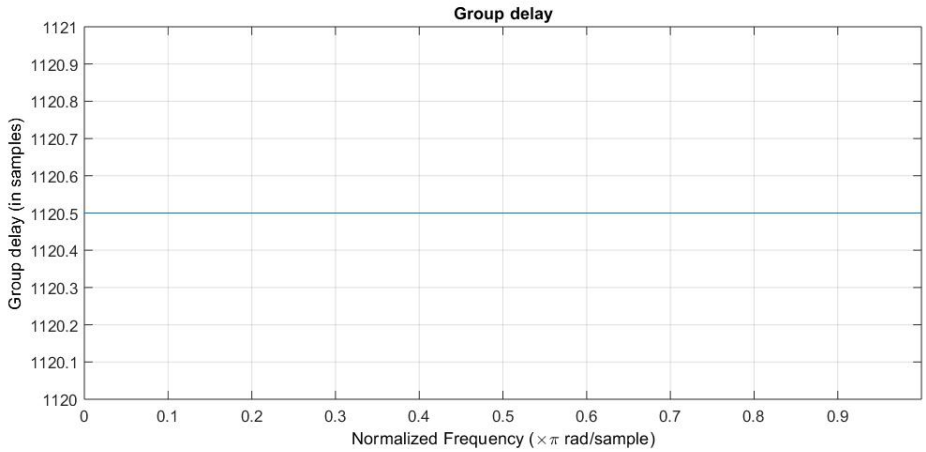

Figure 4.2 Group delay response plot for designed Kaiser window filter

From the frequency response and group delay plots, it can be seen that the Kaiser window filter is designed successfully according to the filter specifications. Therefore the designed Kaiser window filter is applied on the UFR curve for analysing in the frequency domain.

4.2.2 Fourier transforms and parameters derived from power frequency spectrum

It is hypothesised that DU patients may have larger amount of fluctuations at relatively higher frequencies than BOO patients, as they have a higher possibility of not being able to empty the bladder by detrusor contractions thus partially void out urine by abdominal straining. Potentially in the second half of the whole flow, the DU patient may experience detrusor muscle fatigue (Smith et al., 2015). Therefore, the median power frequency analysis is introduced to assess the frequency component difference in UFR curve of each diagnostic group.

To assess UFR curve in the frequency domain, the frequency spectrum is needed to derive the proposed parameter MPF, so the Fast Fourier Transform (FFT) is employed to generate the frequency spectrum. The FFT theory is widely applied in video applications, signal processing and noise reduction.

In general, the Fourier transform decomposes a function of time (a signal or a data sequence) into the frequencies that make it up. The Fourier transform of a function of time itself is a complex-valued function of frequency, whose real value represents the amount of that frequency present in the original function, and whose complex argument

is the phase offset of the basic sinusoid in that frequency. It is called the frequency domain representation of the original signal, which refers to both the frequency domain representation and the mathematical operation that associates the frequency domain representation to a function of time. The algorithm is presented as in equation 4.3, where x_n is the input data sequence with total length N and X_k is the output data sequence.

$$X_k = \sum_{n=0}^{N-1} x_n * e^{-\frac{2\pi i}{N}kn} \quad k = 0, 1, \dots, N-1. \tag{4.3}$$

The Fourier transform is not limited to functions of time, but in order to have a unified language, the domain of the original function is commonly referred to as the time domain. FFT is an efficient implementation of the discrete Fourier transform and could be traced to Gauss's unpublished work in 1805. In MATLAB the FFT functions are based on a library called FFTW which algorithm could be found in Frigo and Johnson paper (1998).

All UFR data is employed for the frequency domain analysis, by using FFT to generate the frequency spectrum and then calculating the power spectrum. The analytic procedures of median power frequency are listed as follows:

1. Pre-process on the starting and end point of the UFR data in Microsoft Excel according to the threshold value of 0.5ml/s
2. Import all data in each diagnostic group into MATLAB and apply designed Kaiser window filter on each data
3. Generate the frequency spectrum by FFT function.
4. Calculate the square of each frequency bin to generate the power spectrum
5. Do an integral of the power spectrum and locate the median point of integral power spectrum

Then the certral point in the power spectrum of is the parameter of median power frequency. The whole flow curve is also divided into two parts in three ways, by half of voiding time, location where half of volume is voided and the Q_{max} point, and median power frequency is calculated in each part as well. An example of the plot output on MPF analysis is presented as in figure 4.3.

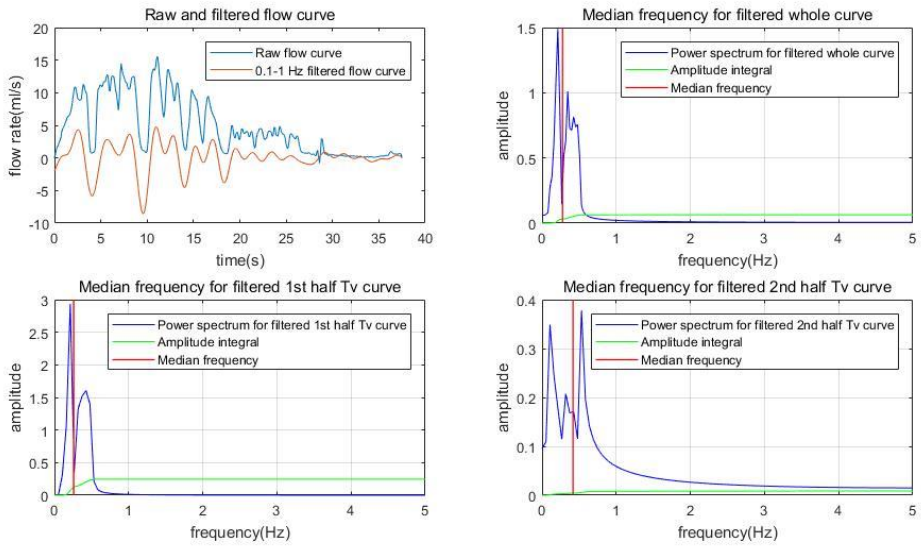

Figure 4.3 Median power frequency analysis on UFR data

The raw flow curve and the Kaiser window filtered flow curve are presented as in the top left sub-plot, in blue and red respectively. The power spectrum is presented in the top right sub-plot in blue and the green line is the integral of the power spectrum, the red line shows the location of median of integral power spectrum. The two sub plots in the bottom present the MPF calculation in two parts of flow divided by the half of voiding time.

The filtered data in the top-left plot of figure 4.3 has a part of negative values since the filtered curve is generating from the raw curve by subtracting the detrusor contraction which last longer than 10 seconds, while the filtered curve contains all fluctuations which are last shorter than 10 seconds. For instance, in the figure 4.3 top-left plot, the fluctuation starting from 0s to approximate 17s is considered as the detrusor contraction and is filtered off, and the smaller fluctuations, such as the small humps and falls, are considered as 'detrusor contractions last shorter than 10s' and 'abdominal straining' which are presented in the filtered curve in red.

The frequency ranges of detrusor contraction and abdominal straining are not a constant value, and they could vary in different patients and different situations. Thus the bandpass range of the designed Kaiser window filter is selected differently apart from 0.1Hz to 1Hz, to verify if any other range could increase the diagnostic power on non-invasively differentiate DU from BOO. The other bandpass ranges are considered as following: 0.1Hz to 0.9Hz, 0.1Hz to 0.8Hz, 0.1Hz to 0.7Hz, 0.2Hz to 1Hz, 0.2Hz to

0.8Hz and 0.2Hz to 0.7Hz. The filtered flow data according to these additional bandpass range are also divided into two parts and assess their diagnostic utility.

The result of the median power frequency analysis holds promise for non-invasively differentiating DU from BOO. However, whereas the original hypothesis was that a DU patient may have higher median power frequency value, on the contrary it appears that the DU patient has a lower median frequency value in the mid-range. The interpretation of result and discussion will be addressed in chapter 6.

4.3 Sum of amplitude changes in the rising slope analysis

The sum of amplitude changes (SAC) in rising slope analysis aims on verify the hypothesis that DU patients may vary their fluctuations greater than BOO patients, since they perform abdominal straining more frequently which are in the frequency range of 0.1Hz to 1Hz (Gammie et al., 2016). To calculate the sum of amplitude in rising slope in desired frequency range, the designed Kaiser window filter is employed. The analytical procedure is conducted as follows:

1. Pre-process on the starting and end point of the UFR data in Microsoft Excel according to the threshold value of 0.5ml/s
2. Import all data in each diagnostic group into MATLAB and apply designed Kaiser window filter on each data
3. Count the amplitude changes of each rising slope in the filtered curve and sum the result to generate the parameter

The figure 4.4 presents an example of SAC analysis on a UFR curve, in which blue line is the raw flow curve, the green and red lines are the Kaiser window filtered curve, and each of green line is the amplitude change in rising slope. The parameter is calculated by taking the sum of amplitude differences in each green line.

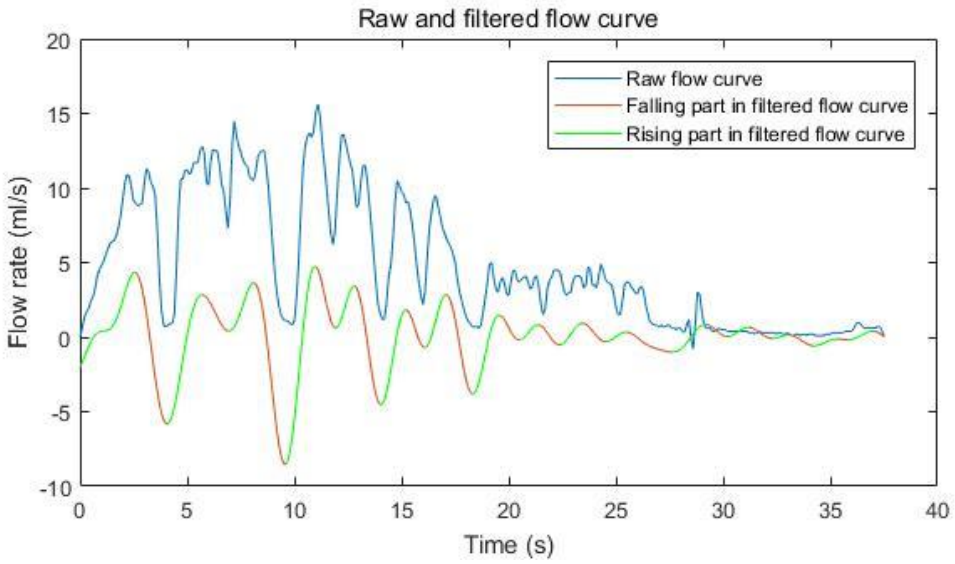

Figure 4.4 Sum of amplitude changes in rising slope analysis

The parameter generated from SAC analysis shows statistical difference between two groups. However it is reported that Q_{max} has significantly statistical difference between DU and BOO patients (Lee et al., 2016), and the statistical difference shown in SAC analysis could be caused by Q_{max} or volume voided differences. Therefore a correlation test has been further conducted to verify if the SAC has significant correlation with Q_{max} in raw curve, Q_{max} in 2 second window filtered curve and volume voided. The result will be further addressed in the chapter 6.

4.4 Wavelet Theory

At the start of frequency domain analysis, the wavelet theory was considered as a possibility to be employed on the UFR curve to assess the time-frequency applicability. Furthermore, it could be an alternative way for reducing spikes by employing wavelet transform decomposition. A figure for wavelet packet tree is presented as in figure 4.5.

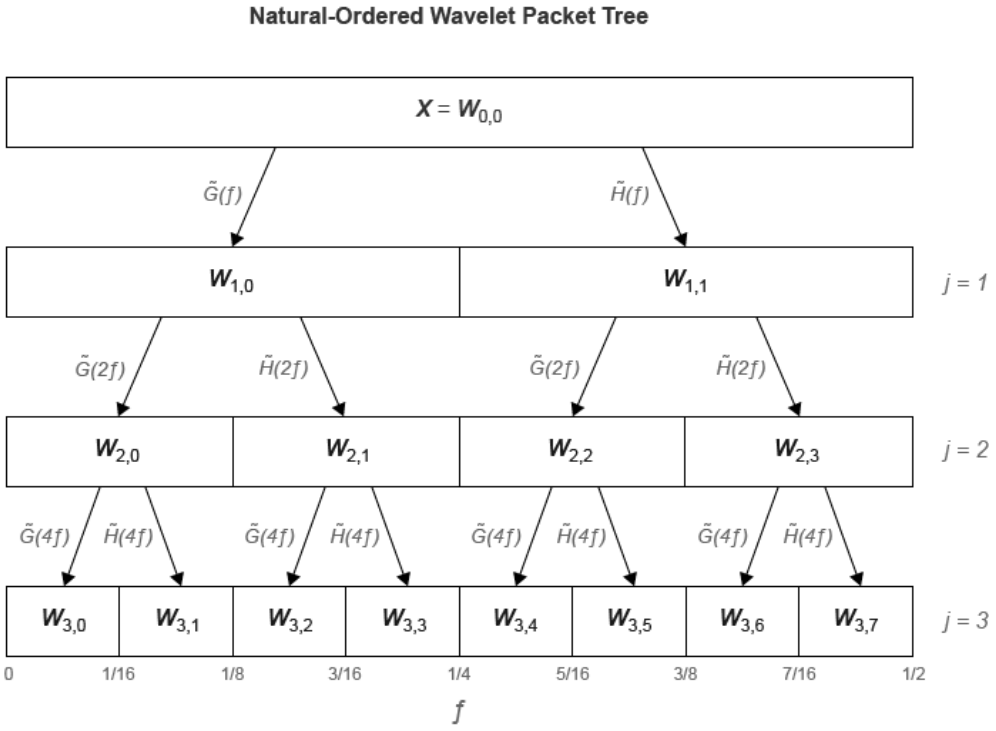

Figure 4.5 Wavelet packet tree in 3 levels

in which at each level, the details and approximations is divided into two parts based on approximated half of prior level frequency. In UFR signals, the sampling frequency is 10Hz, so in level two decomposition we can get approximate frequencies of 0 to 1.25Hz, 1.25Hz to 2.5Hz, 2.5Hz to 3.75Hz and 3.75Hz to 5Hz. It should be easier to perform specified frequency band analysis. For instance, UFR can be analysed on the detail parts in 1.25Hz to 2.5Hz band, or count peak values in approximation part of 0Hz to 1.25Hz band. However the designed bandpass filters provide precise cut-off frequencies thus the Wavelet transform decomposition is not further employed.

Wavelet transforms are divided into continuous wavelet transform (CWT), discrete wavelet transform (DWT) and wavelet packet transform (WPT). The difference between DWT and WPT is that both detail and approximation are decomposed into further level in WPT but in DWT only approximation is decomposed into a higher level. CWT is mainly used on visual inspection as it can be operated at every scale and have the best resolution (Ricker, 1953).

However, the main challenge in using wavelet transform is to select the most optimum mother wavelet. There are at least 20 of different types of mother wavelet families, and almost every mother wavelet has further order specification. To overcome this, similarity between signal and mother wavelet are considered in selecting a mother

wavelet. There are various methods to determine the similarity, but it should be noted there is no standard or general method.

An initial trial of adapting wavelet transform on UFR data has been conducted with db2 mother wavelet which is considered to be one of the most similar mother wavelet to the EMG signal. Additionally, the shape of db2 has the similarity of a flow curve, as presented in the figure 4.6, which shows an asymmetric bell in the beginning and a prolonged falling slope.

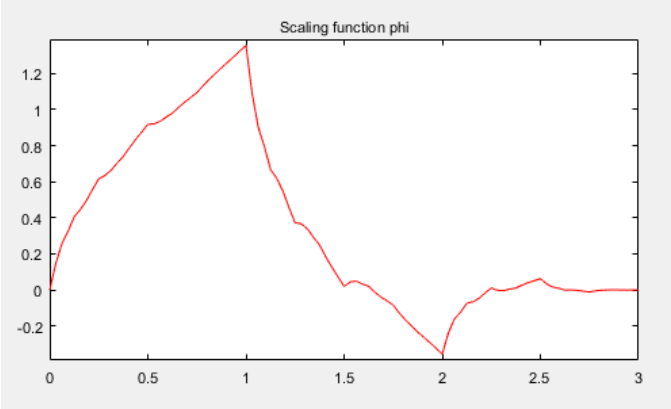

Figure 4.6 db2 mother wavelet

However when adapted on the UFR curve, though the input parameters are set for the best resolution, the output of the time-frequency spectrum could not be used to provide any additional information on time-frequency in UFR curve. The plot is presented as in figure 4.7.

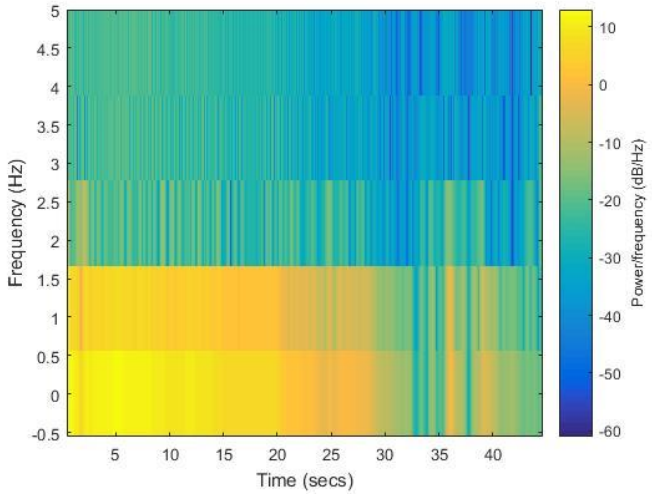

Figure 4.7 Time-frequency plot generated by continues Wavelet transform using db2 mother wavelet

The resolution is poor as there is not much frequency difference between involuntary detrusor contraction and abdominal straining in UFR data. Therefore the Wavelet transform is considered as not suitable for analysing flow curve in the frequency domain.

4.5 Summary

In this chapter, analysing UFR in frequency domain is proposed to assess if there is potential frequency difference between two diagnostic groups. The bandpass filter is designed according to detailed specifications and applied on the UFR data to select desired components in specified frequency range for frequency analysis.

Two frequency analytical methods have been proposed, the median power frequency analysis and the sum of amplitude changes in rising slope analysis, to verify the hypothesis that DU patients may have statistical difference with BOO patients on the frequency domain and on their fluctuation amplitudes. The wavelet theory is also researched but considered it is not suitable for the frequency analysis of UFR data.

With a number of parameters derived from UFR data with statistical difference between two groups proposed, non-invasively differentiation DU from BOO might hold some promise. However each of proposed parameter have limited diagnostic power and is insufficient to serve as a indicator individually.

In the next chapter, three mathematical and statistical methods are considered to be employed on the parameters proposed, for maximising the diagnostic usefulness.

Chapter 5 Statistical Approaches for Optimising Diagnostic Power

5.1 Overview

The UFR curve has been analysed in both time and frequency domain with a number of non-invasive parameters proposed. These parameters need to be tested to verify if they have significantly statistical difference between two groups. However, each of these parameters alone has limited diagnostic usefulness and could not be able to individually differentiate DU from BOO non-invasively. Thus, we now consider developing mathematical and/or statistical models which can combine all proposed parameters to optimise the diagnosing power.

There are numbers of articles using statistical approaches for managing parameters in the urological and nephrology field, mostly by logistic regression, univariate analysis or multivariate analysis (Chung et al., 2013; Groen et al., 1998; Al-Ghazo et al., 2011; Chen et al., 2017). The logistic regression analysis works similar to linear regression but with different output which is a binary variable, for instance 1 stands for DU and 0 stands for BOO. It provides and odds ratio (OR) which indicates the probability of outcome base on the reference group, for instance the intermittency curve may appear in DU group with 2 times probability than appears in BOO group. Its algorithm is given by:

$$\log\left(\frac{OR}{1-OR}\right) = \alpha_0 + \alpha_1 x_1 + \alpha_2 x_2 + \cdots\cdots + \alpha_n x_n \tag{5.1}$$

where *OR* is the odds ratio of an event, α_i are the regression coefficients related with the reference group and x_i input variables (Sperandei, 2014).

While univariate and multivariate analysis serve a similar function to the odds ratio with one independent variable or with multiple factors that influence the variable of interest, the odds ratio has limited diagnostic ability to differentiate DU from BOO.

The statistical analysis in this study is carried out by the following steps:

1. Analyse each proposed non-invasive parameter on its ability to differentiate DU form BOO by calculating the *p* value of each parameter.
2. If the parameter has significantly statistical difference between two groups, the area under curve (AUC) value is then calculated, and derive optimised sensitivity and specificity.
3. Combine the parameters with significantly statistical difference and develop statistical or engineering model to combine parameters for optimising diagnosing utility.

5.2 Statistical analysis on proposed parameters

The t test, also called as Student t-test, is the most commonly used statistical method to investigate the difference of variables in means between two groups, which could be adopted in this study to assess the statistical difference of proposed parameters between two diagnostic groups. However some assumptions should be met prior to adopting the t-test (Pandey, 2015):

1. Parameters in two test groups should follow a normal distribution, otherwise the Mann Whitney U test should be used.
2. Parameters in two test groups should have equal variance.
3. The parameters should be independent variables.

It is accepted that t test could be used even assumption 1 is not fulfilled when the sample size is large enough: normally under 30 samples the assumption is needed to be strictly followed (Hogg and Tanis, 2010). In this study the sample size is 293 which could skip testing normality and use t test directly. In SPSS version 23, input parameters are automatically calculated for variance prior to the t test, if the parameters in two groups do not meet equal variance then the one-way analysis of variance (ANOVA) is conducted to derive the *p* value. Assumption 3 is also fulfilled in this study as all parameters are derived from the independent UFR test. In summary, the *p* value reported in this study is generated from the t test result in SPSS. The t test algorithm is given by

$$t = \frac{\overline{x_1} - \overline{x_2}}{S_p \sqrt{\frac{1}{n_1} + \frac{1}{n_2}}} \tag{5.2}$$

where $\overline{x_1}$ is the mean value of the parameter in the first group and x_2 is the mean value of tested parameter in the second group, n_1 and n_2 is the sample size for two groups, S_p is pooled standard deviation, which algorithm is given by

$$S_p = \frac{(n_1-1)s_1^2+(n_2-1)s_2^2}{n_1+n_2-2} \tag{5.3}$$

where s_1 and s_2 are the standard deviation of tested parameter in each group.

In this study, a p value of less than 0.05 is considered as a significantly statistical difference, an example table of the t test is presented as in table 5.1.

Table 5.1 t test on Q_{max}

		Levene's Test for Equality of Variances		t-test for Equality of Means			
						95% Confidence Interval of the Difference	
		F	Sig.	Sig. (2-tailed)	Mean Difference	Lower	Upper
Q_{max}	Equal variances assumed	28.179	.000	.000	4.006	2.484	5.528
	Equal variances not assumed			.000	4.006	2.421	5.591

It can be seen in the table that the variance of Q_{max} is not equal in two groups, with a p value of less than 0.001 to reject the null hypothesis of equal variances assumed in Levene's test for equality of variances. Therefore the p value of Qmax between two groups is taken the value from 'Sig. (2-tailed)' in the second row which is less than 0.001, and this is considered as Q_{max} has significantly statistical difference between DU and BOO group.

Followed by the t test, parameters which have significantly statistical difference are entered to the receiver operating characteristic (ROC) analysis to calculate the area under curve (AUC) value and to find optimised sensitivity and specificity. The sensitivity, also called the true positive value, in this study measures the proportion of predicted DU data which are actually diagnosed as DU. The specificity, also called as true negative value, measure the proportion of predicted BOO data which are actually

diagnosed as BOO. A table demonstrates the sensitivity and specificity as in table 5.2.

Table 5.2 confusion table

	Diagnosed DU	Diagnosed BOO	
Predicted DU	True positive (TP)	False positive (FP)	Positive predictive value $\frac{TP}{TP+FP}$
Predicted BOO	False negative (FN)	True negative (TN)	Negative predictive value $\frac{TN}{FN+TN}$
	Sensitivity: $\frac{TP}{TP+FN}$	Specificity: $\frac{TN}{FP+TN}$	

The ROC curve is plotted by the sensitivity against 1-specificity value, an instance is presented as in figure 5.1.

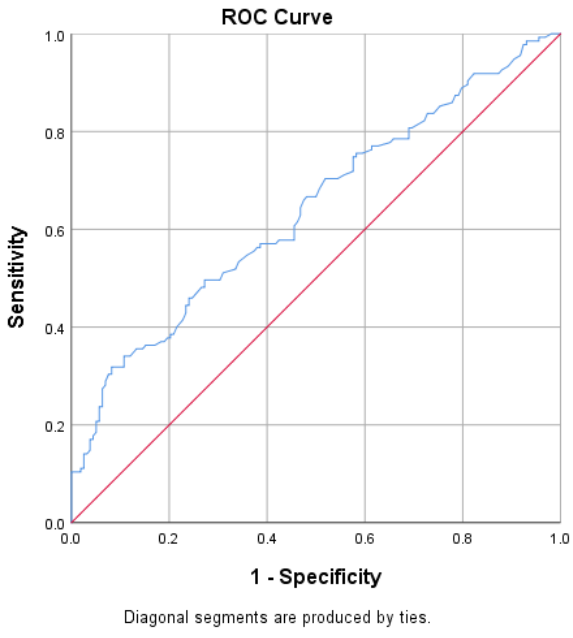

Figure 5.1 ROC curve on Q_{max}

The area under curve value is equal to the probability that a classifier will rank a randomly chosen positive instance higher than a randomly chosen negative one, which algorithm is given by

$$\mathrm{A} = \int_0^1 Sensitivity(t) * (1 - \mathrm{specificity})'(\mathrm{t})\mathrm{dt} \quad (5.4)$$

In SPSS, the ROC analysis also generates a table of sensitivity and (1-specificity) at each cut-off point, then the cut-off value which provides optimised sensitivity and specificity could be calculated as

$$\mathrm{C} = \max(\mathrm{Sensitivity}_i - (1 - \mathrm{Specificity})_i) \quad (5.5)$$

where *i* is the ith number of sensitivity or (1-specificity) generated in the AUC table, the optimised specificity is simply calculated by 1 minus (1-specificity) value.

5.3 Statistical and engineering models on proposed parameters

Each proposed non-invasive parameter could serve as an additional indicator for differentiating DU from BOO, however they have limited diagnosing accuracy individually. To optimise the diagnosing accuracy, statistical and engineering models are now considered to combine the parameters.

In this study, three models are considered for all parameters which have significantly statistical difference between two groups, the multivariance analysis of variance, the classification and regression tree analysis and the neural network theory.

5.3.1 Multivariance analysis of variance

MANOVA is one of the most common multivariate statistical analysis in the biomedical science (Bangert and Baumberger, 2005), which is a member of the General Linear Model family. It is an extension of ANOVA to apply to a situation where analysis of two or more dependent variables are needed to analyse. The experimental design model can be expressed as (Sthle and Wold, 1990):

$$\mathrm{Y} = \mathrm{W} * \beta + \mathrm{E} \quad (5.6)$$

Where Y (N × p) is the observed matrix, W (N × m) is the designed matrix, β (m × p) is the matrix of parameters, E (N × p) is the matrix of random errors, N is the total number of observations, p is the number of dependent variables and m is the number of parameters. Since the rows of W will be identical for all observations in the same cell, the model in terms of cell means can be expressed as

$$Y. = A. * \beta + E. \tag{5.7}$$

where A. is g × m matrix, Y. (g × p) and E. (g × p) denote matrices of means, and g is the number of cells. The reparameterization of the model 5.7 is done by factoring A. into (Bock, 1975; Finn, 1977)

$$A. = K * L \tag{5.8}$$

where K (g × r) forms a column basis for the model, which rank is r. L (r × m) is the constant matrix which contains the coefficients of parameters linearly combined, which can be specified via input value, then K can be derived by $AL'(LL')^{-1}$. After this reparameterization procedure the model can be simplified as

$$Y = A\beta + E = K(L\beta) + E = Kq + E \tag{5.9}$$

where q (r × p) is computed by L (r × n) times β (m × p). Then the parameter estimation is performed by an orthogonal decomposition on K (Golub, 1969)

$$K = QR \tag{5.10}$$

where Q is an orthonormal matrix that $Q'DQ = I$, D is the diagonal matrix of cell frequencies and R is an upper-triangular matrix. Then the normal equation of the model is

$$(K'DK)\,\widehat{\theta} = K'DY \tag{5.11}$$

also as

$$R\hat{\theta} = Q'DY = U \tag{5.12}$$

Therefore, this triangular set can be solved by forming the cross-product matrix.

In SPSS version 23, MANOVA is only available in syntax and not in the graphical interface, the input variables are all the parameters derived from UFR data which have significantly statistical difference between two groups and the group variable is input as 1 and 0 where 1 stands for DU and 0 stands for BOO. The syntax script could be found in appendix IV.

An example of MANOVA by employing Q_{max} and Q_{ave} is presented as in figure 5.2

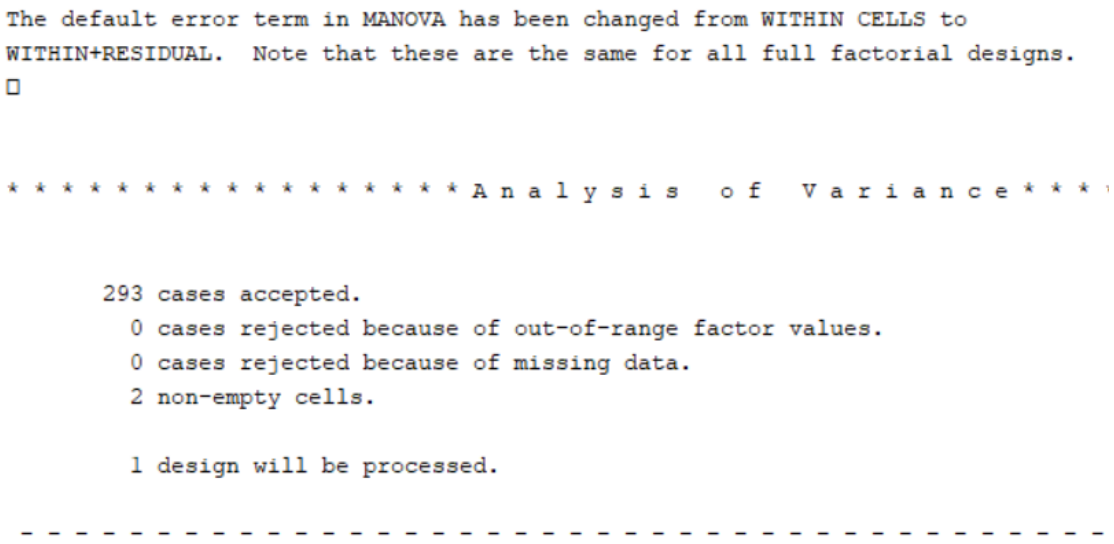

Figure 5.2 Image of MANOVA result of input values

in which shows the 293 cases are all accepted for the MANOVA analysis, and the coefficients estimation result is presented as in figure 5.3

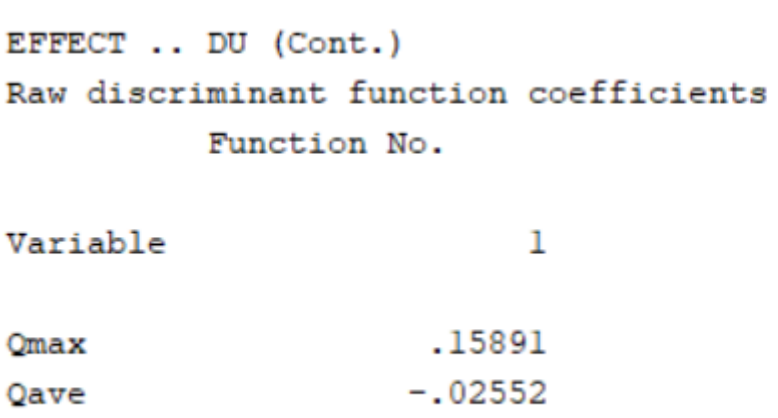

Figure 5.3 Image of Coefficients estimation result

where the coefficients for Q_{max} and Q_{ave} are 0.15891 and -0.02552 respectively, then the new parameter is given by $P_{manova} = 0.15891 * Q_{max} - 0.02552 * Q_{ave}$. The generated parameter is calculated in Excel and then we use the t test to verify the significant statistical difference between the two groups, and generate optimised sensitivity and specificity by ROC analysis.

5.3.2 Classification and regression tree analysis

The Cart analysis is based on classification and regression trees proposed by Breiman

et al. (1984), which is a binary decision tree that is constructed by dividing a parent node into two child nodes repeatedly. The root node contains the whole DU and BOO samples, and the decision is made based on estimating which proposed parameter could provide the best differentiation result between two groups. The tree growing procedure is based on following steps.

1. Assess each parameter's best differentiation utility. Each of parameters is examined to find the best split point to differentiate DU from BOO most precisely.
2. Then choose the best parameter which could serve the best to split the parent node into child nodes.
3. Consider each child node as parent node and repeat step 1 and 2 until stopping rules is fulfilled.

The stopping rules control the tree growing process on every node to stop or to continue, if any following stopping rules are fulfilled then the growing in the node is stopped.

- If a node becomes pure, in which a node has successfully split parent node into pure DU and BOO.
- If the current tree depth reaches the maximum depth growing value which is specified by user.
- If the size of a parent node is less than the minimum node size value which is specified by user.
- If the split of a node results any child node size less than the minimum child node size value which is specified by user.

The node size value and tree depth value affect the accuracy of the CART analysis result, however there is no rule of thumb to quantify the optimised values of node size and depth. In SPSS a validation is provided by separating data into two groups, the testing group and validation group, and to test the robustness of generated CART. In this study, the testing group is set to 70% of randomised total data and validation group set to the rest of 30% of data. Then the node size and depth are tested to find the optimised results, where a 10% difference is accepted between the testing result and validation result.

An example for the CART analysis is presented in figure 5.4, in which Q_{max} and Q_{ave} by voiding time are employed, parent and child nodes are limited to 20 and 5 respectively, and depth is limited to 2 levels.

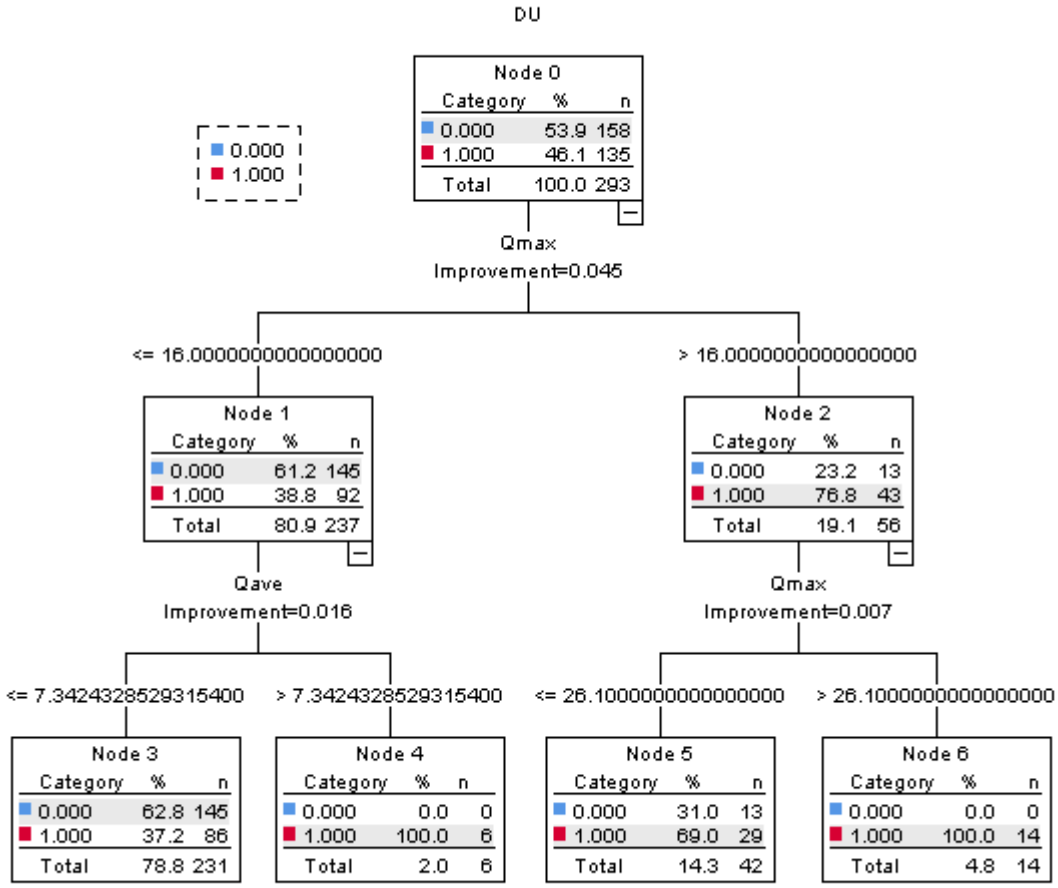

Figure 5.4 Image of CART analysis on Q_{max} and Q_{ave}

and the classification result is presented as in table 5.3

Table 5.3 CART classification result

Classification

	Predicted		
Observed	0	1	Percent Correct
0	145	13	91.8%
1	86	49	36.3%
Overall Percentage	78.8%	21.2%	66.2%

Growing Method: CRT
Dependent Variable: DU

where 1 stands for DU and 0 stands for BOO. The sensitivity and specificity for the generated CART model are 91.8% and 36.3%, with a 66.2% overall diagnosing accuracy. It should be noted that in node 4 and 6, a total of 20 DU patient is diagnosed, which hold the promise to discriminate a partial of DU or BOO patients reliably.

5.3.3 Artificial neural network theory

The artificial neural network (ANN) is a framework for various machine learning algorithms to process complex inputs, which contains layers of computing nodes with information processing characteristics. The advantage of ANN is the feature of nonlinearity which makes it capable of learning and adaptability. Sonke et al. (2000) have evaluated the performance of an ANN model in non-invasive predistortion of BOO in 1903 male data, including Q_{max}, PVR, VV and prostate volume, and yield sensitivity of 71% and specificity of 69%. Djavan et al. (2004) developed an ANN model on International Prostate Symptom Score (IPSS), prostate volume and urinary flow rates to predict BOO in male, and report 82% sensitivity and 77% specificity. In this study, the ANN model is employed to differentiate DU from BOO, with all derived parameters and with flow curve shape as separate inputs.

The ANN is built up with multiple layers and each layer can be expressed as

$$y = a(W * x) + b \tag{5.13}$$

where *x* is the input vector, *y* is the output vector, *b* is the offset vector, *W* is the weight matrix and *a()* is the activation function. In each layer, the input vector *x* is calculated by this simple function to generate the output vector *y*. In general, each layer in neural network performs a linear transformation followed by a non-linear transformation, and training a suitable weight matrix *W* is the main challenge for building up a functional neural network (Schmidhuber, 2015).

In this study, the output of designed neural network is expected to be maximal calculated as the desired diagnostic group, in which 0 is for bladder outlet obstruction and 1 is for detrusor underactivity. Therefore, the training procedure in the designed

neural network is to train the weight matrix in each layer according to the difference of output and the actual diagnosis, where the loss function is employed for measuring the difference. The output, loss, in the loss function represents the difference between neural network output and actual diagnosis, and the aim of the training procedure in designing neural network is to reduce the value of loss. the gradient descent is employed for training, which moves the location of loss value to its backward direction to reduce loss value (Rumelhart and McClelland, 1996). The movement interval is controlled by learning rate.

When calculating the gradient and updating the weight matrix, the time required would be an issue, as the analysis by machine learning usually deal with a large database. In general, the backpropagation method is adapted for gradient calculation. The learning and recognition procedures are presented in figure 5.5 and 5.6 respectively. There are a number of rules of thumb to determine the hidden layer size, for instance it should be between the input size and output layer size (Heaton, 2008). In figure 5.5 and 5.6one hidden layer neural network is presented as an example for demonstrating the training and testing procedure in the ANN model.

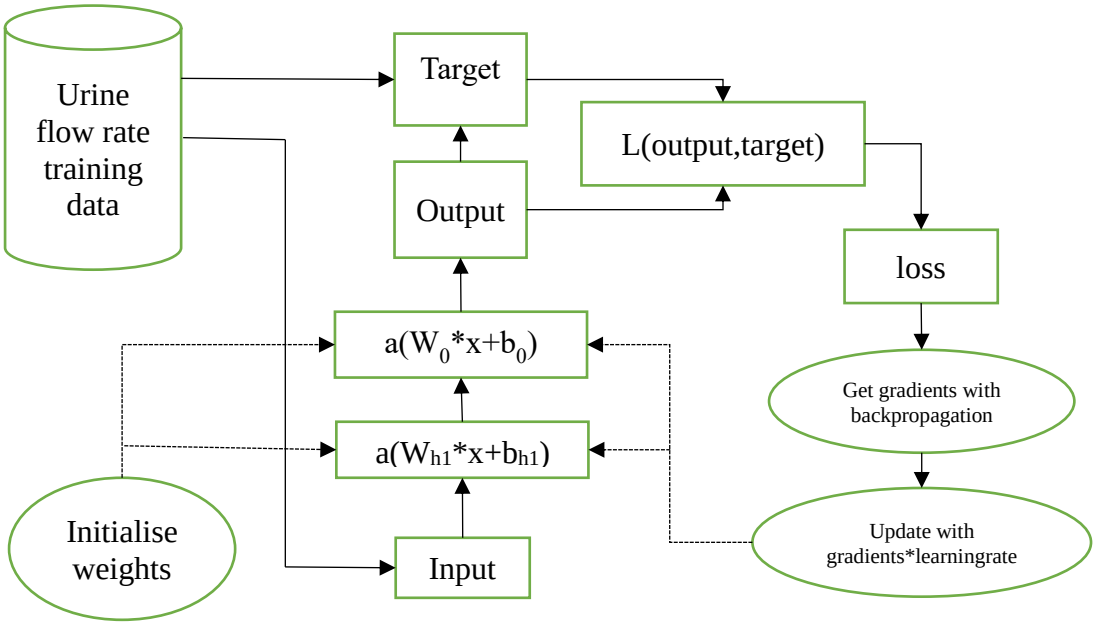

Figure 5.5 Training procedure in ANN model

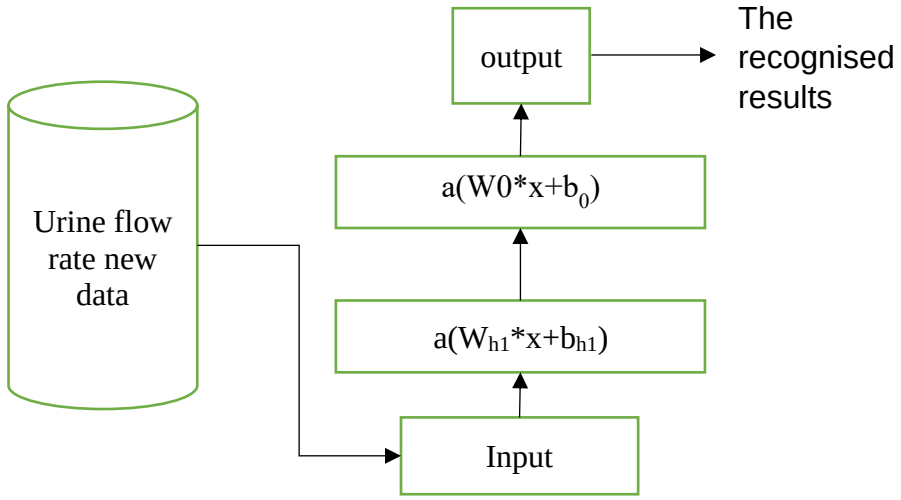

Figure 5.6 Recognition procedure in ANN model

The ANN analysis is conducted in MATLAB version 2018b, with Neural network toolbox. An initial ANN model is set to differentiate DU from BOO, by employing all proposed parameters which have statistical difference between two groups. Then another ANN model is set to assess if urine flow rate shape could discriminate DU and BOO by employing normalised UFR shape data.

5.4 Summary

In this chapter, statistical analysis methods have been proposed to assess if the proposed parameters have statistical difference between two groups by t test. Three statistical approaches for maximising the diagnosing accuracy have been developed, including MANOVA test, CART analysis and ANN model. In next chapter, statistical analysis result will be interpreted.

Chapter 6 Interpretation of Results

6.1 Overview

In this chapter, the statistical analysis results of derived parameters and proposed statistical models are presented. All derived parameters are categorised in the following two groups according to their difficulties to compute.

- **Parameters obtained or derived from raw curve and filtered curve**: this group includes the parameters which could be obtained from the uroflowmetry, for instance Q_{max}, VV, $Q_{max2sec}$, voiding time and flow time, and parameters which could be derived from UFR raw data or 2 seconds window filtered data with minimum calculation, for instance Q_{ave} by T_v, Q_{ave} by T_f, mean flow rate in rising and falling part, ratio of T_v against T_f.
- **Parameters derived by complex mathematical calculation of raw UFR data**: this group includes parameters derived from raw data by filtering technique and frequency analysis, for instance MPF variables, ratio of peak numbers in different filtered curve, time constant value in raw and filtered curve, SAC variables and parameters derived in shape template analysis.

All parameters are tested for their statistical difference between two diagnostic groups, and those which have significantly statistical difference are employed in the MANOVA, CART and neural network analysis. The results of statistical models are then presented as well.

6.2 Statistical analysis results for derived parameters

The analytical methods of derived parameters have been presented in chapter 3 and 4, and the statistical analysis method is explained in chapter 5 section 2. All statistical analysis is performed in SPSS version 23.

The power analysis is conducted in the G*Power version 3.1.9.4, with selected t test, Mann-Whitney test and inputted effect size of 0.5 and sample size for two groups, the power of Mann-Whitney test is 0.966 out of 1, which demonstrates the reliability and

robustness of the analytical results.

6.2.1 Parameters derived from raw curve and filtered curve

Raw curve parameters are most easily obtained from uroflowmetry outputs, however it is reported the artefacts are needed to be removed prior to report the values of uroflowmetry parameters, either by a two seconds window filter applied on the UFR curve or manually by an experienced urologist (Schaefer et al., 2002). The two seconds window filter could smooth the curve in time domain but may lose valuable information in frequency domain. Therefore, in this study a 0.5Hz low pass filter is also applied on the UFR data to derive parameters, which have the same roll-off point as the two seconds window filter but could keep the information in frequency domain.

The definitions of derived parameters in the first group is presented as in table 6.1.

Table 6.1 Variables in the first group and their definition

Variables	Definition
Qmax	Maximum flow rate in raw curve
Qave	Average flow rate by flow time in raw curve
Volume voided	Integral of flow data sequence
Up time/Down time	Ratio of rising time against falling time
Flow time	Void time - (sample number of value less than 0.5)/10
Void time	Data length / sampling rate of 10
Flow time/Void time	Ratio of flow time against void time
Flow index (Qave/Qmax)	Ratio of Q_{ave} against Q_{max} in raw curve
Mean rate in raising part	Mean flow rate in rising slope
Mean rate in falling part	Mean flow rate in falling slope
Ratio of mean up/down	Ratio of mean flow rate in rising against in falling slope
DeltaQ	Q_{max} - Q_{ave} in raw curve
Qmax 0.5Hz	Q_{max} in 0.5Hz filtered curve
Qave 0.5Hz	Q_{ave} in 0.5Hz filtered curve
Ut/Dt 0.5Hz	Ratio of rising time against falling time in 0.5Hz filtered curve
Qave/Qmax 0.5Hz	Ratio of Q_{ave} against Q_{max} in 0.5Hz filtered curve
meanUFRupward 0.5Hz	Mean flow rate in rising slope in 0.5Hz filtered curve
meanUFRdownward 0.5Hz	Mean flow rate in falling slope in 0.5Hz filtered curve
FI0.5Hz	Ratio of Q_{ave} against Q_{max} in 0.5Hz filtered curve
DeltaQ0.5Hz	Q_{max} -Q_{ave} in 0.5Hz filtered curve
Qmax2sec	Q_{max} in 2 seconds window filtered curve
QaveTv2sec	Q_{ave} by void time in 2 seconds window filtered curve
QaveTf2sec	Q_{ave} by flow time in 2 seconds window filtered curve
FI2sec	Ratio of Q_{ave} against Q_{max} in 2 seconds window filtered curve
Ut/Dt2sec	Ratio of rising time against falling time in 2sec filtered curve

DeltaQ2sec	Q_{max} -Q_{ave} in 2 seconds window filtered curve
MUP2sec	Mean flow rate in rising slope in 2 seconds filtered curve
MDOWN2sec	Mean flow rate in falling slope in 2 seconds filtered curve
RMU/D2sec	Ratio of two variables above
TQmax	Time to Q_{max} in raw curve
TQmax2sec	Time to Q_{max} in 2 seconds window filtered curve
TQmax/T_v	Ratio of time to Q_{max} against void time in raw curve
TQmax2sec/T_v	Ratio of time to Q_{max} against void time in 2sec filtered curve

in which flow index (FI) and DeltaQ are proposed to serve as indicator for overactive bladder and BOO respectively (Futyma et al., 2015; Lee et al., 2016), and in this study these two non-invasive parameters are tested to see if they have statistical difference between DU and BOO groups. The descriptive statistical analysis result of derived parameters is presented as in table 6.2. Column DU is the group variable in which 1 stands for DU and 0 stands for BOO.

Table 6.2 Group statistics

	DU	N	Mean	Std. Deviation
Qmax	1	135	13.65	8.23
	0	158	9.64	4.79
Qave	1	135	4.95	3.16
	0	158	3.81	1.95
Volume voided	1	135	180.12	136.23
	0	158	149.96	102.81
Up time/Down time	1	135	1.08	2.28
	0	158	.72	1.31
Flow time	1	135	31.84	18.93
	0	158	35.63	24.71
Void time	1	135	41.33	25.38
	0	158	42.48	31.53
Flow time/Void time	1	135	.80	.17
	0	158	.85	.13
Flow index (Qave/Qmax)	1	135	.37	.14
	0	158	.41	.13
Mean rate in raising part	1	135	6.59	4.35
	0	158	5.27	2.63
Mean rate in falling part	1	135	4.16	2.77
	0	158	3.28	1.85
Ratio of mean up/down	1	135	1.90	1.23
	0	158	1.80	1.20

DeltaQ	1	135	8.70	6.21
	0	158	5.83	3.56
Qmax 0.5Hz	1	135	12.20	7.08
	0	158	8.41	4.07
Qave 0.5Hz	1	135	4.95	3.16
	0	158	3.81	1.95
Ut/Dt 0.5Hz	1	135	.72	.88
	0	158	.67	1.26
Qave/Qmax 0.5Hz	1	135	.41	.14
	0	158	.46	.12
meanUFRupward 0.5Hz	1	135	6.74	4.37
	0	158	5.31	2.57
meanUFRdownward 0.5Hz	1	135	4.17	2.79
	0	158	3.32	1.82
FI0.5Hz	1	135	2.21	1.64
	0	158	1.96	1.22
DeltaQ0.5Hz	1	135	7.25	4.96
	0	158	4.60	2.66
Qmax2sec	1	135	11.51	6.44
	0	158	8.23	3.54
QaveTv2sec	1	135	2.81	2.45
	0	158	2.21	1.54
QaveTf2sec	1	135	3.46	2.73
	0	158	2.59	1.66
FI2sec	1	135	5.53	3.54
	0	158	4.83	2.80
Ut/Dt2sec	1	135	.37	1.03
	0	158	.28	.59
DeltaQ2sec	1	135	8.39	6.09
	0	158	5.34	3.97
MUP2sec	1	135	6.67	4.47
	0	158	5.19	2.64
MDOWN2sec	1	135	2.40	2.14
	0	158	1.90	1.39
RMU/D2sec	1	135	3.79	2.94
	0	158	3.42	2.16
TQmax	1	135	13.30	12.86
	0	158	11.65	15.27
TQmax2sec	1	135	12.69	10.63
	0	158	12.11	15.14
TQmax/Tv	1	135	.35	.23

	0	158	.28	.20
TQmax2sec/Tv	1	135	.34	.20
	0	158	.28	.17

The t test result for group 1 parameters is presented as in table 6.3. Levene's Test for equality of variances determines the *p* value to be used in t test: if the Levene's test has a significant statistical result of less than 0.05 then the *p* value is taken the second row in the 'sig. (2-tailed)' column. The parameters which have statistically significant difference of *p* value less than 0.05 are highlighted by *, *p* value less than 0.01 by ** and *p* value less than 0.001 by ***.

Table 6.3 t test result for group 1 parameters

		Levene's Test for Equality of Variances		t-test for Equality of Means
		F	Sig.	Sig. (2-tailed)
Qmax***	Equal variances assumed	28.179	.000	.000000
	Equal variances not assumed			.000001
Qave***	Equal variances assumed	21.360	.000	.000214
	Equal variances not assumed			.000369
Volume voided*	Equal variances assumed	4.772	.030	.031891
	Equal variances not assumed			.035861
Up time/Down time	Equal variances assumed	3.176	.076	.094469
	Equal variances not assumed			.108492
Flow time	Equal variances assumed	3.956	.048	.147165
	Equal variances not assumed			.139004
Void time	Equal variances assumed	.526	.469	.732268
	Equal variances not assumed			.727908
Flow time/Void time**	Equal variances assumed	7.318	.007	.007536
	Equal variances not assumed			.008848
Flow index	Equal variances assumed	2.876	.091	.013164
(Qave/Qmax)*	Equal variances not assumed			.013951
Mean rate in raising	Equal variances assumed	29.212	.000	.001533
part**	Equal variances not assumed			.002316
Mean rate in falling	Equal variances assumed	15.867	.000	.001284
part**	Equal variances not assumed			.001824
Ratio of mean	Equal variances assumed	3.153	.077	.506409
up/down	Equal variances not assumed			.507293
DeltaQ***	Equal variances assumed	25.049	.000	.000001

	Equal variances not assumed			.000004
Qmax 0.5Hz***	Equal variances assumed	36.418	.000	.000000
	Equal variances not assumed			.000000
Qave 0.5Hz***	Equal variances assumed	21.379	.000	.000214
	Equal variances not assumed			.000368
Ut/Dt 0.5Hz	Equal variances assumed	.193	.661	.691543
	Equal variances not assumed			.683390
Qave/Qmax 0.5Hz**	Equal variances assumed	4.126	.043	.001658
	Equal variances not assumed			.001887
meanUFRupward	Equal variances assumed	33.967	.000	.000606
0.5Hz**	Equal variances not assumed			.001003
meanUFRdownward	Equal variances assumed	18.069	.000	.001935
0.5Hz**	Equal variances not assumed			.002728
FI0.5Hz	Equal variances assumed	9.368	.002	.138930
	Equal variances not assumed			.148217
DeltaQ0.5Hz***	Equal variances assumed	34.242	.000	.000000
	Equal variances not assumed			.000000
Qmax2sec***	Equal variances assumed	37.834	.000	.000000
	Equal variances not assumed			.000000
QaveTv2sec*	Equal variances assumed	13.783	.000	.010744
	Equal variances not assumed			.013874
QaveTf2sec**	Equal variances assumed	15.413	.000	.000994
	Equal variances not assumed			.001543
FI2sec	Equal variances assumed	4.627	.032	.060261
	Equal variances not assumed			.065149
Ut/Dt2sec	Equal variances assumed	2.125	.146	.320015
	Equal variances not assumed			.339513
DeltaQ2sec***	Equal variances assumed	19.147	.000	.000001
	Equal variances not assumed			.000001
MUP2sec***	Equal variances assumed	33.502	.000	.000545
	Equal variances not assumed			.000905
MDOWN2sec*	Equal variances assumed	14.437	.000	.017895
	Equal variances not assumed			.022054
RMU/D2sec	Equal variances assumed	6.087	.014	.220159
	Equal variances not assumed			.231284
TQmax	Equal variances assumed	.025	.874	.330627
	Equal variances not assumed			.324261
TQmax2sec	Equal variances assumed	11.489	.352	.708233
	Equal variances not assumed			.700704
TQmax/Tv**	Equal variances assumed	3.674	.056	.005938
	Equal variances not assumed			.006338

TQmax2sec/Tv**	Equal variances assumed	2.792	.025	.008484
	Equal variances not assumed			.009228

From table 6.2 and 6.3, the variables Qmax, Qave, DeltaQ have a *p* value less than 0.001 in raw curve and filtered curves, mean flow rate in rising slope and falling slope also have a *p* value less than 0.01 in raw and filtered curves. The *p* value for Q_{max} and DeltaQ are similar with Lee et al.'s findings (2016), though mean value and standard deviation (SD) of Q_{max} in each diagnostic group is significantly different comparing with their findings. In this study's database, BOO and DU have 2 seconds window filtered Q_{max} with mean value ± SD of 8.23 ± 3.54 and11.51 ± 6.44 respectively, on the contrary, in Lee's data, the mean value of Q_{max} in BOO group is higher than in DU group in their database.

The volume voided shows significantly statistical difference between two groups, which not surprisingly has statistically significant linear relationships with Q_{max} (p<0.001), mean flow rate in rising part (p<0.001) and mean flow rate in the falling part (p<0.001). The ratio of T_f against T_v is lower in DU group compared to the BOO group and has statistically significant difference, which indicates that DU patients may have a higher chance of performing an intermittent flow shape than BOO patients.

Q_{ave} has limited reports in the literature that it could discriminate DU from BOO, and indeed in this study the Q_{ave} in raw curve and 2 seconds window filtered curve have statisticaly significant difference between two groups. Moreover, in two seconds filtered curve Q_{ave} by flow time has better statistical difference than Q_{ave} by voiding time, which may be worth further research in different cohorts.

The ratio of time to Q_{max} against voiding time in 2 seconds window filtered curve variable has significantly statistical difference between two groups with a *p* value of less than 0.01, for which mean value in DU group is higher than in BOO group (0.34±0.20 vs 0.28±0.17). This result indicates that the shape of DU flow curve may show a different pattern than BOO flow curve, as reported by Abrams and others, which is verified in the flow shape template analysis.

There are a number of parameters showing statistically significant differences between DU and BOO groups, which thus hold promise to differentiate DU from BOO non-

invasively and will be employed for developing statistical models, combined with parameters having significant statistically difference in group 2.

6.2.2 Parameters derived by complex mathematical calculation of raw UFR data

The parameters derived by complex mathematical calculation may not be as easy to generate compared to uroflowmetry parameters, but these parameters could further improve the diagnosing accuracy if they have significantly statistical difference to discriminate DU from BOO.

The parameters in this group are defined as in table 6.4.

Table 6.4 parameters in group 2 and their definitions

Parameters	Definitions
T1	Time constant value on rising part in raw curve
T2	time constant value on falling part in raw curve
T1/T2	Ratio of T1 against T2 in raw curve
TC1 0.5Hz	Time constant value on rising part in 0.5Hz filtered curve
TC2 0.5Hz	Time constant value on falling part in 0.5Hz filtered curve
ratio of TC1/2 0.5Hz	Ratio of time constant value in 0.5Hz filtered curve
TC1 0.1Hz	Time constant value on rising part in 0.1Hz filtered curve
TC2 0.1Hz	Time constant value on falling part in 0.1Hz filtered curve
ratio TC1/2 0.1Hz	Ratio of time constant value in 0.1Hz filtered curve
TC12sec	Time constant value on rising part in 2sec window filtered curve
TC22sec	Time constant value on falling part in 2sec window filtered curve
RTC1/22sec	Ratio of time constant value in 2sec window filtered curve
Normalised TC2	Time constant value on falling part in normalised 2sec filtered flow curve
Peak counting ratio 1Hz/0.1Hz	Ratio of peak numbers in 0.1Hz against 1Hz filtered curve
Peak counting ratio raw/0.1Hz	Ratio of peak numbers in raw against 1Hz filtered curve
0.1-1 MPF whole flow	MPF in 0.1Hz-1Hz filtered curve
0.1-1 MPF first half volume	MPF in 0.1Hz-1Hz first half VV part of raw curve
0.1-1 MPF 1st/2nd Qmax	Ratio of MPF in 0.1Hz-1Hz 1st against 2nd half part divided by Q_{max}
0.1-1 MPF first half T	MPF in 0.1Hz-1Hz first half Tv part
0.1-1 MPF whole/2nd Qmax	Ratio of MPF in 0.1Hz-1Hz whole against 2nd Q_{max} half part
0.2-0.9 MPF whole flow	MPF in 0.2Hz-0.9Hz in whole curve
0.2-0.9 MF first half Volumes	MPF in 0.2Hz-0.9Hz in first half VV part
0.1-0.7 MPF whole flow	MPF in 0.1Hz-0.7Hz filtered curve

0.1-0.8 MPF whole flow	MPF in 0.1Hz-0.8Hz filtered curve
0.1-0.9 MPF whole flow	MPF in 0.1Hz-0.9Hz filtered curve
0.1-0.9 MPF 1st/2nd Qmax	Ratio of MPF in 0.1Hz-0.9Hz 1st against 2nd half part divided by Q_{max}
0.2-0.7 MPF first half volume	MPF in 0.2Hz-0.7Hz in first half VV part
0.2-0.8 MPF whole flow	MPF in 0.2Hz-0.8Hz in whole curve
0.2-0.8 MPF first half volume	MPF in 0.2Hz-0.8Hz in first half VV part
0.2-1 MPF whole flow	MPF in 0.2Hz-1Hz in whole curve
0.2-1 MPF first half volume	MPF in 0.2Hz-1Hz in first half VV part
Peak2sec	peak numbers in 2sec filtered curve
Peakraw	peak numbers in raw curve
peak0.5Hz	peak numbers in 0.5Hz filtered curve
peak1Hz	peak numbers in 1Hz filtered curve
peak0.1Hz	peak numbers in 0.1Hz filtered curve
2sec/0.1	Ratio of peak numbers in 2sec against in 0.1Hz filtered curve
0.5/0.1	Ratio of peak numbers in 0.5Hz against in 0.1Hz filtered curve
Amplitude change in raising slope	SAC value in 0.1Hz-1Hz filtered curve
Amp change/Qmax	SAC against Q_{max} in raw curve
Amp change/VV	SAC against VV

The descriptive statistical analysis result of derived parameters in group 2 is presented in table 6.5. Column DU is the group variable in which 1 stands for DU and 0 stands for BOO.

Table 6.5 Statistics of parameters in group 2

	DU	N	Mean	Std. Deviation
T1	1	135	600.50	8183.16
	0	158	255.54	5515.51
T2	1	135	145.27	122.79
	0	158	171.61	145.70
T1/T2	1	135	4.64	63.25
	0	158	3.32	68.64
TC1 0.5Hz	1	135	-71.70	1023.93
	0	158	-10.58	745.67
TC2 0.5Hz	1	135	102.68	98.78
	0	158	133.27	122.52
ratio of TC1/2 0.5Hz	1	135	-1.89	20.40
	0	158	.70	6.16

TC1 0.1Hz	1	135	47.59	369.55
	0	158	76.59	342.43
TC2 0.1Hz	1	135	155.08	130.88
	0	158	181.40	153.82
ratio TC1/2 0.1Hz	1	135	.09	4.26
	0	158	.47	2.64
TC12sec	1	135	15.35	746.57
	0	158	166.38	2222.06
TC22sec	1	135	157.40	111.51
	0	158	183.84	118.40
RTC1/22sec	1	135	-.21	8.17
	0	158	3.45	45.60
Normalised TC2	1	135	327.86	199.20
	0	158	396.16	174.14
Peak counting ratio	1	135	8.63	3.73
1Hz/0.1Hz	0	158	11.08	5.42
Peak counting ratio	1	135	16.22	8.14
raw/0.1Hz	0	158	20.87	10.33
0.1-1 MPF whole flow	1	135	.43	.10
	0	158	.49	.10
0.1-1 MPF first half volume	1	135	.39	.16
	0	158	.46	.19
0.1-1 MPF 1st/2nd Qmax	1	135	1.35	.56
	0	158	1.61	.69
0.1-1 MPF first half T	1	135	.47	.14
	0	158	.53	.14
0.1-1 MPF whole/2nd Qmax	1	135	.83	.26
	0	158	.97	.30
0.2-0.9 MPF whole flow	1	135	.50	.08
	0	158	.55	.07
0.2-0.9 MF first half Volumes	1	135	.46	.12
	0	158	.53	.14
0.1-0.7 MPF whole flow	1	135	.34	.07
	0	158	.39	.08
0.1-0.8 MPF whole flow	1	135	.37	.08
	0	158	.42	.09
0.1-0.9 MPF whole flow	1	135	.40	.09
	0	158	.47	.10
0.1-0.9 MPF 1st/2nd Qmax	1	135	1.06	.54
	0	158	1.26	.60
0.2-0.7 MF first half Volumes	1	135	.37	.08

	0	158	.40	.08
0.2-0.7 MPF first half volume	1	135	.47	.09
	0	158	.53	.10
0.2-0.8 MPF whole flow	1	135	.47	.07
	0	158	.52	.07
0.2-0.8 MPF first half volume	1	135	.51	.10
	0	158	.58	.12
0.2-1 MPF whole flow	1	135	.53	.09
	0	158	.59	.08
0.2-1 MPF first half volume	1	135	.57	.12
	0	158	.66	.14
Peak2sec	1	135	11.72	9.52
	0	158	15.86	15.60
Peakraw	1	135	37.84	24.52
	0	158	46.46	37.22
peak0.5Hz	1	135	10.81	7.26
	0	158	11.86	9.55
peak1Hz	1	135	20.18	12.30
	0	158	24.03	18.79
peak0.1Hz	1	135	2.47	1.73
	0	158	2.37	2.15
2sec/0.1	1	135	5.13	3.76
	0	158	7.32	4.75
0.5/0.1	1	135	4.84	2.62
	0	158	5.76	2.89
Amplitude change in raising	1	135	25.72	18.77
slope	0	158	18.35	15.70
Amp change/Qmax	1	135	2.13	1.55
	0	158	1.96	1.40
Amp change/VV	1	135	.17	.11
	0	158	.15	.16

The t test result for group 2 parameters is presented as in table 6.6. The parameters which have statistically significant difference with *p* value less than 0.05 are highlighted by *, *p* value less than 0.01 by ** and *p* value less than 0.001 by ***.

Table 6.6 t test result for group 2 parameters

	Levene's Test for Equality of Variances	t-test for Equality of Means

		F	Sig.	Sig. (2-tailed)
T1	Equal variances assumed	.799	.372	.668826
	Equal variances not assumed			.678006
T2	Equal variances assumed	2.126	.146	.098631
	Equal variances not assumed			.094207
T1/T2	Equal variances assumed	.091	.764	.864902
	Equal variances not assumed			.864040
TC1 0.5Hz	Equal variances assumed	.809	.369	.556034
	Equal variances not assumed			.565597
TC2 0.5Hz*	Equal variances assumed	2.064	.152	.020707
	Equal variances not assumed			.018680
ratio of TC1/2 0.5Hz	Equal variances assumed	4.487	.035	.129688
	Equal variances not assumed			.156751
TC1 0.1Hz	Equal variances assumed	.394	.531	.486630
	Equal variances not assumed			.489265
TC2 0.1Hz	Equal variances assumed	1.781	.183	.119311
	Equal variances not assumed			.114714
ratio TC1/2 0.1Hz	Equal variances assumed	3.044	.082	.348962
	Equal variances not assumed			.366034
TC12sec	Equal variances assumed	.650	.421	.451443
	Equal variances not assumed			.422973
TC22sec	Equal variances assumed	.765	.382	.051323
	Equal variances not assumed			.050248
RTC1/22sec	Equal variances assumed	1.525	.218	.359005
	Equal variances not assumed			.323952
Normalised TC2**	Equal variances assumed	1.843	.176	.001915
	Equal variances not assumed			.002149
Peak counting ratio	Equal variances assumed	17.976	.000	.000013
1Hz/0.1Hz***	Equal variances not assumed			.000007
Peak counting ratio	Equal variances assumed	7.154	.008	.000031
raw/0.1Hz***	Equal variances not assumed			.000023
0.1-1 MPF whole	Equal variances assumed	.218	.641	.000000
flow***	Equal variances not assumed			.000000
0.1-1 MPF first half	Equal variances assumed	4.003	.046	.002402
volume**	Equal variances not assumed			.002117
0.1-1 MPF 1st/2nd	Equal variances assumed	3.541	.061	.000481
Qmax***	Equal variances not assumed			.000386
0.1-1 MPF first half	Equal variances assumed	.066	.797	.000035
T***	Equal variances not assumed			.000036
0.1-1 MPF whole/2nd	Equal variances assumed	2.975	.086	.000024

Qmax***	Equal variances not assumed			.000019
0.2-0.9 MPF whole	Equal variances assumed	.295	.587	.000001
flow***	Equal variances not assumed			.000001
0.2-0.9 MF first half	Equal variances assumed	2.931	.088	.000010
Volumes***	Equal variances not assumed			.000008
0.1-0.7 MPF whole	Equal variances assumed	.526	.469	.000003
flow***	Equal variances not assumed			.000002
0.1-0.8 MPF whole	Equal variances assumed	.823	.365	.000000
flow***	Equal variances not assumed			.000000
0.1-0.9 MPF whole	Equal variances assumed	.397	.529	.000000
flow***	Equal variances not assumed			.000000
0.1-0.9 MPF 1st/2nd	Equal variances assumed	1.316	.252	.004052
Qmax**	Equal variances not assumed			.003792
0.2-0.7 MF first half	Equal variances assumed	.001	.979	.003938
Volumes**	Equal variances not assumed			.004034
0.2-0.7 MPF first half	Equal variances assumed	.708	.401	.000001
volume***	Equal variances not assumed			.000001
0.2-0.8 MPF whole	Equal variances assumed	.346	.557	.000001
flow***	Equal variances not assumed			.000001
0.2-0.8 MPF first half	Equal variances assumed	2.185	.140	.000000
volume***	Equal variances not assumed			.000000
0.2-1 MPF whole	Equal variances assumed	.442	.507	.000000
flow***	Equal variances not assumed			.000000
0.2-1 MPF first half	Equal variances assumed	1.801	.181	.000000
volume***	Equal variances not assumed			.000000
Peak2sec**	Equal variances assumed	11.409	.001	.007640
	Equal variances not assumed			.005742
Peakraw*	Equal variances assumed	7.741	.006	.022294
	Equal variances not assumed			.018472
peak0.5Hz	Equal variances assumed	2.331	.128	.295267
	Equal variances not assumed			.285137
peak1Hz*	Equal variances assumed	6.459	.012	.042375
	Equal variances not assumed			.036291
peak0.1Hz	Equal variances assumed	1.389	.240	.685978
	Equal variances not assumed			.680992
2sec/0.1***	Equal variances assumed	10.627	.001	.000021
	Equal variances not assumed			.000015
0.5/0.1**	Equal variances assumed	5.651	.018	.004842
	Equal variances not assumed			.004524
Amplitude change in	Equal variances assumed	6.325	.012	.000303
raising slope***	Equal variances not assumed			.000371

Amp change/Qmax	Equal variances assumed	.689	.407	.328993
	Equal variances not assumed			.332802
Amp change/VV	Equal variances assumed	.021	.885	.166333
	Equal variances not assumed			.153331

From tables 6.5 and 6.6, the results of time constant value analysis only show statistically significant difference between two groups in the falling part of raw curve with a *p* value of 0.018. The normalised TC2 variable derived in falling part of normalised flow curves, which has statistically significantly difference between two groups with a *p* value of 0.002. This result verifies the finding in the flow template analysis that the major difference in shape between DU and BOO happens in the falling part, and it provides improvement of accuracy to discriminate between DU and BOO.

For a graphical inspection, one parameter from each analytical method with highest statistical difference is presented as boxplots in appendix VI. The parameters included are Qmax2sec, mean rate in falling part, DeltaQ2sec, MUP2sec, TQmax/Tv, Peak counting ratio 1Hz/0.1Hz, 0.1-1 MPF whole flow and amplitude change in raising slope.

The MPF variables hold promise to differentiate DU form BOO non-invasively, however the result is contrary to the hypothesis, which show the mean value of median power frequency in 0.1Hz to 1Hz filtered curve in BOO group is higher than in DU group, with mean value ± SD of 0.43±0.1 and 0.49±0.1 for DU and BOO groups respectively.

The peak numbers in raw, 1Hz, 2sec window, 0.5Hz and 0.1Hz filtered curve individually have limited statistical difference between two groups, however the ratio of peak numbers in raw/0.1Hz, 2sec/0.1Hz and 1Hz/0.1Hz have much stronger statistical difference. It can be seen in the table 6.5 that the mean values of peak numbers in DU group in raw, 1Hz filtered and 2 seconds window filtered curves are greater than in BOO group, but are lower in 0.1Hz filtered curve. This could be because DU patients could not sustain a reasonable detrusor contraction and therefore perform multiple contractions of relatively short duration each and/or abdominal straining. Considering the MPF analysis result that DU has lower mean value of MPF than BOO, we hypothesise that DU patient may contract the detrusor more often than BOO patient. However, this is only in hypothesis and needs to be verified with PFS.

Sum of amplitude changes in rising slope shows statistically significant difference between two groups, and not surprisingly this variable has a linear correlation with Q_{max} and volume voided with *p* values less than 0.001.

The parameters which have statistically significant difference are employed in generating statistical models, with the parameters mentioned in the group 1.

6.2.3 Parameter derived by flow template analysis

The flow template analysis shows that the shape difference could be a potential indicator for differentiating DU from BOO, but its usefulness needs further validation. The parameters derived from flow template analysis is defined as in table 6.7.

Table 6.7 Parameters derived from flow template analysis and definitions

Parameters	Definition
RES with DU in 0.5-98	Sum square errors comparing with DU template in normalised 0.5%-98% VV part
RES with BOO in 0.5-98	Sum square errors comparing with BOO template in normalised 0.5%-98% VV part
RES in 0.5-98	Ratio of two parameters above, DU/BOO
RES with DU in RAW	Sum square errors comparing with DU template in normalised raw curve
RES with BOO in RAW	Sum square errors comparing with BOO template in normalised raw curve
Ratio RES in raw	Ratio of two parameters above, DU/BOO
RES with DU in 2sec	Sum square errors comparing with DU template in 2sec filtered raw curve
RES with BOO in 2sec	Sum square errors comparing with BOO template in 2sec filtered raw curve
Ratio RES in 2sec	Ratio of two parameters above, DU/BOO
EUS with bell shape	Sum square errors comparing with bell shape in 2sec filtered raw curve

The intermittency detection result by the criteria stated in the chapter 3 section 4 is presented as in the table 6.8, in which 0 stands for non-intermittent curve and 1 stands for intermittent curve in the row below ‘intermittency’. It can be observed that intermittency prevalence of intermittency in DU group is 43.7% and in BOO group is 33.3%. This result verifies the hypothesis made in the peak counting analysis that DU patients have lower mean peak numbers in 0.1Hz filtered curve than BOO patients, due to more higher frequency strain peaks being filtered out.

Table 6.8 DU * Intermittency Crosstabulation

Count

		Intermittency		
		0	1	Total
DU	0	107	51	158
	1	76	59	135
Total		183	110	293

The statistics result of proposed parameters in the non-intermittent curves are presented in the table 6.9, in which 1 stands for DU and 0 stands for BOO in column 'DU' respectively.

Table 6.9 Parameters derived in non-intermittency curve by shape template analysis

	DU	N	Mean	Std. Deviation
RES with DU in 0.5-98	1	76	80.22	57.64
	0	107	71.11	52.27
RES with BOO in 0.5-98	1	76	71.88	53.73
	0	107	42.69	37.31
Ratio RES in 0.5-98	1	76	1.50	1.15
	0	107	2.15	1.54
RES with DU in RAW	1	76	181.55	112.15
	0	107	168.41	98.94
RES with BOO in RAW	1	76	135.14	89.71
	0	107	110.68	79.59
Ratio RES in raw	1	76	1.40	.36
	0	107	1.65	.31
RES with DU in 2sec	1	76	136.15	99.39
	0	107	118.70	84.22
RES with BOO in 2sec	1	76	96.91	77.82
	0	107	68.25	58.90
Ratio RES in 2sec	1	76	1.51	.56
	0	107	1.97	.62
EUS with bell shape	1	76	112.38	87.57
	0	107	122.74	85.00

It can be witnessed that DU data have higher mean value of sum of square errors comparing with DU template than BOO data, which is because DU flow shape varies

and Q_{max} could appear anywhere from the very beginning of the flow curve to very end of the flow curve. However when comparing DU and BOO data with BOO template, the mean value of square errors is much smaller in BOO group in normalised raw curve, 2 seconds filtered curve and 0.5% to 98% volume voided part in 2 seconds filtered curve. The *t* test result for these parameters in non-intermittent curve is presented as in table 6.10. The parameters having statistically significant difference with *p* value less than 0.05 is marked a *, *p* value less than 0.01 is marked a ** and *p* value less than 0.001 is marked a ***.

Table 6.10 *t* test result for shape template analysis in non-intermittent curve

		Levene's Test for Equality of Variances		t-test for Equality of Means
		F	Sig.	Sig. (2-tailed)
RES with DU in 0.5-98	Equal variances assumed	.556	.457	.267585
	Equal variances not assumed			.275796
RES with BOO in 0.5-98***	Equal variances assumed	8.741	.004	.000024
	Equal variances not assumed			.000077
Ratio RES in 0.5-98**	Equal variances assumed	.943	.333	.002090
	Equal variances not assumed			.001264
RES with DU in RAW	Equal variances assumed	1.234	.268	.403505
	Equal variances not assumed			.413673
RES with BOO in RAW	Equal variances assumed	1.400	.238	.053606
	Equal variances not assumed			.058880
Ratio RES in raw***	Equal variances assumed	.181	.671	.000002
	Equal variances not assumed			.000004
RES with DU in 2sec	Equal variances assumed	1.155	.284	.202009
	Equal variances not assumed			.215084
RES with BOO in 2sec**	Equal variances assumed	3.590	.060	.005090
	Equal variances not assumed			.007669
Ratio RES in	Equal variances assumed	.017	.897	.000001

2sec***	Equal variances not assumed			.000001
EUS with bell shape	Equal variances assumed	.014	.905	.423194
	Equal variances not assumed			.425687

in which the mean values of sum of square errors in three groups do not have significant statistical difference when comparing non-intermittent data with DU template. However when compared with the BOO template, sum of square errors have statistical difference in 0.5% to 98% volume voided part and in 2 second filtered curve with *p* value of 0.01. The most significant statistically difference is found in the ratio of sum square errors in two seconds filtered data with a *p* value of 0.000001. The AUC value in the ROC test is 0.719 with optimised sensitivity and specificity of 70% and 60% respectively.

The analytical results show that the flow shape template hold promise to differentiate DU from BOO, but it only works on the non-intermittent curves. Therefore the parameters derived by shape template analysis are not included in the statistical models generating, though they still could serve as an additional indicator for discriminating DU from BOO non-invasively.

6.2.4 Area under curve analysis and optimised sensitivity/specificity for parameters proposed in group 1 and 2

The t test result presented in 6.2.1 and 6.2.2 verifies that a number of derived parameters hold promise to differentiate DU from BOO, and their individual usefulness is analysed in the ROC analysis in this section. One parameter from each analytical method with highest statistical difference is presented in ROC curve, showing the AUC value and optimised sensitivity/specificity. The parameters included are Qmax2sec, mean rate in falling part, DeltaQ2sec, MUP2sec, TQmax/Tv, Peak counting ratio 1Hz/0.1Hz, Normalised TC2, 0.1-1 MPF whole flow and amplitude change in raising slope. The ROC curve for these selected parameters are presented as in figure 6.1 and 6.2.

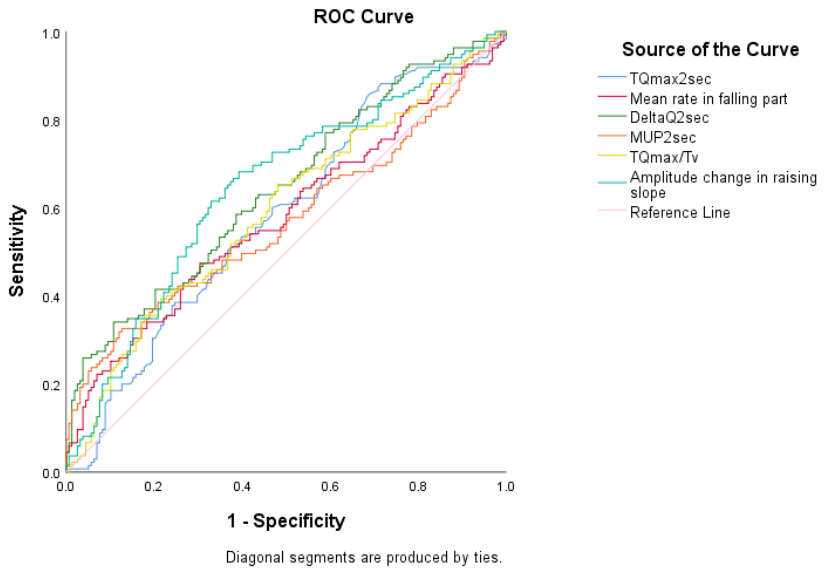

Figure 6.1 ROC curve for 7 proposed parameters which greater value indicates positive classification

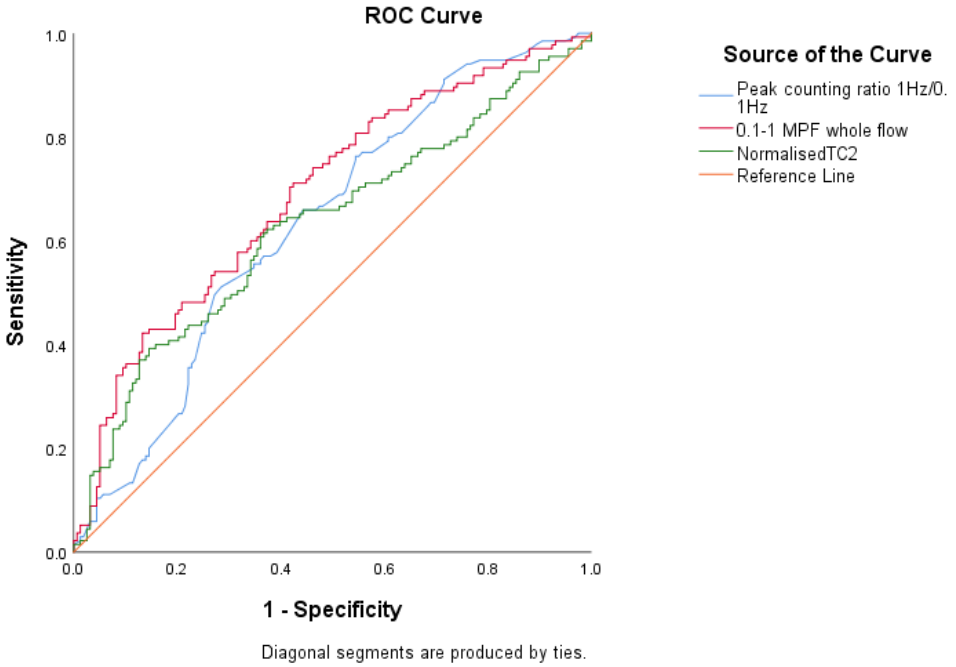

Figure 6.2 ROC curve for 3 proposed parameters which smaller value indicates positive classification

Their AUC values and optimised sensitivity and specificity are presented as in table 6.11.

Table 6.11 Area under curve value and sensitivity and specificity

Test Result Variable(s)	AUC value	Sensitivity	Specificity
TQmax2sec	0.583	86%	31%
Mean rate in falling part	0.581	47%	70%

DeltaQ2sec	0.644	34%	89%
MUP2sec	0.571	33%	81%
TQmax/Tv	0.594	36%	82%
Amplitude change in raising slope	0.645	68%	60%
Peak counting ratio 1Hz/0.1Hz	0.634	51%	72%
0.1-1 MPF whole flow	0.690	42%	87%
NormalisedTC2	0.629	62%	63%

The largest AUC value is provided by the parameter of 0.1-1 MPF whole flow with 42% sensitivity and 87% specificity, followed by amplitude change in raising slope and DeltaQ2sec. Though each of parameters has statistically significant difference between the two groups, they individually still cannot differentiate DU from BOO. Therefore the statistical models are developed in next section to test if the combined parameters could serve as a more powerful indicator for discriminating DU with BOO.

6.3 Statistical models and their diagnostic utility

Based on the statistical analysis result in last section, 49 parameters which have significant statistical difference between two groups are employed in the CART and neural network analysis. 3 variables, DeltaQ in raw curve and 0.5Hz/2sec filtered curve, have linear relationship with Q_{max} and Q_{ave}, are excluded in MANOVA analysis. A total of 46 parameters are employed in MANOVA analysis to generate a linear combination 'super' parameter which could maximise diagnosing accuracy.

6.3.1 Statistical model of MANOVA

The statistics for generated MANOVA variable are presented as in table 6.12, and *t* test result is presented in table 6.13.

Table 6.12 MANOVA variable statistics

	DU	N	Mean	Std. Deviation
MANOVA variable	1	135	6.26	1.08
	0	158	8.01	.92

Table 6.13 t test result of MANOVA variable

		Levene's Test for Equality of Variances		t-test for Equality of Means
		F	Sig.	Sig. (2-tailed)
MANOVA variable	Equal variances assumed	3.004	.084	.000
	Equal variances not assumed			.000

where the *p* value of MANOVA variable between two groups is $1.2*10^{-37}$. This results shows promise to differentiate DU from BOO non-invasively, but its diagnostic utility need to be further investigated. The ROC curve is presented as in figure 6.3.

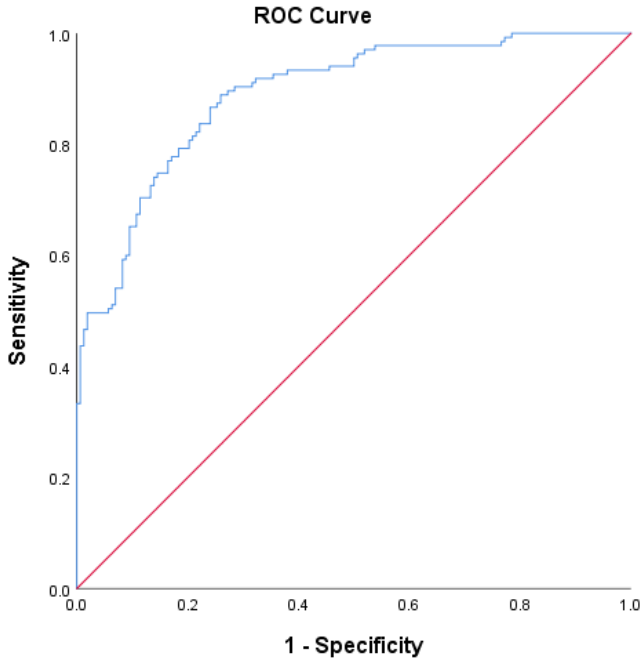

Figure 6.3 ROC curve of MANOVA variable

The AUC value of MANOVA variable is 0.89, with optimised sensitivity of 89% and specificity of 74% at the cut-off value of 7.37. However the MANOVA does not support cross validation. Therefore the robustness of MANOVA method is tested by discriminant analysis, which performs a similar algorithm that linearly combines parameters into a new variable with an binary output of 1 and 0. The cross validation

result is presented in the table 6.14.

Table 6.14 Cross validation using discriminant analysis

			Predicted Group Membership		
		DU	0	1	Total
Original	Count	0	130	28	158
		1	26	109	135
	%	0	82.3	17.7	100.0
		1	19.3	80.7	100.0
Cross-validated[b]	Count	0	117	41	158
		1	36	99	135
	%	0	74.1	25.9	100.0
		1	26.7	73.3	100.0

a. 81.6% of original grouped cases correctly classified.

b. Cross validation is done only for those cases in the analysis. In cross validation, each case is classified by the functions derived from all cases other than that case.

c. 73.7% of cross-validated grouped cases correctly classified.

The cross validation results in a 73.7% of accuracy comparing to testing result of 81.6% classified accuracy. A less than 10% classification difference shows the MANOVA result is robust.

The MANOVA variable could additionally serve as a preliminary test for screening out a part of DU patients who are definitely not diagnosed as BOO. For instance, a cut-off value of 5.78 provides 33% sensitivity and 100% specificity, which means 33 out of 100 DU patients could be securely predicted and do not need to go through uncomfortable PFS. On the contrary, a cut-off value of 8.79 provides 100% sensitivity and 21% specificity, that 21 out of 100 BOO patients could be accurately predicted and need to further investigate if they need an immediate surgery with PFS.

The MANOVA variable could be potentially used as a score test to evaluate the likelihood of DU/BOO. The higher score in MANOVA, the higher chance of suffering BOO, and vice versa. The patients with middle scores may need to go through PFS for an accurate diagnosis. However the MANOVA variable needs a large database to secure a higher robustness, and the coefficients need to be updated accordingly when a new UFR data analysed with confirmed diagnosis.

6.3.2 Statistical model of CART

With 49 parameters inputted to generate the classification and regression tree, the data was split into 70% of training and 30% of testing. Considering that there are 207 data in the training start node, the tree maximum tree depth is set to 3, minimum cases in parent nodes set to 20 and in child node set to 7. The training CART model is presented as in figure 6.4 and testing in figure 6.5.

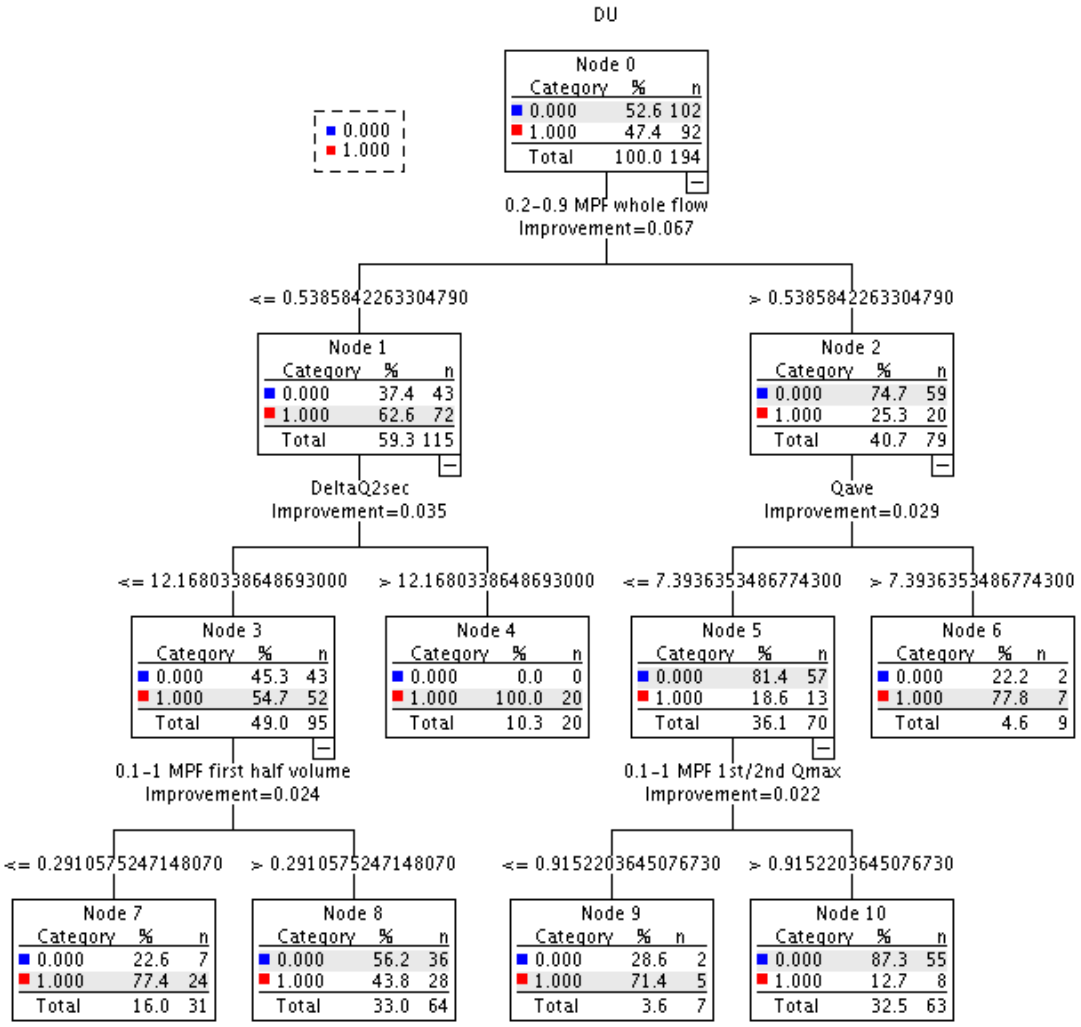

Figure 6.4 Training CART model with 70% of data

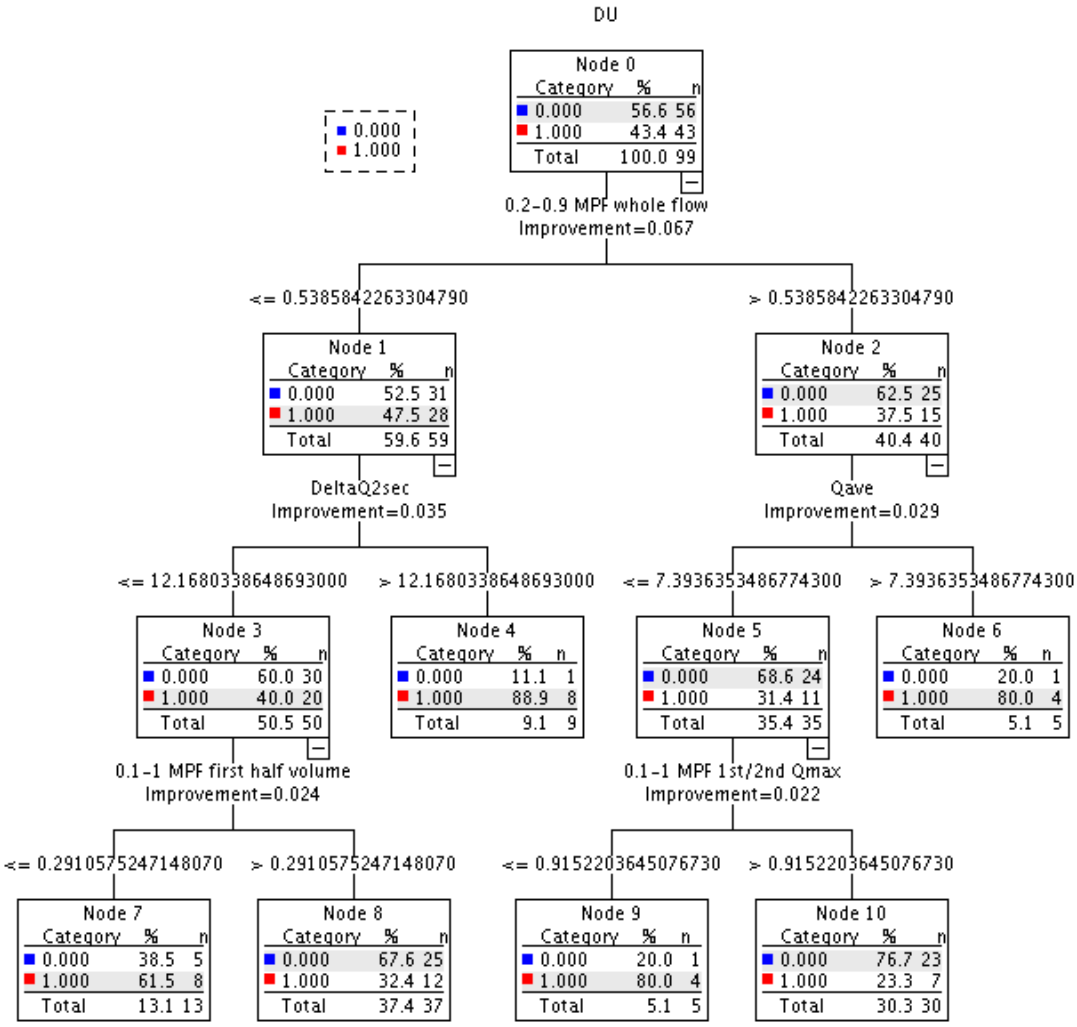

Figure 6.5 Testing CART model with 30% of data

The classification and verification table is presented as in table 6.15.

Table 6.15 Classification and verification table

		Predicted		
Sample	Observed	0	1	Percent Correct
Training	0	91	11	89.2%
	1	36	56	60.9%
	Overall Percentage	65.5%	34.5%	75.8%
Test	0	48	8	85.7%
	1	19	24	55.8%
	Overall Percentage	67.7%	32.3%	72.7%

Growing Method: CRT
Dependent Variable: DU

The difference of percent correct between training and testing is 3% which shows the robustness of the built-up CART model. The most promising finding is in training level 2 node 4 there are 20 DU patients has been classified in a pure group, with 0 of BOO, but in testing the same node has 8 DU patients mixed with 1 BOO patient.

The CART could indicate a higher chance of either BOO or DU when the data is classified into a child node, but it could not make a clear suggestion for differentiating DU from BOO, since the child node normally contains data from both diagnostic groups. However the 74% overall diagnosing accuracy is an improvement compared to use individual parameter to discriminate DU with BOO.

It should be noted that CART model has lower robustness than MANOVA model, as at each node decision only one parameter is employed, though the algorithm guarantees the most accuracy decisions are made in every growing node. The robustness of MANOVA model is based on its multiple parameters, the final predicted result will not be much affected when a few parameters failed to discriminate DU with BOO in some special cases. However if a larger scale of database applied, CART model has potential to be further grown into a greater number of layers, and may have a much improved diagnosing accuracy, though the training and testing procedures are even more time consuming.

6.3.3 Artificial Neural network model

In the artificial neural network (ANN) model, all proposed parameters have been employed for generating a robust model. 293 data are divided into three group: 70% for training, 15% for validation and 15% for testing the model. To avoid over fitting, a simple feed forward neural network with 1 hidden layer is designed. The choice of hidden neurons numbers is by using five-fold cross validation on overall accuracy.

The number of hidden neurons is normally between input number and output number, but could go up to twice as input number. In this study the input parameters are 49 and output number is 1, therefore the hidden neurons number test starts from 25 and end at 55. For this, the highest accuracy in five-fold cross validation is employed. The five-fold cross validation result is presented as in table 6.16.

Table 6.16 five-fold cross validation result

Neurons	First	Second	Third	Fourth	Fifth	Overall
25	75.1%	74.7%	77.8%	73.7%	72.4%	74.7%
26	71.7%	73.4%	77.8%	74.4%	77.1%	74.9%
27	75.4%	77.5%	74.1%	74.7%	71.7%	74.7%
28	76.5%	74.4%	75.1%	79.5%	76.5%	76.4%
29	80.5%	76.1%	73.4%	74.4%	80.2%	76.9%
30	77.8%	73.0%	75.8%	69.3%	74.7%	74.1%
31	73.7%	72.4%	77.1%	70.3%	75.8%	73.9%
32	74.4%	74.1%	75.4%	76.8%	75.8%	75.3%
33	78.5%	78.5%	73.0%	74.4%	70.0%	74.9%
34	73.7%	76.1%	74.7%	70.0%	69.6%	72.8%
35	75.8%	79.5%	74.1%	77.5%	76.5%	76.7%
36	74.1%	79.2%	77.8%	74.1%	70.6%	75.2%
37	73.7%	76.5%	75.1%	81.6%	69.6%	75.3%
38	81.6%	79.2%	75.4%	73.4%	75.4%	77.0%
39	71.0%	75.1%	67.2%	68.9%	71.3%	70.7%
40	79.2%	74.1%	79.9%	75.1%	69.3%	75.5%
41	78.5%	75.8%	71.3%	79.2%	73.7%	75.7%
42	76.5%	74.1%	68.3%	74.7%	69.3%	72.6%
43	75.4%	75.1%	73.4%	80.2%	75.8%	76.0%
44	77.5%	75.1%	70.3%	73.0%	76.5%	74.5%
45	75.4%	71.0%	77.1%	71.3%	72.7%	73.5%
46	77.5%	78.2%	80.2%	76.8%	75.4%	77.6%
47	77.8%	75.8%	72.4%	74.7%	77.5%	75.6%
48	73.0%	72.4%	75.4%	75.1%	78.5%	74.9%
49	78.2%	72.0%	73.7%	81.9%	76.8%	76.5%
50	68.9%	76.5%	74.4%	81.9%	80.5%	76.4%
51	77.1%	73.0%	75.8%	65.9%	76.1%	73.6%
52	72.0%	79.2%	70.3%	77.8%	79.5%	75.8%
53	75.1%	80.5%	78.2%	76.5%	79.5%	78.0%
54	69.6%	72.7%	77.1%	71.0%	75.1%	73.1%
55	77.5%	74.1%	72.4%	77.8%	73.4%	75.0%

It can be seen from table 6.16, in 30 times five-fold cross validation the overall accuracy does not vary a lot, in which the average accuracy is around 75%. The best accuracy in five-fold cross verification is in 53 neurons, therefore the neural network is designed with 1 hidden layer with 53 hidden neurons. The plots of ROC curve and confusion box are presented as in figure 6.6 and 6.7 respectively.

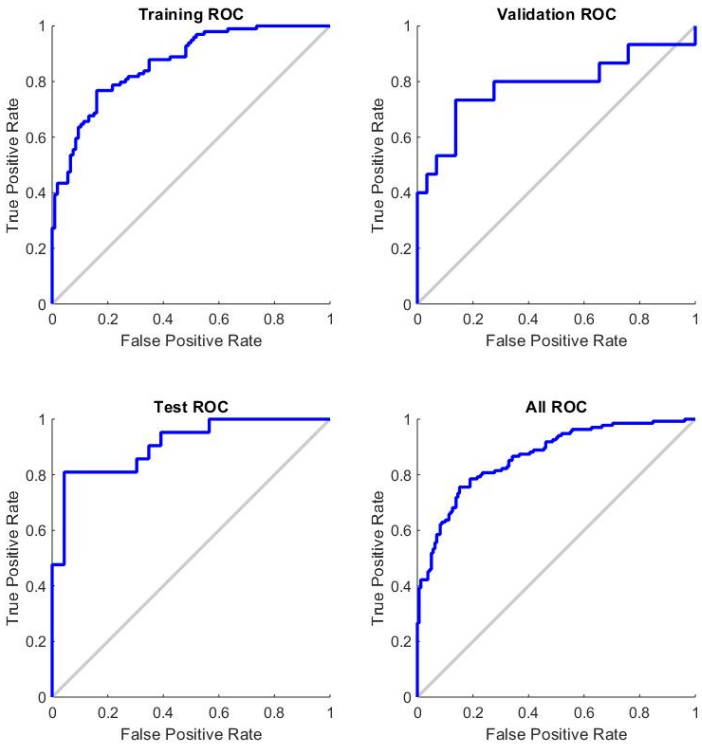

Figure 6.6 ROC curve of designed neural network

Figure 6.7 Confusion box of designed neural network

Designed neural network has overall sensitivity of 75.6%, and specificity of 82.9% with discrimination accuracy of 79.5%. This result shows a more robust model than MANOVA and CART model.

Another neural network model is built up to assess if the shape of flow could be a discriminator of DU with BOO by employing normalised UFR data in which each data is normalised with 1000 resample points and the maximum amplitude of 1 to represent the pure flow shape. In this analysis all UFR data are input in three groups in percentage of 70, 15, 15 for training, validation, testing respectively. Due to input number of 1000 variables, the five-fold cross validation is not presented. The final model has 1 hidden layer with 815 neurons, and its ROC curve and confusion box are presented as in figure 6.8 and 6.9 respectively.

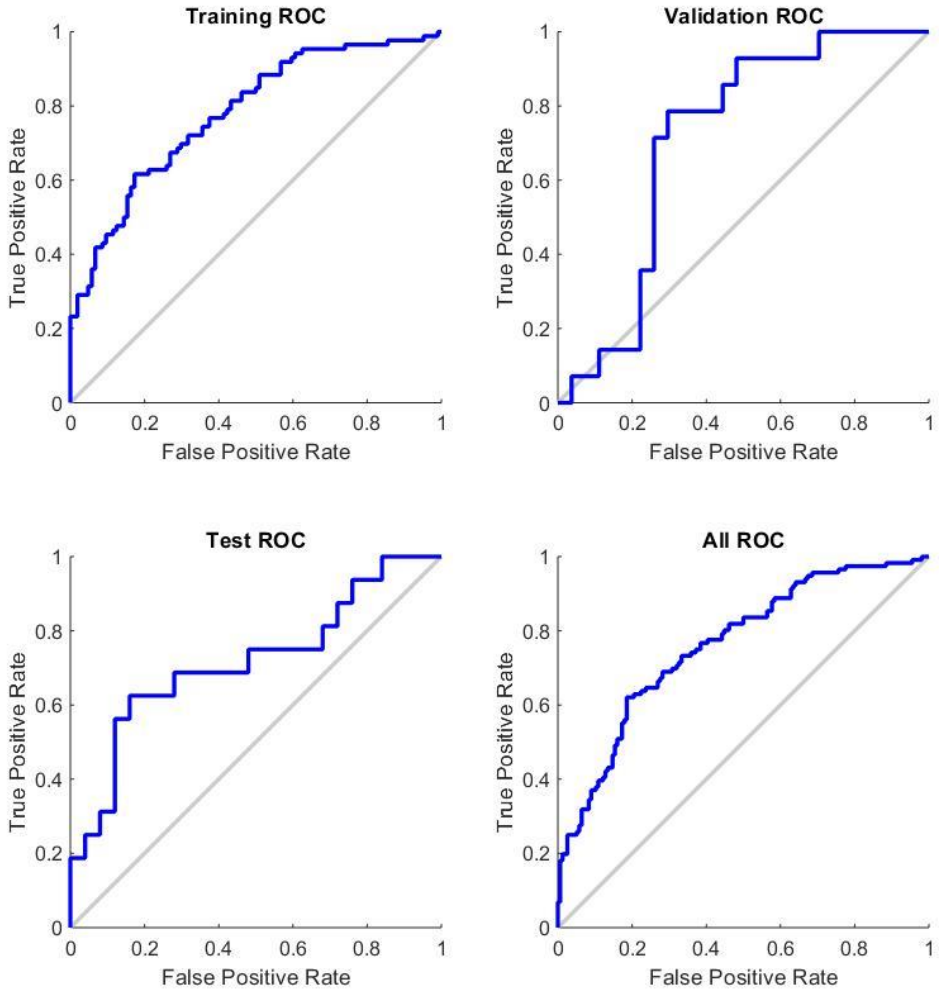

Figure 6.8 ROC curve of designed neural network for flow shape

Figure 6.9 confusion box of designed neural network for flow shape

The designed neural network has 54.3% sensitivity and 82.7% specificity to discriminate DU with BOO, with an overall accuracy of 70.6%. Though it is still poor accuracy compared with CART or MANOVA models, it has better accuracy than any non-invasive parameters alone and hold the promise to differentiate DU from BOO if a larger group of data is employed.

It should be noted that in this study neural network application is an initial exploration on its applicability to differentiate DU from BOO, in which the basic artificial neural network is designed and tested. There are other type of neural networks, such as convolutional neural network and recurrent neural network, and a number of different active functions available for a possible further research.

6.4 Summary

In this chapter, the proposed parameters have been statistically analysed and presented their diagnostic utility to differentiate DU from BOO. The novel indicators which proposed in this study, time constant variables, MPF variables, peak counting variables and flow template variables have statistically significant difference between two groups and hold the promise to serve as predictors to differentiate DU from BOO.

Three statistical models, MANOVA, CART and artificial neural network have been designed and tested to combine proposed parameters for maximising the diagnosing accuracy. All three models show an average of around 80% accuracy in discrimination DU with BOO, and are possible for a clinical trial.

Chapter 7 Conclusions and Future Research

7.1 Conclusions

The overall aim of this PhD research is to non-invasively differentiate DU from BOO, by using existing non-invasive parameters and combining them with derived parameters which have statistical difference between two groups. Moreover, we aim to establish a possible model which can combine the parameters for maximising discriminating accuracy.

In this study, the non-invasive diagnostic methods for diagnosing BOO/DU and differentiation DU from BOO are surveyed. The flow shape definition and their descriptors in literature are summarised and we make suggestions for a consistent use.

The UFR data are initially analysed in the time domain. To reduce the artefact a low-pass filter is designed and tested, then applied on the UFR data to derive peak numbers in different filtered curves. The modelling methods of flow curve is proposed, and we use Least Squares method to approximate the model, in which time constant value is derived and found to have significantly statistical difference in two groups. A novel study on the flow template is conducted, with shape template generated for each diagnostic group. It is also found that he normalised flow curve could improve the diagnostic usefulness of time constant variables, especially in the falling part.

With a hypothesis that DU patient may have relatively higher value of mean mid-range frequency, UFR data are further analysed in the frequency domain, where a newly designed bandpass filter provides precise cut-offs. The bandpass filtered curve is analysed by Fast Fourier transform to generate the frequency spectrum, and to derive median power frequency variables and sum of amplitude changes variable which have statistically significant difference in two groups. However the MPF result reveals the mid-range frequency is lower in DU group than BOO group. A trial analysis of Wavelet is presented, but unfortunately it may not be suitable for applying to the UFR data.

All proposed parameters are assessed for their statistical significance for DU against BOO. In this study we proposed 49 non-invasively parameters which have significant

statistical difference between two groups, and which could serve as additional indicators for non-invasively differentiating DU from BOO. Each parameter is examined in SPSS to assess their mean value in each diagnostic group and *p* value of statistical significance. Then three statistical/mathematical models are established to combine proposed parameters for maximising discriminant utility, with an average of 75% to 80% accuracy.

7.2 In three generated and tested statistical models, MANOVA result could serve as a score indicator for differentiating DU with BOO and further contributes to 27% of patients being accurately predicted on their diagnosis, which is considered as the most robust model in three. CART model is relatively easier to be affected by the type I error when making decisions on splitting the parent nodes into child nodes, and it is considered to have the lowest robustness. The ANN model is fairly robust due to the current number of data analysed, and its robustness could be improved by employing a larger scale of data or further analysing on recurrent neural network models. **Contributions**

The contributions of this thesis are mainly

- The first study of analysing UFR curve in frequency domain to explore the frequency content and difference between two LUT dysfunction groups, with a number of parameters proposed which have significant statistical difference.
- The parameter generated by multivariance analysis, classification and regression tree and neural network methods on all proposed parameters hold the promise to differentiate DU with BOO non-invasively, and it is close to a potential clinical trial.
- The data employed in this study are free-flow UFR data, which is simpler to collect and is relatively economical as no additional equipment is required, is more convenient and less risky for the patient and the parameter derivation procedure could be automatically processed in MATLAB with code provided in appendix.
- The shape of flow is also reported to associate with one or more voiding

abnormalities, but some of the terms to describe abnormally shaped flow rate curves are confusing. This study also includes a survey on flow shape and their descriptors in relevant published articles and makes suggestions on standardisation of shape descriptors.

- This study introduces the archetype of DU and BOO flow shapes, and recommends quantitative definition of 'intermittency' to avoid early and end dribbles counted as a part of flow.
- The proposed non-invasive analytical methods may also be suitable for other LUT dysfunctions, such as DO, or in female population, for serving as additional diagnostic indicators.

7.3 Further research

Though a number of articles proposed non-invasive methods to diagnose DU or differentiate with BOO, there is no effective non-invasive diagnostic method and PFS is the only gold standard for assessing LUT dysfunctions. To continue this study for overcoming this situation, some potential expansion of the present study can be summarised as follows and could be further researched in post doctorate study.

- To investigate the frequency range of detrusor contraction and abdominal straining, which could provide a precise cut-off frequency value in frequency domain analysis.
- To test the proposed parameters in a different database, to verify the robustness of their diagnostic utility.
- Analysing UFR in a larger database, which could be managed by a multicentre trial, to possibly further increase the discriminant accuracy, and to improve the reliability of statistical models.
- Conduct a comprehensive analysis on application of neural network in UFR data, possibly using recurrent neural network for flow shape and convolutional neural network for combining parameters.
- Test the possibility of applying proposed parameters in other diagnostic groups, and in females.

Reference List:

Abdel-Aal, A., El-Karamany, T., Al-Adl, A.M., Abdel-Wahab, O. and Farouk, H. (2011) Assessment of noninvasive predictors of bladder outlet obstruction and acute urinary retention secondary to benign prostatic enlargement. *Arab Journal of Urology*. 9 (3), pp.209-214.

Abrams, P. (1999) Bladder outlet obstruction index, bladder contractility index and bladder voiding efficiency: three simple indices to define bladder voiding function. *BJU International*, 84 (1), pp.14-15.

Abrams, P., Cardozo, L., Fall, M., Griffiths, D., Rosier, P., Ulmsten, U., van Kerrebroeck, P., Victor, A. and Wein, A. (2002) The Standardisation of Terminology of Lower Urinary Tract Function. *Neurourology and Urodynamics*. 21 (2), pp.167-178

Abrams, P. (2006) *Urodynamics*. 3rd ed. London: Springer.

Abrams, P., Cardozo, L., Wagg, A. and Wein, A.J. (2017) *Incontinence*, 6th ed International Consultation on Incontinence, Tokyo, September 2016. International Continence Society.

Al-Ghazo, M. A., Ghalayini, I. F., Al-Azab, R., Hani, O. B., Matani, Y. S. and Haddad, Y. (2011) Urodynamic detrusor overactivity in patients with overactive bladder symptoms. *International neurourology journal*, 15(1), pp. 48-54.

Angkoon, P., Sirinee, T., Huosheng H., Pornchai P. and Chusak, L. (2012). The Usefulness of Mean and Median Frequencies in Electromyography Analysis, Computational Intelligence in Electromyography Analysis - A Perspective on Current Applications and Future Challenges, Dr. Ganesh R. Naik (Ed.), InTech, available from DOI: 10.5772/50639.

Austin, P.F., Bauer, S.B., Bower, W., Chase, J., Franco, I., Hoebeke, P., Rittig, S., Walle, J.V., von Gontard, A., Wright, A., Yang, S.S. and Nevéus, T., (2016) The standardization of terminology of lower urinary tract function in children and adolescents: Update report from the standardization committee of the International Children's Continence Society. *Neurourology and Urodynamic*s 35(4), pp.471-481.

Babu, R., Harrison, S.K. and Hutton, K.A. (2004) Ballooning of the foreskin and physiological phimosis: is there any objective evidence of obstructed voiding? *BJU Int*. 94 (3), pp.384-7.

Bangert, A.W. and Baumberger, J.P. (2005) Research and Statistical Techniques Used in the Journal of Counseling & Development: 1990–2001. *Journal of Counseling & Development*, 83 (4), pp. 480-487.

Bock, R.D. (1975) *Multivariate statistical methods in behavioral research.* New York: McGraw-Hill.

Bradley, A.E., Benjamin, N.B. and Jack, W.M. (2010) The use of uroflowmetry to diagnose recurrent stricture after urethral reconstructive surgery. International braz j urol 36 (5). pp.639-640.

Berges, R., and Oelke, M. (2011). Age-stratified normal values for prostate volume, PSA, maximum urinary flow rate, IPSS, and other LUTS/BPH indicators in the German male community-dwelling population aged 50 years or older. *World Journal of Urology*, 29(2), 171–178.

Boothroyd, A.E., Dixon, P.J., Christmas, T.J., Chapple, C.R. and Rickards, D. The ultrasound cystodynamogram--a new radiological technique. The British Journal of Radiology, 63 (749), pp.331-332.

Breiman, L., Friedman, J.H., Olshen, R.A. and Stone, C.J. (1984) *Classification and Regression Trees*. New York: Chapman & Hall/CRC.

Chancellor, M.B., Blaivas, J.G., Kaplan, S.A. and Axelrod, S. (1991) Bladder outlet obstruction versus impaired detrusor contractility: the role of outflow. Journal of Urology, 145 (4), pp.810–812.

Chen, S.L., Ng, S.C., Huang, Y.H. and Chen, G.D. (2017) Are patients with bladder oversensitivity different from those with urodynamically proven detrusor overactivity in female overactive bladder syndrome? *Journal of the Chinese Medical Association*, 80 (10), pp. 644–650.

Chia, S.J., Heng, C.T., Chan, S.P. and Foo, K.T. (2003) Correlation of intravesical prostatic protrusion with bladder outlet obstruction. *BJU International*. 91, pp.371-374.

Chou, T.P., Gorton, E., Stanton, S.L., Atherton, M., Baessler, K. and Rienhardt, G. (2000) Can uroflowmetry patterns in women be reliably interpreted? *International Urogynecology J Pelvic Floor Dysfunction*. 11(3), pp.142-7.

Chung, D.E., Dillon, B., Kurta, J., Maschino, A., Cronin, A. and Sandhu, J. S. (2013) Detrusor underactivity is prevalent after radical prostatectomy: A urodynamic study including risk factors. *Canadian Urological Association*, 7(1-2), pp. E33-37.

Djavan, B., Fong, Y.K., Harik, M., Milani, S., Reissigl, A., Anagnostou, T., Bagheri, F., Waldert, M., Kreuzer, S., Fajkovic, H. and Marberger, M. (2004) Longitudinal study of men with mild symptoms of bladder outlet obstruction treated with watchful waiting for four years. *Urology* 64 (6), pp. 1144–1148.

ElSaied, W., Mosharafa, A., ElFayoumy, H., ElGhoniemy, M., Ziada, A., ElGhamrawy, H., Lbrahim, A. and Abdel-Azim, M. (2013) Detrusor wall thickness compared to other non-invasive methods in diagnosing men with bladder outlet obstruction: A prospective controlled study. *African Journal of Urology*. 19 (4), pp.160-164.

Fantl, J.A., Smith, P.J., Schneider, V., Hurt, W.G. and Dunn, L.J. (1983) Fluid weight uroflowmetry in women. *American Journal of Obstetrics and Gynecology.* 145(8). pp.1017-1024.

Finazzi Agrò, E., Lamorte, F., Patruno, G., Bove, P., Petta, F., Topazio, L. and Di Santo, A. (2012) *Non Invasive Urodynamics: The Penile Cuff Test in Patients Candidate to Turp*. Beijing, 15 October 2012. ICS.

Finn, J.D. (1977) *Multivariate analysis of variance and covariance. In: Statistical Methods for Digital Computers,* Volume 3. New York: John Wiley & Sons, Inc.

Frigo, M. and Johnson, S.G. (1998) FFTW: An Adaptive Software Architecture for the FFT. *Proceedings of the International Conference on Acoustics, Speech, and Signal Processing*. 3, pp. 1381-1384.

Gammie, A., Clarkson, B., Constantinou, C., Damaser, M., Drinnan, M., Geleijnse, G., Griffiths, D., Rosier, P., Schäfer, W., van Mastrigt, R. and International Continence Society Urodynamic Equipment Working Group (2014) International Continence Society guidelines on urodynamic equipment performance. *Neurourology and Urodynamics*. 33 (4), pp.370-379.

Gammie, A., Kaper, M., Dorrepaal, C., Kos, T., and Abrams, P. (2016). Signs and Symptoms of Detrusor Underactivity: An Analysis of Clinical Presentation and Urodynamic Tests From a Large Group of Patients Undergoing Pressure Flow Studies. *European Urology*, 69 (2), pp.361–369.

Gammie, A., Yoshida, S., Steup, A., Kaper, M., Dorrepaal, C., Kos, T. and Abrams, P. (2016) Flow time and voiding time – definitions and use in identifying detrusor underactivity. *Neurourology and Urodynamics*. 35 (supplement 2), pp.s68-s69.

Gammie, A., Kaper, M., Dorrepaal, C., Kos, T. and Abrams, P. (2016). Signs and Symptoms of Detrusor Underactivity: An Analysis of Clinical Presentation and Urodynamic Tests From a Large Group of Patients Undergoing Pressure Flow Studies. European Urology, 69 (2), pp.361–369.

Ghobish, A.A. (2000) Quantitative and qualitative assessment of flowmetrograms in patients with prostatodynia. European Urology, 38(5), pp.576-83.

Golub, G. H. (1969) Matrix decompositions and statistical calculations. New York, Academic Press.

Gratzke, C., Bachmann, A., Descazeaud, A., Drake, M.J., Madersbacher, S., Mamoulakis, C., Oelke, M., Tikkinen, K.A. and Gravas, S. (2015) EAU Guidelines on the Assessment of Non-neurogenic Male Lower Urinary Tract Symptoms including Benign Prostatic Obstruction. *European Urology,* 67 (6), pp. 1099-1109

Griffiths, H.J., Castro, J. (1970) An evaluation of the importance of residual urine. *Br J Radiol*. 43, pp. 409-413.

Griffiths, D., Höfner, K., van Mastrigt, R., Rollema, H.J., Spångberg, A. and Gleason, D. (1997) Standardization of terminology of lower urinary tract function: Pressure-flow studies of voiding, urethral resistance, and urethral obstruction. *Neurourology and Urodynamics*. 16 (1), pp.1-18.

Griffiths, C.J., Rix, D., MacDonald, A.M., Drinnan, M.J., Pickard, R.S. and Ramsden, P.D. (2002) Noninvasive measurement of bladder pressure by controlled inflation of a penile cuff. *The Journal of Urology*, 167 (3), pp. 1344–1347.

Groen, J.M, Klijn, A.J, Bosch, J.L.H.R, Nijman, R.J.M, and van Mastrigt, R. (1998) Diagnosis and grading of detrusor instability using a computerized algorithm. *The Journal of Urology*, 159 (5), pp. 1669–1674.

Gutierrez, S.C. (1997) Urine flow in childhood: a study of flow chart parameters based on 1,361 uroflowmetry tests. *Journal of Urology*. 157 (4), pp. 1426-8.

Guzel, O., Aslan, Y., Balci, M., Tuncel, A., Keten, T., Erkan, A. and Atan, A. (2015) Can Bladder Wall Thickness Measurement Be Used for Detecting Bladder Outlet Obstruction? *Urology*. 86 (3), pp. 439-444.

Hagan, M.T. and Demuth, H.B. (2014) *Neural Network Design.* 2nd Ed, Martin Hagan.

Harding, C., Horsburgh, B., Dorkin, T.J. and Thorpe, A.C. (2012) Quantifying the effect of urodynamic catheters on urine flow rate measurement. *Neurourology and Urodynamics*. 31 pp.139-142.

Harding, C.K., Robson, W., Drinnan, M.J., Griffiths, C.J., Ramsden, P.D. and Pickard, R.S. (2004) An automated penile compression release maneuver as a noninvasive test for diagnosis of bladder outlet obstruction. *The Journal of Urology*. 172 (6), pp. 2312-2315.

Haylen, B.T., de Ridder, D., Freeman, R.M., Swift, S.E., Berghmans, B., Lee, J., Monga, A., Petri, E., Rizk, D.E., Sand, P.K. and Schaefer, G.N. (2010) An International Urogynecological Association (IUGA)/International Continence Society (ICS) joint report on the terminology for female pelvic floor dysfunction. *International Urogynecology Journal*. 21 (1), pp. 5-26.

Heaton, J. (2008) *Introduction to Neural Networks with Java*, 2nd ed, Heaton Research, Incorporated.

Hogg, R.V. and Tanis, E.A. (2010) Probability and Statistical Inference. 8th Ed, Pearson.

Huang Foen Chung, J.W.N.C., Bohnen, A.M., Pel, J.J.M., Bosch, J.L.H.R., Niesing, R., and van Mastrigt, R. (2004) Applicability and reproducibility of condom catheter method for measuring isovolumetric bladder pressure. *Urology*, 63 (1), pp. 56–60.

Jensen, K.M., Nielsen, K.K., Jensen, H., Pedersen, O.S. and Krarup, T. (1983) Urinary flow studies in normal kindergarten--and schoolchildren. *Scandinavian Journal of Urology and Nephrology*. 17 (1), pp.11-21.

Jeong, S.J., Kim, H.J., Lee, Y.J., Lee, J.K., Lee, B.K., Choo, Y.M., Oh, J.J., Lee, S.C., Jeong, C.W., Yoon, C.Y., Hong, S.K., Byun, S.S. and Lee, S.E. (2012) Prevalence and Clinical Features of Detrusor Underactivity among Elderly with Lower Urinary Tract Symptoms: A Comparison between Men and Women. *Korean Journal of Urology.* 53 (5), pp. 342-348.

Jørgensen, J. B., Jensen, K. M., Klarskov, P., Bernstein, I., Abel, I. and Mogensen, P. (1990) Intra- and inter- observer variations in classification of urinary flow curve patterns. *Neurourology and Urodynamics*, 9 (5), pp. 535-539.

Jørgensen, J.B., Colstrup, H. and Frimodt-Møller, C. Uroflow in women: an overview and suggestions for the future. *International Urogynecology Journal of Pelvic Floor Dysfunction*. 9 (1), pp. 33-36.

Kim, M., Cheeti, A., Yoo, C., Choo, M., Paick, J. and Oh, S. (2014) Non-Invasive Clinical Parameters for the Prediction of Urodynamic Bladder Outlet Obstruction: Analysis Using Causal Bayesian Networks. *PLoS One*. 9 (11), pp. 20.

Kinahan, T.J., Churchill, B.M., McLorie, G.A., Gilmour, R.F. and Khoury, A.E. (1992) The efficiency of bladder emptying in the prune belly syndrome. *Journal of Urology*. 148, pp. 600-603.

Kolman, C., Girman, C.J., Jacobsen, S.J. and Lieber, M.M. (1999) Distribution of post-void residual urine volume in randomly selected men. *Journal of Urology*, 161 (1), pp. 122-127

Laghari, W.M., Baloch, M.U., Mengal, M.A. and Shah, S.J. (2014) Performance Analysis of Analog Butterworth Low Pass Filter as Compared to Chebyshev Type-I Filter, Chebyshev Type-II Filter and Elliptical Filter. *Circuits and Systems*. 5, pp. 209-216.

Leblanc, G., Tessier, J., Schick, E. 1995 The importance and significance of post-micturitional bladder residue in the evaluation of prostatism. *Prog Urol*. 5 (4), pp. 511-514.

Lee, K.S., Song, P.H. and Ko, Y.H. (2016) Does uroflowmetry parameter facilitate discrimination between detrusor underactivity and bladder outlet obstruction?. *Investigative and clinical urology*, 57 (6), pp. 437-441.

Li, R., Gammie, A., Zhu, Q. and Nibouche, M. (2018) Urine flow rate curve shapes and their descriptors, *Neurourology and Urodynamics*. 37 (8). pp. 2938-2944

Lim, K.B., Ho, H., Foo, K.T., Wong, M.Y.C. and Fook-Chong, S. (2006) Comparison of intravesical prostatic protrusion, prostate volume and serum prostatic-specific antigen in the evaluation of bladder outlet obstruction. *International Journal of Urology*. 13, pp. 1509-1513.

Mattsson, S. and Spångberg, A. (1994) Urinary flow in healthy schoolchildren. *Neurourology and Urodynamics*, 13 (3), pp. 281-96.

Mostafavi, S.H., Hooman, N., Hallaji, F., Emami, M., Aghelnezhad, R., Moradi-Lakeh, M. and Otukesh, H. (2012) The correlation between bladder volume wall index and the pattern of uroflowmetry/external sphincter electromyography in children with lower urinary tract malfunction. *Journal of Pediatric Urology*. 8 (4), pp. 367-74.

Oelke, M., Höfner, K., Jonas, U., de la Rosette, J.J., Ubbink, D.T. and Wijkstra, H.

(2007) Diagnostic Accuracy of Noninvasive Tests to Evaluate Bladder Outlet Obstruction in Men: Detrusor Wall Thickness. *Uroflowmetry*. 52 (3), pp. 827-835.

Ozawa, H., Chancellor, M.B., Ding, Y.Y., Nasu, Y., Yokoyama, T. and Kumon, H. (2000) Noninvasive urodynamic evaluation of bladder outlet obstruction using Doppler ultrasonography. *Urology*. 56 (3), pp. 408-412.

Paick, S.H., Choi, W.S., Park, H.K., Jeong, S.J., Lee, H., Seo, J.T., Park, W.H., Kim, H.W. and Kim, H.G. (2014) *Hand Grip Strength as a Predictor of Detrusor Underactivity in Male Patients with Lower Urinary Tract Symptoms*. In: ICS 2014 conference, Rio de Janeiro, 20 October 2014.

Pandey, R.M. (2015) Commonly used t-tests in medical research. *Journal of the Practice of Cardiovascular Sciences*, 4 (2), pp. 185-188.

Patel, N.D. and Parsons, J.K. (2014) Epidemiology and etiology of benign prostatic hyperplasia and bladder outlet obstruction. *Indian Journal of Urology*, 30 (2), pp.170-176.

Pauwels, E., De Wachter, S. and Wyndaele, J.J. (2005) A normal flow pattern in women does not exclude voiding pathology. *International Urogynecology Journal of Pelvic Floor Dysfunction*, 16 (2), pp. 104-8.

Pel, J.J.M. and van Mastrigt, R. (1999) Non-invasive measurement of bladder pressure using an external catheter. *Neurourology and Urodynamics*, 18 (5), pp. 455–469.

Pel, J.J.M., and van Mastrigt, R. (2001) THE VARIABLE OUTFLOW RESISTANCE CATHETER: A NEW METHOD TO MEASURE BLADDER PRESSURE NONINVASIVELY. *The Journal of Urology*, 165 (2), pp. 647–652.

Pel, J.J.M., Bosch, J.L.H.R., Blom, J.H.M., Lycklama à Nijeholt, A.A.B., and van Mastrigt, R. (2002) Development of a non-invasive strategy to classify bladder outlet obstruction in male patients with LUTS. *Neurourology and Urodynamics*, 21 (2), pp. 117–125.

Ricker, N. (1953) WAVELET CONTRACTION, WAVELET EXPANSION, AND THE CONTROL OF SEISMIC RESOLUTION. *Geophysics*, 18 (4), pp. 769-792.

Rikken, B., Pel, J.J., van Mastrigt, R. (1999) Repeat noninvasive bladder pressure measurements with an external catheter. *Journal of Urology*, 162 (2), pp. 474-479.

Prando, A. (2010) Ultrasound assessment of intravesical prostatic protrusion and detrusor wall thickness--new standards for noninvasive bladder outlet obstruction diagnosis*?*. *International Brazil Journal Urology*. 36 (6), pp. 766-766.

Rademakers, K.L.J., van Koeveringe, G.A. and Oelke, M. (2016) Ultrasound detrusor wall thickness measurement in combination with bladder capacity can safely detect detrusor underactivity in adult men. *World Journal of Urology*, 35 (1), pp. 153-159.

Reynard, J.M., Peters, T.J., Lamond, E. and Abrams, P. (1995) The significance of

abdominal straining in men with lower urinary tract symptoms. *British journal of Urology*, 75 (2), pp. 148-153.

Reynard, J., Lim, C. and Abrams, P. (1996) Significance of intermittency in men with lower urinary tract symptoms. *Urology*. 47 (4), pp. 491-496.

Reynard, J.M., Peters, T.J., Lamond, E. and Abrams, P. (1995) The significance of abdominal straining in men with lower urinary tract symptoms. *British Journey of Urology*. 75 (2), pp. 148-153.

Rollema, H.J. 1981 *Uroflowmetry in males: Refrence values and clinical application in benign prostatic hypertrophy*. PhD, University of Groningen.

Rumelhart, D.E. and McClelland, James. (1986). *Parallel Distributed Processing: Explorations in the Microstructure of Cognition*. Cambridge, MIT Press.

Schaefer, W., Abrams, P., Liao, L., Mattiasson, A., Pesce, F., Spangberg, A., Sterling, A.M., Zinner, N.R., Kerrebroeck, P.V. and International Continence Society (2002) Good urodynamic practices: Uroflowmetry, filling cystometry, and pressure‐flow studies. *Neurourology and Urodynamics*, 21 (3), pp. 261-274.

Schaefer, W. (2018) RE: Futyma et al. use of uroflow parameters in diagnosing an overactive bladder—Back to the drawing board and ICS News 613. *Neurourology and Urodynamics*, 37 (1), pp. 510-512.

Schmidhuber, J. (2015) Deep Learning in Neural Networks: An Overview. *Neural Networks*. 61, pp. 85–117.

Shin, S.H., Kim, J.W., Kim, J.W., Oh, M.M. and Moon, D.G. (2013) The degree of intravesical prostatic protrusion in association with bladder outlet obstruction. *Korean Journal of Urology*. 54 (6), pp. 369-372.

Smith, P., Pregenzer, G., Galffy, A. and Kuchel, G. (2015) Underactive bladder and detrusor underactivity represent different facets of volume hyposensitivity and not impaired contractility. *Bladder*, 2 (2), pp. e17.

Soderstrom, T. and Stoica, P. (1989) *System Identification*. 1st ed. Hemel Heampstead, UK: Prentice Hall International.

Sonke, G.S., Heskes, T., Verbeek, A.L., de la Rosette, J.J. and Kiemeney, L.A. (2000) Prediction of bladder outlet obstruction in men with lower urinary tract symptoms using artificial neural networks. *Journal of Urology*, 163 (1), pp. 300-305.

Sperandei, S. (2014) Understanding logistic regression analysis. *Biochemia medica*, 24 (1), pp. 12-18.

Sthle, L. and Wold, S., (1990) Multivariate analysis of variance (MANOVA). *Chemometrics and Intelligent Laboratory Systems*, 9, pp. 127–141.

Stulen, F. B., and De Luca, C. J. (1981) Frequency Parameters of the Myoelectric Signal

as a Measure of Muscle Conduction Velocity. *IEEE Transactions on Biomedical Engineering*, BME-28 (7), pp. 515–523.

Swithinbank, L.V. and Webster, L.M. (2012) Basic understanding of urodynamics. *Obstetrics, Gynaecology & Reproductive Medicine*. 22 (11), pp.315-320.

Uren, A. D., Cotterill, N., Harding, C., Hillary, C., Chapple, C., Klaver, M., Bongaerts, D., Hakimi, Z. and Abrams, P. (2017) Qualitative Exploration of the Patient Experience of Underactive Bladder. *European Urology*, 72 (3), pp.402–407.

Uren, A.D. and Drake, M.J. (2017) Definition and symptoms of underactive bladder. *Investigative and Clinical Urology*, 58 (Supplement 2), pp. S61-S67.

van der Vis-Melsen, M.J., Baert, R.J., Rajnherc, J.R., Groen, J.M., Bemelmans, L.M. and De Nef, J.J. (1989) Scintigraphic assessment of lower urinary tract function in children with and without outflow tract obstruction. *British Journal of Urology*. 64 (3), pp.263-9.

Wein A, Chapple C. (2017) *Underactive bladder*. Switzerland: Springer.

Wen, J.G., Cui, L.G., Li, Y.D., Shang, X.P., Zhu, W., Zhang, R.L., Meng, Q.J. and Zhang, S.J. (2013) Urine flow acceleration is superior to Qmax in diagnosing BOO in patients with BPH. *Journal of Huazhong University of Science and Technology*, 33 (4), pp. 563-566.

Williams, A.B. (2006) *Electronic Filter Design Handbook*. 4th ed. London: McGraw-Hill.

Wyndaele, J. (1999) Normality in urodynamics studied in healthy adults. *Journal of Urology*, 161 (3). pp.899-902.

Zellner, A. (1962) An Efficient Method of Estimating Seemingly Unrelated Regressions and Tests for Aggregation Bias. *Journal of the American Statistical Association*, 57 (298), pp. 348-368.

Appendix

I) Matlab code for urodynamic model and peak counting

```
% started: 12/11/2013
% updated: 03/10/2015

% This program, using least squares approach,estimate the parameters
from
% measured urine data, which is a 2*N matrix, the first column is
input
% vectors and the second column is measured vectors

% Data processing, using butterworth filter with first order, 1Hz and
0.1Hz
folder='C:\Users\rui li\Desktop\project\Out files\out files
2017.6.30\excel'
d=dir(folder);
aa={d.name};
bb=aa(~cellfun(@isempty,regexp(aa,'.+(?=\.xlsx)','match')));
for i=1:numel(bb)
  Q1=xlsread(bb{i});

[b,a]=butter(1,0.2); % design the 1Hz filter parameters
Q2=filter(b,a,Q1);  % filter the data and save to Q2
[c,d]=butter(1,0.02);  % design the 0.1Hz filter parameters
Q3=filter(c,d,Q1);  % filter the data and save to Q3
[e,f]=butter(3,0.2);
Q4=filter(e,f,Q1);
[g,h]=butter(3,0.02);
Q5=filter(g,h,Q1);

% Assume the model structure is given as
% Q(t)=a*Q(t-1)+b*P(t)
% par is the martix for the parameters
% par=[-a,b]
% By Z transform, the descrete transfer function is
% Q(z)=b1*z/(z-a)


%(I)data processing for raw data
% Using least square to estimate the value of a,b and then calculate
the
% time constant
[n2 m2]=size(Q1);  %measure the data sequence length
[Q_max k]=max(Q1); %find the pick value and its position
                   %to section upward and downward data
Q=Q1;              %for symbolic short
V=sum(Q1)/10
% 1) For upward model parameter estimation from raw data
P=Q_max*ones(k,1); %set up input/stinulate sequence as step
PHI=[Q(1:k-1,1),P(2:k,1)];
par=inv(PHI'*PHI)*(PHI'*Q(2:k,1)); %estimate parameters
Traw1=-1/log(par(1,1)) %calculate time constant value for upward part
%{
%plot model output response for raw data
Q_Mopt(2,1)=Q(2,1); %setup initial values
```

```
for t=3:k
Q_Mopt(t,1)=par(1,1)*Q_Mopt(t-1,1)+abs(par(2,1))*P(t,1);
end
plot(Q_Mopt)
%}
% 2) For downward model parameter estimation from raw data
P=zeros(n2,1); %set up input/stinulate sequence as impulse
P(k,1)=Q_max;
PHI=[Q(k-1:n2-1,1),P(k:n2,1)]; % Build up PHI, and estimate the value
of par
par=inv(PHI'*PHI)*(PHI'*Q(k:n2,1)); %estimate parameters
Traw2=-1/log(par(1,1)) %calculate time constant value for downward
part
%{
%plot model output response for raw data
for t=k:n2
Q_Mopt(t,1)=par(1,1)*Q_Mopt(t-1,1)+par(2,1)*P(t,1);
end
t=1:n2;
figure(1)
plot(t',Q_Mopt, t', Q,'linewidth',2)
xlabel('time(0.1s)')
ylabel('flow rate(ml/s)')
legend('estimated model curve','raw data curve')
title('original data curve fitting')


%(II)data processing for 1Hz filtered data
%plot the 1Hz filtered data
figure(2)
plot(Q2)
xlabel('time(0.1s)')
ylabel('flow rate(ml/s)')
legend('1Hz filtered data curve')
title('1Hz filtered data')
%}

%(III)data processing for 0.1Hz filtered data
[n2 m2]=size(Q3); %measure the data sequence length
[Q_max3 k]=max(Q3); %find the pick value and its position
                    %to section upward and downward data
Q=Q3; %for symbolic short

% 1) For upward model parameter estimation from filtered data
P=Q_max3*ones(k,1); %set up input/stinulate sequence as step
PHI=[Q(2:k-1,1),P(3:k,1)];
par=inv(PHI'*PHI)*(PHI'*Q(3:k,1)); %estimate parameters
Tfilter1=-1/log(par(1,1)) %calculate time constant value for upward
part
%{
%plot model output response for 0.1Hz filtered data
Q_Mopt(2,1)=Q(2,1); %setup initial values
for t=3:k
Q_Mopt(t,1)=par(1,1)*Q_Mopt(t-1,1)+par(2,1)*P(t,1);
end
%plot(Q_Mopt)
%}
% 2) For downward model parameter estimation from filtered data
P=zeros(n2,1); %set up input/stinulate sequence as impulse
P(k,1)=Q_max3;
```

```
PHI=[Q(k-1:n2-1,1),P(k:n2,1)]; % Build up PHI, and estimate the value
of par
par=inv(PHI'*PHI)*(PHI'*Q(k:n2,1)); %estimate parameters
Tfilter2=-1/log(par(1,1))%calculate time constant value for downward
part
%{
%plot model output response for 0.1Hz filtered data
for t=k:n2
Q_Mopt(t,1)=par(1,1)*Q_Mopt(t-1,1)+par(2,1)*P(t,1);
end
t=1:n2;
figure(3)
plot(t',Q_Mopt, t', Q,'linewidth',2)
xlabel('time(0.1s)')
ylabel('flow rate(ml/s)')
legend('estimated model curve','0.1 Hz filtered data curve')
title('0.1Hz filtered data and curve fitting')
%}
meanUFRupward=sum(Q1(1:k))/k %the mean UFR for the upward part
meanUFRdownward=sum(Q1((k+1):n2))/(n2-k-1) % the mean URF for the
downward part
UtDt=k/(n2-k) % the ratio of upward time and downward time
if Q_max<5
    peak1=findpeaks(Q1,'MINPEAKHEIGHT',0.5);
    peak1=length(peak1);%count the number of peaks in raw data
    peak2=findpeaks(Q4,'MINPEAKHEIGHT',0.5);
    peak2=length(peak2);%count the number of peaks in 1Hz filtered
data
    peak3=findpeaks(Q5,'MINPEAKHEIGHT',0.5);
    peak3=length(peak3);%count the number of peaks in 0.1Hz filtered
data
else
    peak1=findpeaks(Q1,'MINPEAKHEIGHT',1);
    peak1=length(peak1);%count the number of peaks in raw data
    peak2=findpeaks(Q4,'MINPEAKHEIGHT',1);
    peak2=length(peak2);%count the number of peaks in 1Hz filtered
data
    peak3=findpeaks(Q5,'MINPEAKHEIGHT',1);
    peak3=length(peak3);%count the number of peaks in 0.1Hz filtered
data
end

Ft=length(find(Q1>0.5))/10;
Vt=n2/10;
Q_ave=V/Vt;

if k<11
    QmaxW=Qmax;
else
    QmaxW=0.05*sum(Q1((k-10):(k+9)));
end
Excel=[Q_max Q_ave V 0 0 Tfilter1 Tfilter2 Tfilter1/Tfilter2 UtDt
peak1 peak2 peak3 0 0 0 peak2/peak3 peak1/peak3 Ft Vt Ft/Vt
Q_ave/Q_max meanUFRupward meanUFRdownward
meanUFRupward/meanUFRdownward QmaxW];

Excelall(i,:)=Excel;
end
```

II) Matlab code for verification of filter order in peak counting analysis

```
[g,h]=butter(3,0.2);  % design the 1Hz filter parameters
Q2=filter(g,h,Q1);    % filter the data and save to Q2
[g,h]=butter(3,0.16); % design the 0.8Hz filter parameters
Q3=filter(g,h,Q1);    % filter the data and save to Q3
[g,h]=butter(3,0.12); % design the 0.6Hz filter parameters
Q4=filter(g,h,Q1);    % filter the data and save to Q4
[g,h]=butter(3,0.1);  % design the 0.5Hz filter parameters
Q5=filter(g,h,Q1);    % filter the data and save to Q5
[g,h]=butter(3,0.06); % design the 0.3Hz filter parameters
Q6=filter(g,h,Q1);    % filter the data and save to Q6
[g,h]=butter(3,0.02); % design the 0.1Hz filter parameters
Q7=filter(g,h,Q1);    % filter the data and save to Q7
[g,h]=butter(3,0.016); % design the 0.05Hz filter parameters
Q8=filter(g,h,Q1);    % filter the data and save to Q8
[g,h]=butter(3,0.012);% design the 0.01Hz filter parameters
Q9=filter(g,h,Q1);    % filter the data and save to Q9

if max(Q1)>5
    peak1=findpeaks(Q1,'MINPEAKHEIGHT',1);
    peak1=length(peak1);%count the number of peaks in raw data
    peak2=findpeaks(Q2,'MINPEAKHEIGHT',1);
    peak2=length(peak2);%count the number of peaks in 1Hz filtered
data
    peak3=findpeaks(Q3,'MINPEAKHEIGHT',1);
    peak3=length(peak3);%count the number of peaks in 0.1Hz filtered
data
    peak4=findpeaks(Q4,'MINPEAKHEIGHT',1);
    peak4=length(peak4);%count the number of peaks in raw data
    peak5=findpeaks(Q5,'MINPEAKHEIGHT',1);
    peak5=length(peak5);%count the number of peaks in 1Hz filtered
data
    peak6=findpeaks(Q6,'MINPEAKHEIGHT',1);
    peak6=length(peak6);%count the number of peaks in 0.1Hz filtered
data
    peak7=findpeaks(Q7,'MINPEAKHEIGHT',1);
    peak7=length(peak7);%count the number of peaks in raw data
    peak8=findpeaks(Q8,'MINPEAKHEIGHT',1);
    peak8=length(peak8);%count the number of peaks in 1Hz filtered
data
    peak9=findpeaks(Q9,'MINPEAKHEIGHT',1);
    peak9=length(peak9);%count the number of peaks in 0.1Hz filtered
data
else
    peak1=findpeaks(Q1,'MINPEAKHEIGHT',0.5);
    peak1=length(peak1);%count the number of peaks in raw data
    peak2=findpeaks(Q2,'MINPEAKHEIGHT',0.5);
    peak2=length(peak2);%count the number of peaks in 1Hz filtered
data
    peak3=findpeaks(Q3,'MINPEAKHEIGHT',0.5);
    peak3=length(peak3);%count the number of peaks in 0.1Hz filtered
data
    peak4=findpeaks(Q4,'MINPEAKHEIGHT',0.5);
    peak4=length(peak4);%count the number of peaks in raw data
    peak5=findpeaks(Q5,'MINPEAKHEIGHT',0.5);
    peak5=length(peak5);%count the number of peaks in 1Hz filtered
data
```

```
    peak6=findpeaks(Q6,'MINPEAKHEIGHT',0.5);
    peak6=length(peak6);%count the number of peaks in 0.1Hz filtered
data
    peak7=findpeaks(Q7,'MINPEAKHEIGHT',0.5);
    peak7=length(peak7);%count the number of peaks in raw data
    peak8=findpeaks(Q8,'MINPEAKHEIGHT',0.5);
    peak8=length(peak8);%count the number of peaks in 1Hz filtered
data
    peak9=findpeaks(Q9,'MINPEAKHEIGHT',0.5);
    peak9=length(peak9);%count the number of peaks in 0.1Hz filtered
data
end
Peak=[peak1 peak2 peak3 peak4 peak5 peak6 peak7 peak8 peak9];
```

III) Matlab code for MPF analysis

```
folder= C:\Users\Rui2L\Desktop\project\Out files\Male\UFR data\BOO
and DU'
d=dir(folder);
a={d.name};
b=a(~cellfun(@isempty,regexp(a,'.+(?=\.xlsx)','match')));
for k=1:numel(b)
  Q1=xlsread(b{k});
  Fs = 10;                                                  % Sampling
Frequency
Fn = Fs/2;                                                % Nyquist
Frequency
L1=length(Q1);
[e,f] = ellip(3,2,50,[0.06 0.2],'bandpass');              % Design
bandpass filter vector
Q2=filter(e,f,Q1);                                        % Filtered
whole curve
Q3=Q2(1:fix(L1/2));                                       % First half
curve
L3=length(Q3);
Q4=Q2(fix(L1/2):L1);                                      % Second
half curve
L4=length(Q4);

% Find median power frequency in the whole filtered flow
FTs = fft(Q2)/L1;
Fv = linspace(0, 1, fix(L1/2)+1)*Fn;                      % Frequency
Vector
Iv = 1:length(Fv);                                        % Index
Vector
absFTs=abs(FTs(Iv));                                      % Absolute
value of FFT
PabsFTs=absFTs.^2;                                        % Power
spectrum
CumAmp = cumtrapz(Fv, PabsFTs);                           % Integrate
power spectrum amplitude
MedPFreq = interp1(CumAmp, Fv, CumAmp(end)/2);            % Use
'interp1' To Find ¡®MPF¡¯
CumAmpS = cumtrapz(Fv, abs(FTs(Iv)));                     % Integrate
FFT Amplitude
MedFreq = interp1(CumAmpS, Fv, CumAmpS(end)/2);           % Use
¡®interp1¡¯ To Find ¡®MF¡¯

% Find median power frequency in the first and second half of
filtered flow
FTs3 = fft(Q3)/L3;
Fv3 = linspace(0, 1, fix(L3/2)+1)*Fn;                     % Frequency
Vector
Iv3 = 1:length(Fv3);                                      % Index
Vector
absFTs3=abs(FTs3(Iv3));                                   % Absolute
value of FFT
PabsFTs3=absFTs3.^2;                                      % Power
spectrum
CumAmp3 = cumtrapz(Fv3, PabsFTs3);                        % Integrate
FFT Amplitude
MedPFreq1 = interp1(CumAmp3, Fv3, CumAmp3(end)/2);         % MPF in
1st half
```

```
CumAmpS3 = cumtrapz(Fv3, abs(FTs3(Iv3)));                    %
Integrate FFT Amplitude
MedFreq1 = interp1(CumAmpS3, Fv3, CumAmpS3(end)/2);            % Use
¡®interp1¡¯ To Find ¡®MF¡¯

FTs4 = fft(Q4)/L4;
Fv4 = linspace(0, 1, fix(L4/2)+1)*Fn;                    % Frequency
Vector
Iv4 = 1:length(Fv4);                                     % Index
Vector
absFTs4=abs(FTs4(Iv4));                                  % Absolute
value of FFT
PabsFTs4=absFTs4.^2;                                     % Power
spectrum
CumAmp4 = cumtrapz(Fv4, PabsFTs4);                       % Integrate
FFT Amplitude
MedPFreq2 = interp1(CumAmp4, Fv4, CumAmp4(end)/2);        % MPF in
2nd half
CumAmpS4 = cumtrapz(Fv4, abs(FTs4(Iv4)));                    %
Integrate FFT Amplitude
MedFreq2 = interp1(CumAmpS4, Fv4, CumAmpS4(end)/2);

MPF=[MedPFreq MedPFreq1 MedPFreq2 MedFreq MedFreq1 MedFreq2];

% MF and MPF calculation on two part of flow, splited by Qmax point
[m,n]=max(Q1);
Q3=Q2(1:n);                                              % First half
curve
L3=length(Q3);
Q4=Q2((n+1):L1);                                         % Second
half curve
L4=length(Q4);

% Find median power frequency in the first and second half of
filtered flow
FTs3 = fft(Q3)/L3;
Fv3 = linspace(0, 1, fix(L3/2)+1)*Fn;                    % Frequency
Vector
Iv3 = 1:length(Fv3);                                     % Index
Vector
absFTs3=abs(FTs3(Iv3));                                  % Absolute
value of FFT
PabsFTs3=absFTs3.^2;                                     % Power
spectrum
CumAmp3 = cumtrapz(Fv3, PabsFTs3);                       % Integrate
FFT Amplitude
MedPFreq1 = interp1(CumAmp3, Fv3, CumAmp3(end)/2);        % MPF in
1st half
CumAmpS3 = cumtrapz(Fv3, abs(FTs3(Iv3)));                    %
Integrate FFT Amplitude
MedFreq1 = interp1(CumAmpS3, Fv3, CumAmpS3(end)/2);            % Use
¡®interp1¡¯ To Find ¡®MF¡¯

FTs4 = fft(Q4)/L4;
Fv4 = linspace(0, 1, fix(L4/2)+1)*Fn;                    % Frequency
Vector
Iv4 = 1:length(Fv4);                                     % Index
Vector
absFTs4=abs(FTs4(Iv4));                                  % Absolute
value of FFT
```

```
PabsFTs4=absFTs4.^2;                                    % Power
spectrum
CumAmp4 = cumtrapz(Fv4, PabsFTs4);                      % Integrate
FFT Amplitude
MedPFreq2 = interp1(CumAmp4, Fv4, CumAmp4(end)/2);       % MPF in
2nd half
CumAmpS4 = cumtrapz(Fv4, abs(FTs4(Iv4)));                    %
Integrate FFT Amplitude
MedFreq2 = interp1(CumAmpS4, Fv4, CumAmpS4(end)/2);

MPF(7:10)=[MedPFreq1 MedPFreq2 MedFreq1 MedFreq2];

% MF and MPF calculation on two part of flow, splited by the half of
volume voided point
CumAmpW = cumtrapz(1:length(Q1), Q1);                   % Integrate
FFT Amplitude
[~, n]=min(abs(CumAmpW(:)-CumAmpW(end)/2));             % MPF in 2nd
half

Q3=Q2(1:n);                                             % First half
curve
L3=length(Q3);
Q4=Q2((n+1):L1);                                        % Second
half curve
L4=length(Q4);

% Find median power frequency in the first and second half of
filtered flow
FTs3 = fft(Q3)/L3;
Fv3 = linspace(0, 1, fix(L3/2)+1)*Fn;                   % Frequency
Vector
Iv3 = 1:length(Fv3);                                    % Index
Vector
absFTs3=abs(FTs3(Iv3));                                 % Absolute
value of FFT
PabsFTs3=absFTs3.^2;                                    % Power
spectrum
CumAmp3 = cumtrapz(Fv3, PabsFTs3);                      % Integrate
FFT Amplitude
MedPFreq1 = interp1(CumAmp3, Fv3, CumAmp3(end)/2);      % MPF in 1st
half
CumAmpS3 = cumtrapz(Fv3, abs(FTs3(Iv3)));               % Integrate
FFT Amplitude
MedFreq1 = interp1(CumAmpS3, Fv3, CumAmpS3(end)/2);     % Use
¡®interp1¡¯ To Find ¡®MF¡¯

FTs4 = fft(Q4)/L4;
Fv4 = linspace(0, 1, fix(L4/2)+1)*Fn;                   % Frequency
Vector
Iv4 = 1:length(Fv4);                                    % Index
Vector
absFTs4=abs(FTs4(Iv4));                                 % Absolute
value of FFT
PabsFTs4=absFTs4.^2;                                    % Power
spectrum
CumAmp4 = cumtrapz(Fv4, PabsFTs4);                      % Integrate
FFT Amplitude
MedPFreq2 = interp1(CumAmp4, Fv4, CumAmp4(end)/2);      % MPF in 2nd
half
CumAmpS4 = cumtrapz(Fv4, abs(FTs4(Iv4)));               % Integrate
```

```
FFT Amplitude
MedFreq2 = interp1(CumAmpS4, Fv4, CumAmpS4(end)/2);
MPF(11:14)=[MedPFreq1 MedPFreq2 MedFreq1 MedFreq2];
MPFall(k,1:14)=MPF;
end
```

IV) SPSS syntax script for MANOVA

```
MANOVA Qmax Qave Volumevoided FlowtimeVoidtime FlowindexQaveQmax
Meanrateinraisingpart Meanrateinfallingpart
   Peakcountingratio1Hz0.1Hz Peakcountingratioraw0.1Hz @0.11MPFwholeflow
   @0.11MPFfirsthalfvolume @0.11MPF1st2ndQmax @0.11MPFfirsthalfT
@0.11MPFwhole2ndQmax
   @0.20.9MPFwholeflow @0.20.9MFfirsthalfVolumes @0.10.7MPFwholeflow
@0.10.8MPFwholeflow
   @0.10.9MPFwholeflow @0.10.9MPF1st2ndQmax @0.20.7MFfirsthalfVolumes
@0.20.7MPFfirsthalfvolume
   @0.20.8MPFwholeflow @0.20.8MPFfirsthalfvolume @0.21MPFwholeflow
@0.21MPFfirsthalfvolume Qmax0.5Hz
   TC20.5Hz QaveQmax0.5Hz meanUFRupward0.5Hz meanUFRdownward0.5Hz
   Qmax2sec QaveTv2sec QaveTf2sec DeltaQ2sec MUP2sec
   MDOWN2sec Peak2sec Peakraw peak1Hz @2sec0.1 @0.50.1
   Amplitudechangeinraisingslope TQmaxTv TQmax2secTv NormalisedTC2
   BY DU (0,1)  % performing MANOVA analysis on all input parameters
which have significant statistically difference between two groups
 /DISCRIM=STAN RAW CORR  % generating discriminant parameters
 /PRINT=SIGNIF(MULTIV,UNIV,EIGEN,DIMENR) % present if
Multivariate F tests, Eigenvalues matrix, dimension-reduction
analysis or univariate F tests have statistical difference between
two groups
 /DESIGN.
```

V) MATLAB code for flow normalisation analysis

```
folder='C:\Users\Rui2L\Desktop\project\Out files\Male\UFR data\BOO
and DU'
d=dir(folder);
aa={d.name};
bb=aa(~cellfun(@isempty,regexp(aa,'.+(?=\.xlsx)','match')));

for i=1:numel(bb)
    Q1=xlsread(bb{i});
    Q11=Q1;
    Q11(11:(length(Q1)+10))=Q11;
    Q11(1:10)=zeros(1,10);
    Q11((length(Q1)+11):(length(Q1)+20))=zeros(1,10);
    for j=1:length(Q1)
        Q1f(j,1)=(sum(Q11(j:(j+20))))/21;
    end
    VV = cumtrapz(1:length(Q1f),Q1f);
    ST= find(VV>VV(end)*0.005, 1, 'first'); %locate 0.5% VV point
    ET= find(VV>VV(end)*0.98, 1, 'first'); %locate 98% VV point
    xq=1:((length(Q1f(ST:ET))-1)/999):length(Q1f(ST:ET));
    vq = interp1(Q1f(ST:ET),xq);
    vqn=vq/max(vq);

    xq1=1:((length(Q1)-1)/999):length(Q1);
    vq1 = interp1(Q1,xq1);
    vqn1=vq1/max(vq1);

    xq2=1:((length(Q1f)-1)/999):length(Q1f);
    vq2 = interp1(Q1f,xq2);
    vqn2=vq2/max(vq2);

    loc1=find(Q1f(ST:ET)<0.5);
    if isempty(loc1)
        inte(i,1)=0;
        %Excel(i,:)=vqn;
        %eUs1=sum((vqn-TU).^2);
        %eOs1=sum((vqn-TO).^2);
        %TD(i,2:3)=[eUs1,eOs1];
    else
        inte(i,1)=1;
        %Excel(i,:)=0;
    end

    eUs1=sum((vqn-TD).^2);
    eOs1=sum((vqn-TB).^2);
    inte(i,2:3)=[eUs1,eOs1];

    eUs2=sum((vqn1-TD).^2);
    eOs2=sum((vqn1-TB).^2);
    inte(i,4:5)=[eUs2,eOs2];

    eUs3=sum((vqn2-TD).^2);
    eOs3=sum((vqn2-TB).^2);
    inte(i,6:7)=[eUs3,eOs3];

    clear Q1f Q11
end
```

VI) Boxplot for selected parameters

Following figures, from figure 40 to figure 47, are boxplots generated by SPSS, which are summary plots of 8 parameters, graphically depicting the median, quartiles, and extreme values. The box represents the interquartile (IQ) range which contains the middle 50% of the records. The whiskers are lines that extend from the upper and lower edge of the box to the highest and lowest values which are no greater than 1.5 times the IQ range. A line across the box indicates the median. Outliers are cases with values between 1.5 and 3 times the IQ range, i.e., beyond the whiskers. Extremes are cases with values more than 3 times the IQ range.

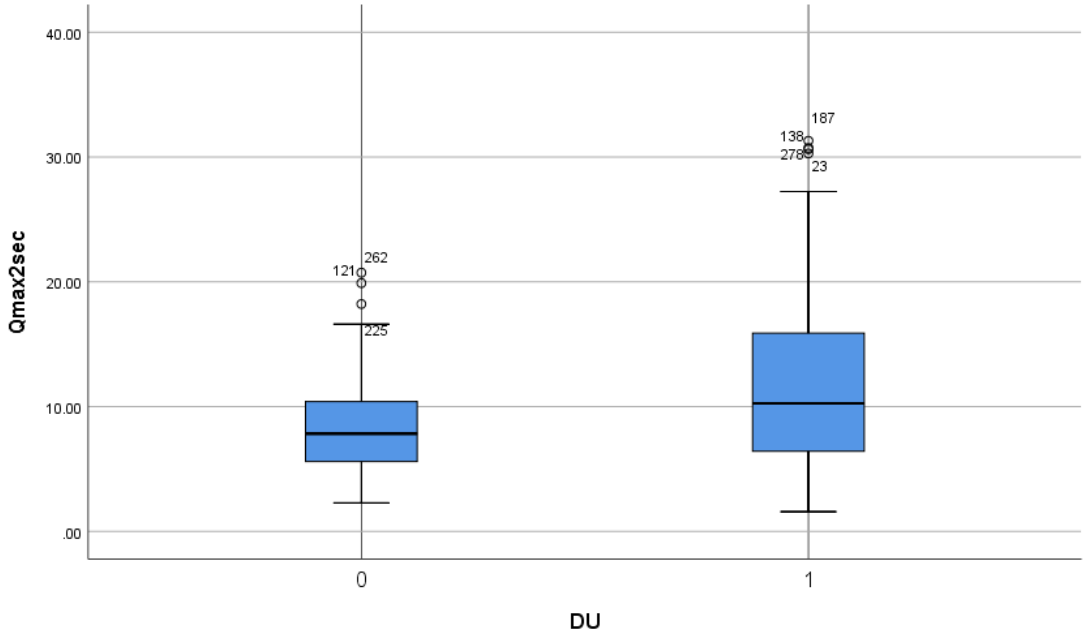

Figure 10 Qmax2sec boxplot

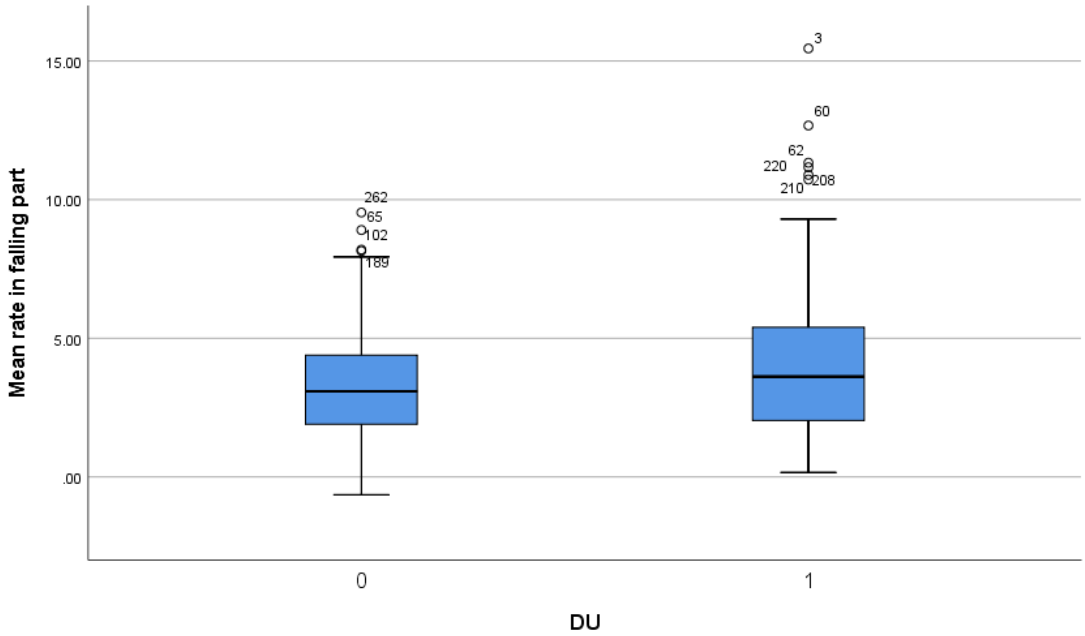

Figure 11 Mean rate in falling part box plot

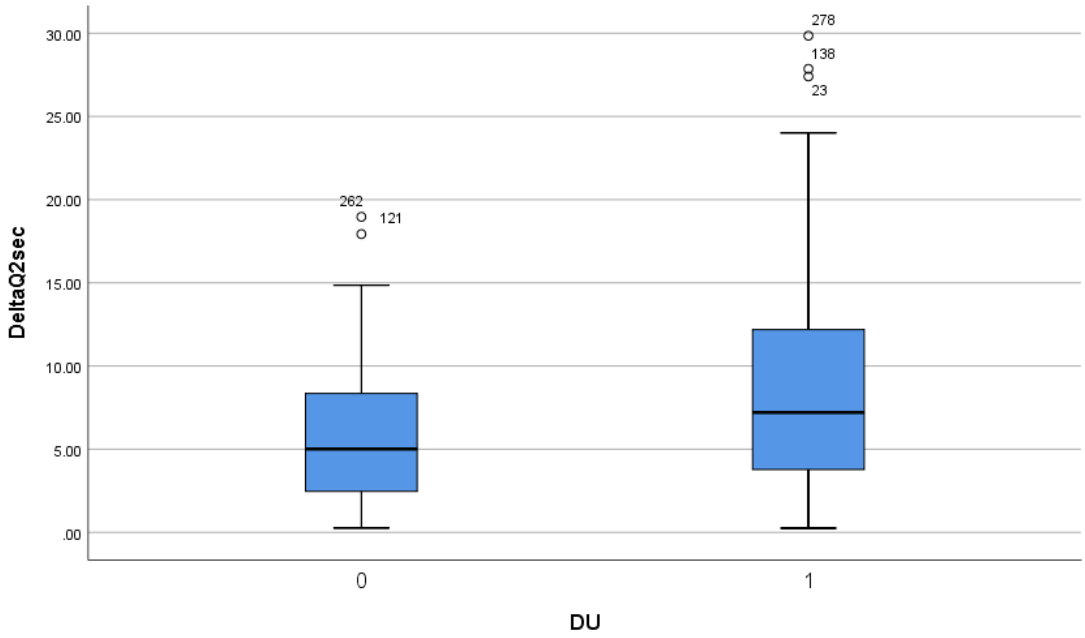

Figure 12 DeltaQ2sec boxplot

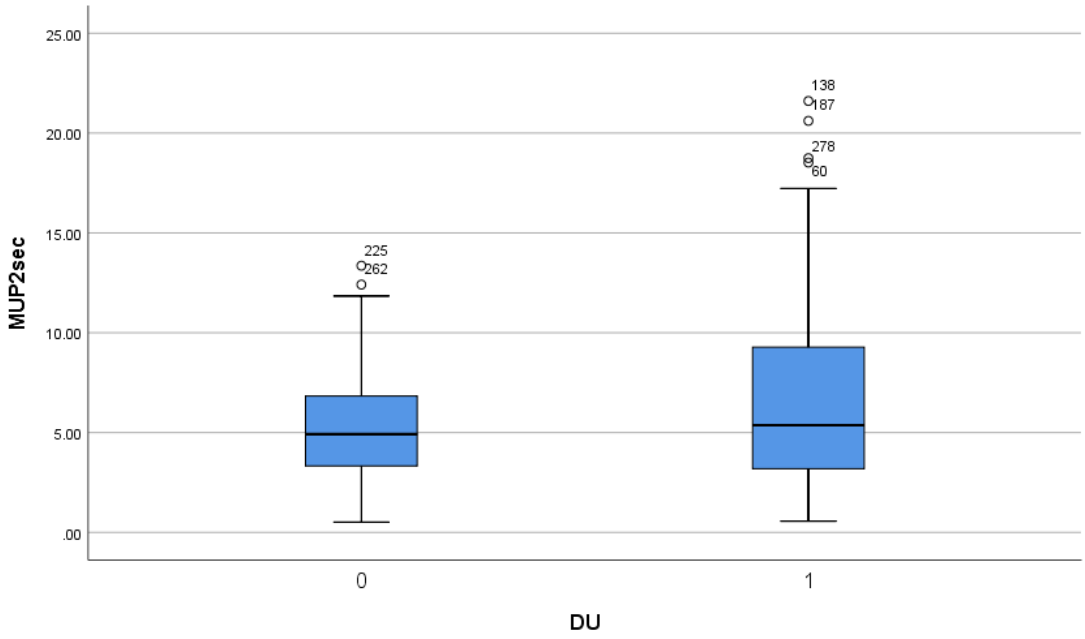

Figure 13 Mup2sec boxplot

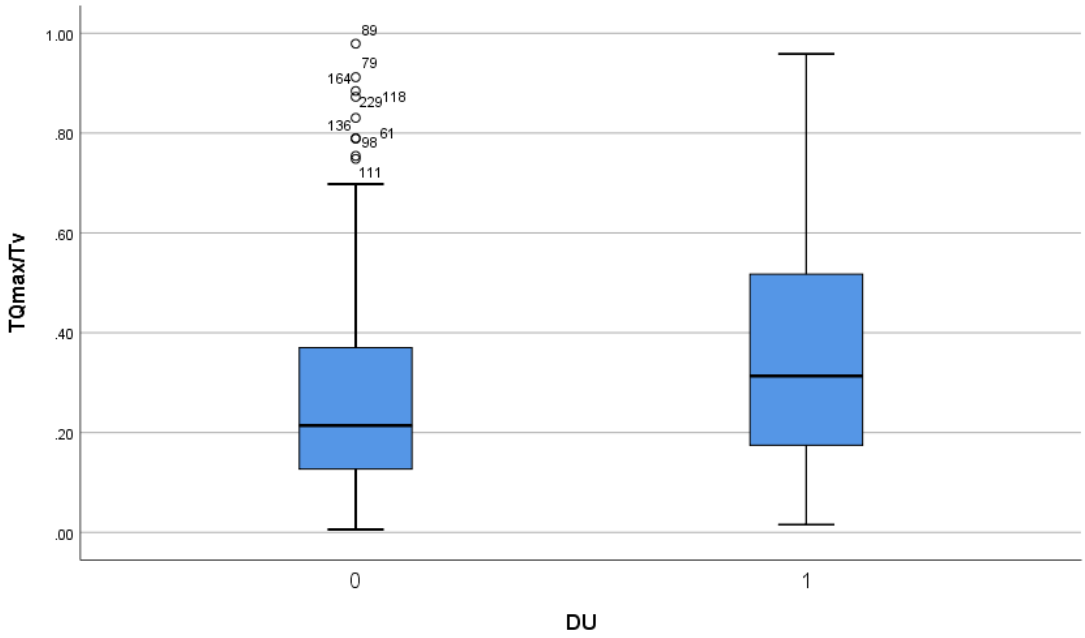

Figure 14 TQmax/Tv boxplot

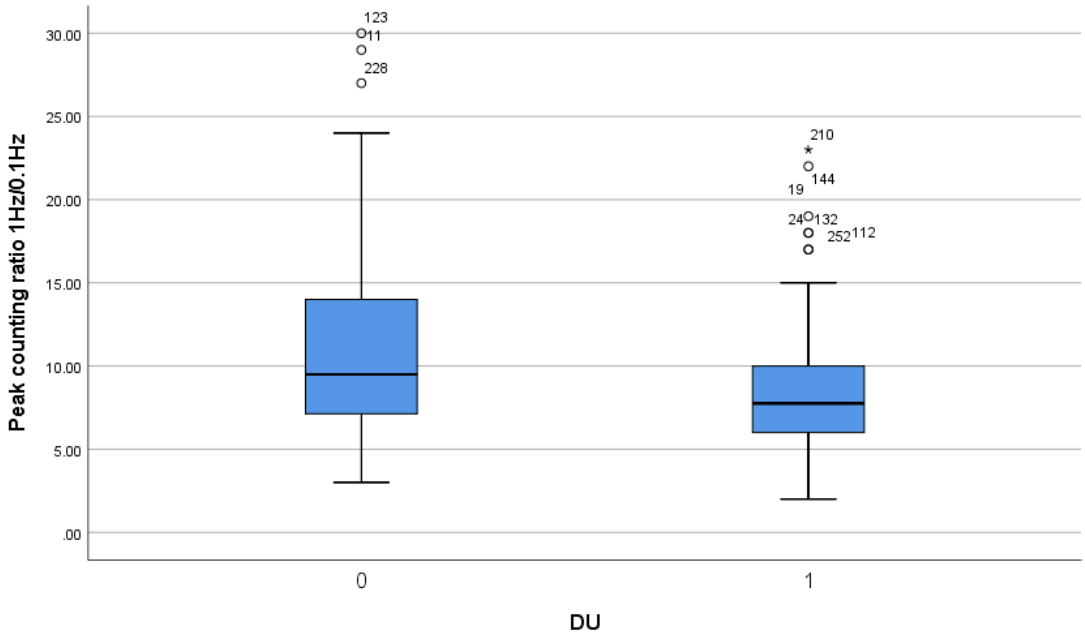

Figure 15 Peak counting ratio 1Hz/0.1Hz boxplot

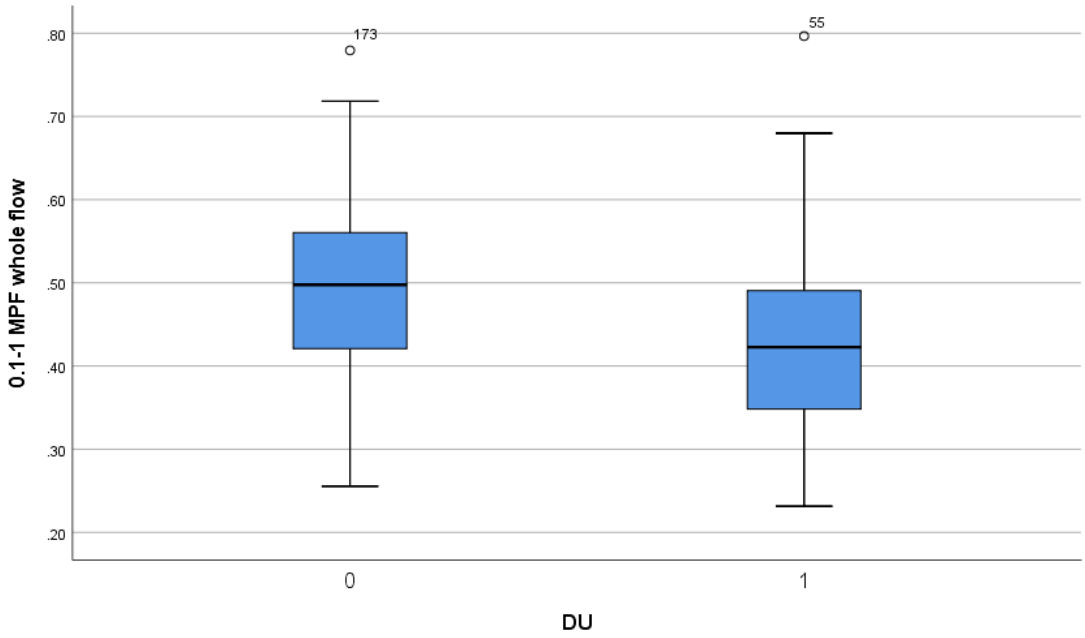

Figure 16 0.1-1 MPF whole flow boxplot

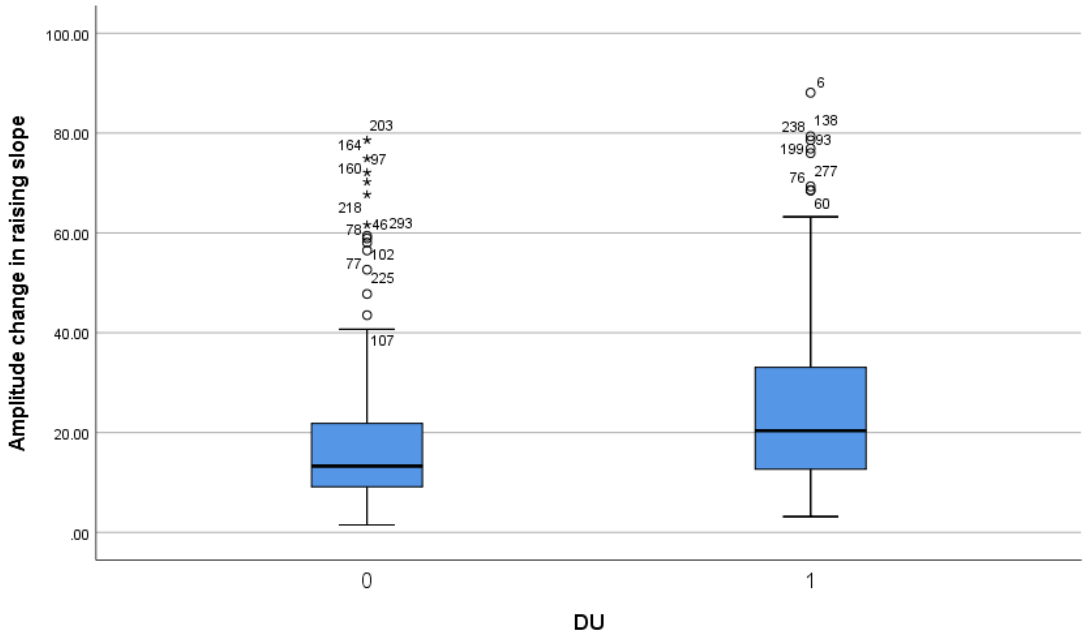

Figure 17 amplitude change in raising slope boxplot

VII) DU urine flow rate curve plots

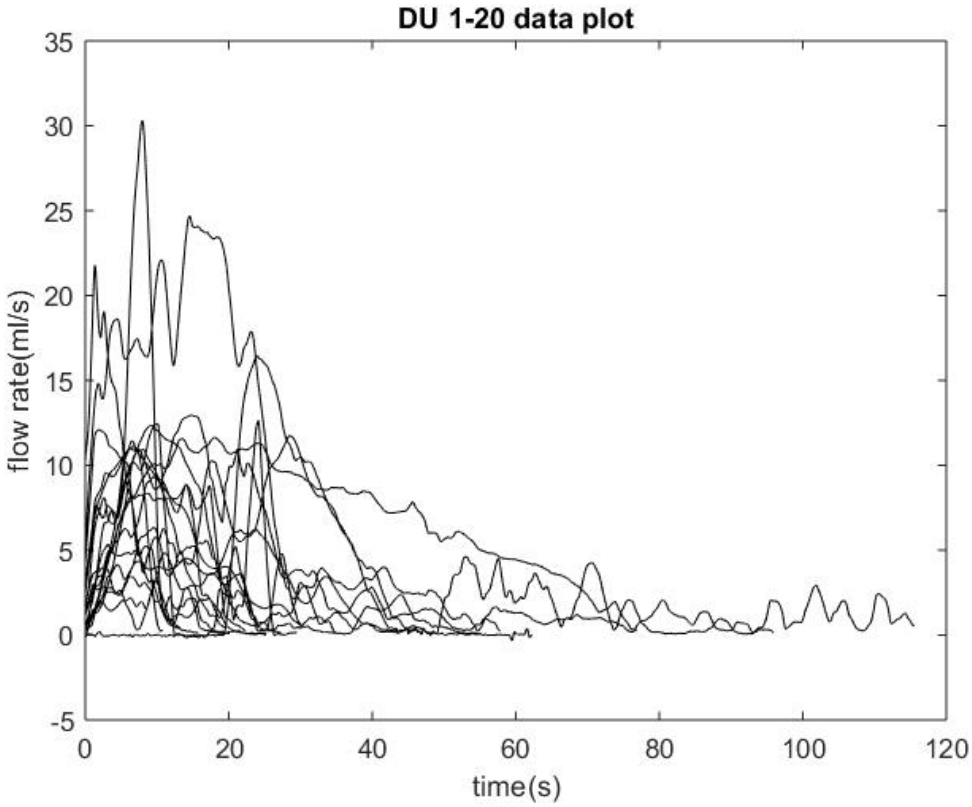

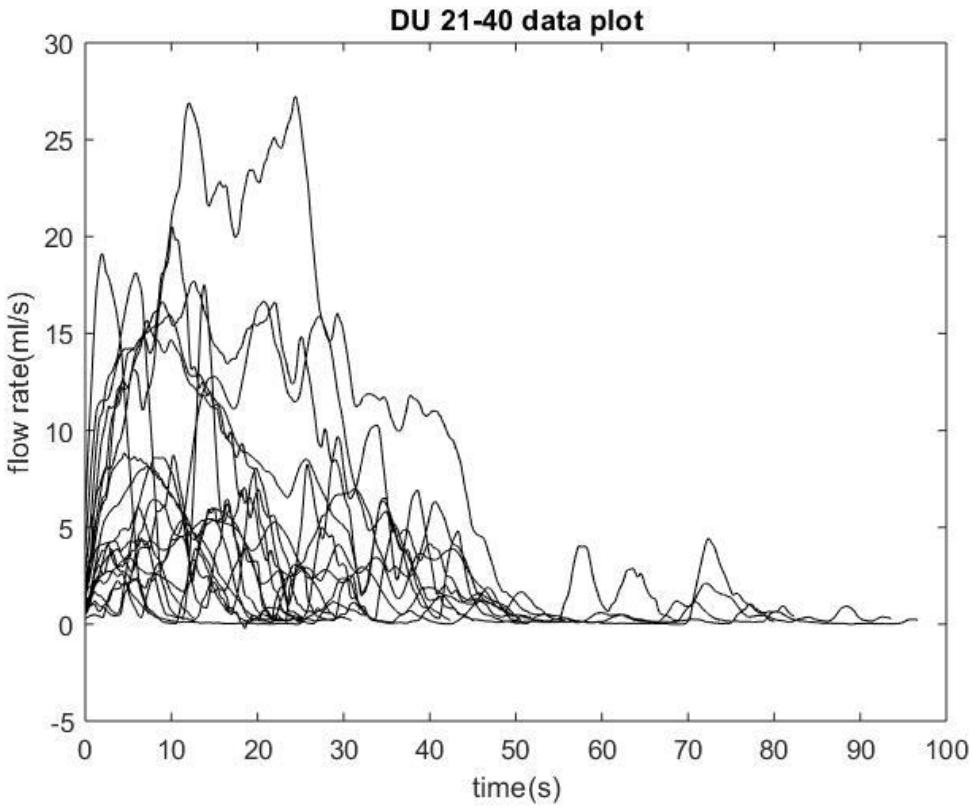

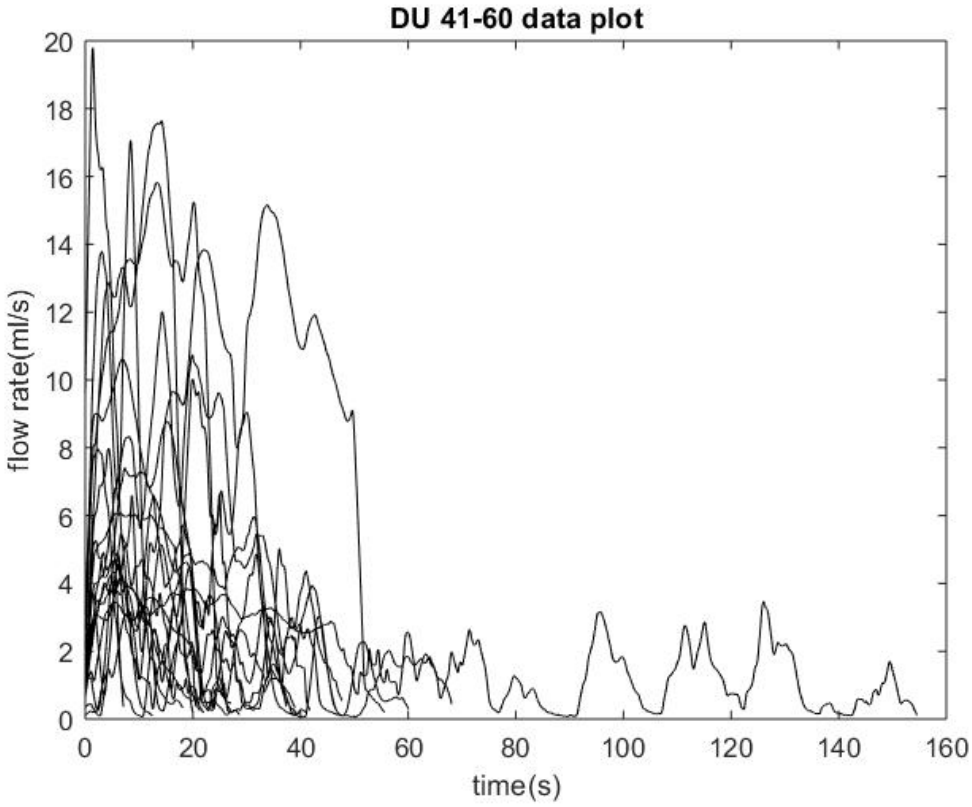
DU 41-60 data plot
flow rate(ml/s)
time(s)
0
2
4
6
8
10
12
14
16
18
20
0
20
40
60
80
100
120
140
160

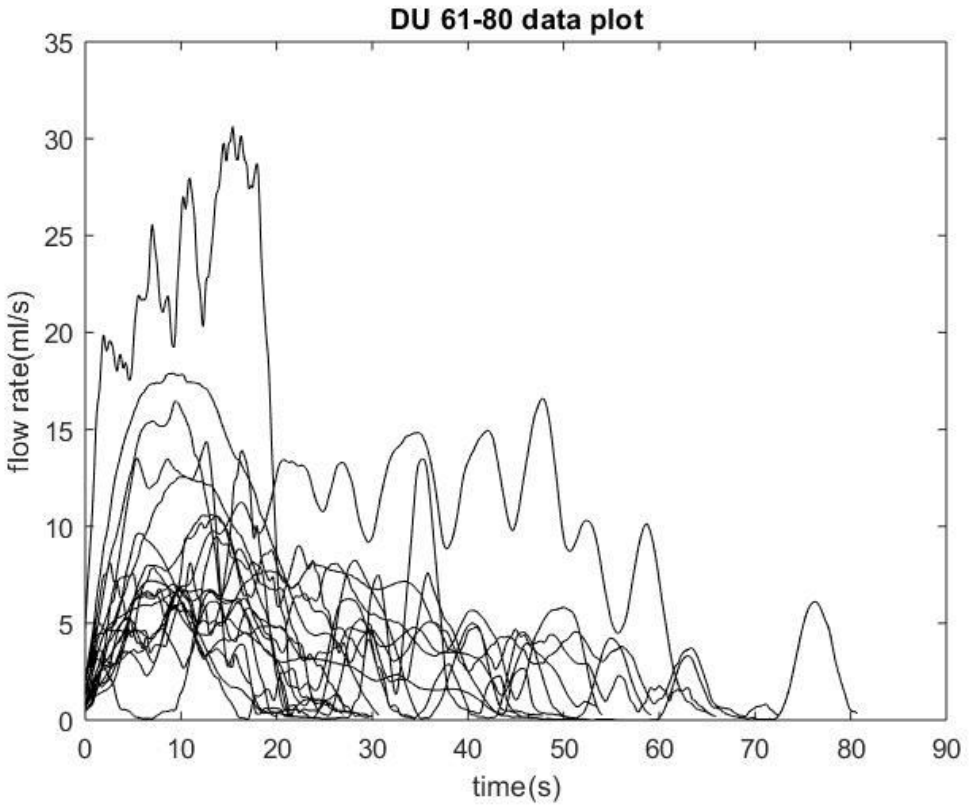
DU 61-80 data plot
flow rate(ml/s)
time(s)
0
5
10
15
20
25
30
35
0
10
20
30
40
50
60
70
80
90

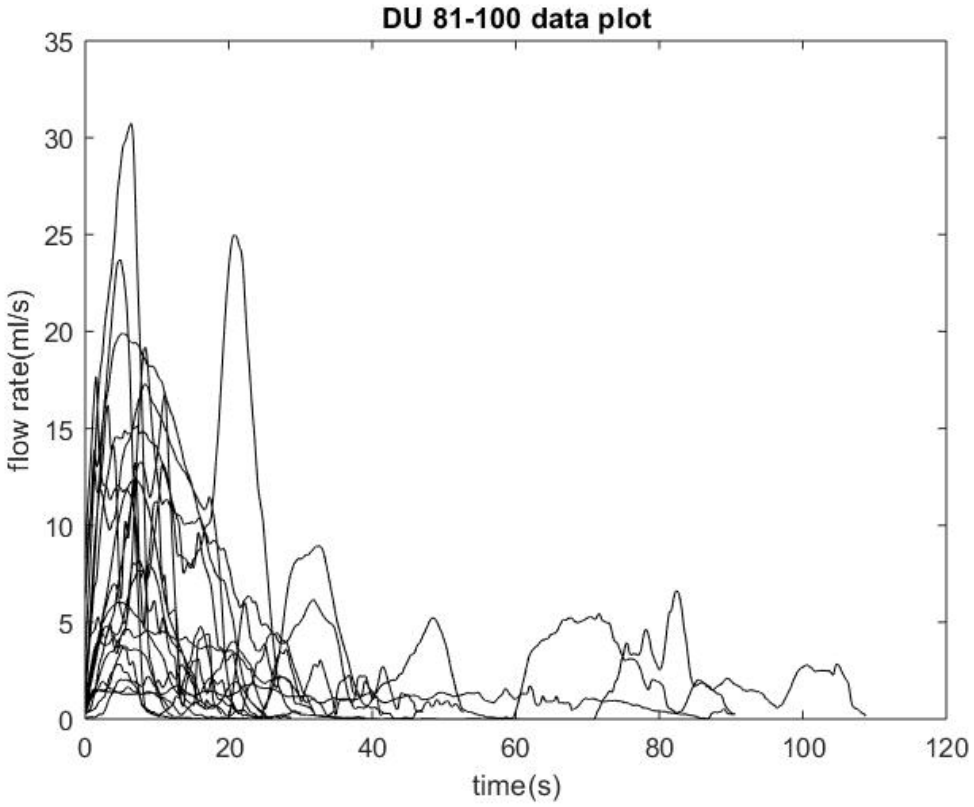
DU 81-100 data plot
flow rate(ml/s)
time(s)
0
5
10
15
20
25
30
35
0
20
40
60
80
100
120

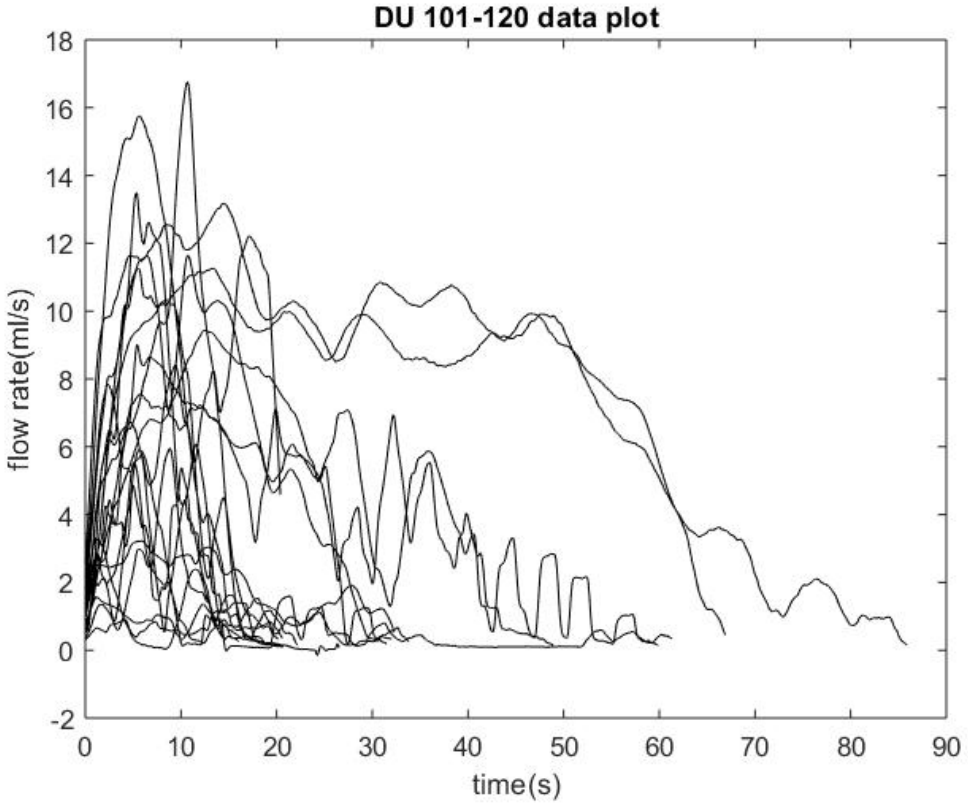
DU 101-120 data plot
flow rate(ml/s)
time(s)
-2
0
2
4
6
8
10
12
14
16
18
0
10
20
30
40
50
60
70
80
90

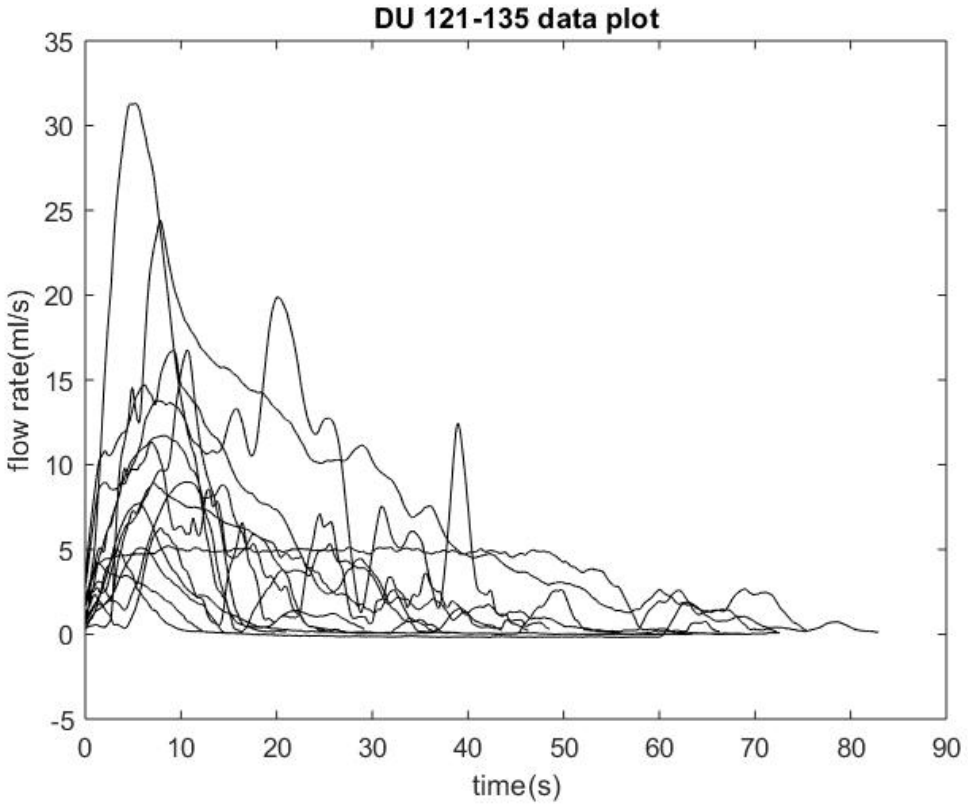
DU 121-135 data plot
flow rate(ml/s)
time(s)
35
30
25
20
15
10
5
0
-5
0
10
20
30
40
50
60
70
80
90

VIII) BOO urine flow rate curve plots

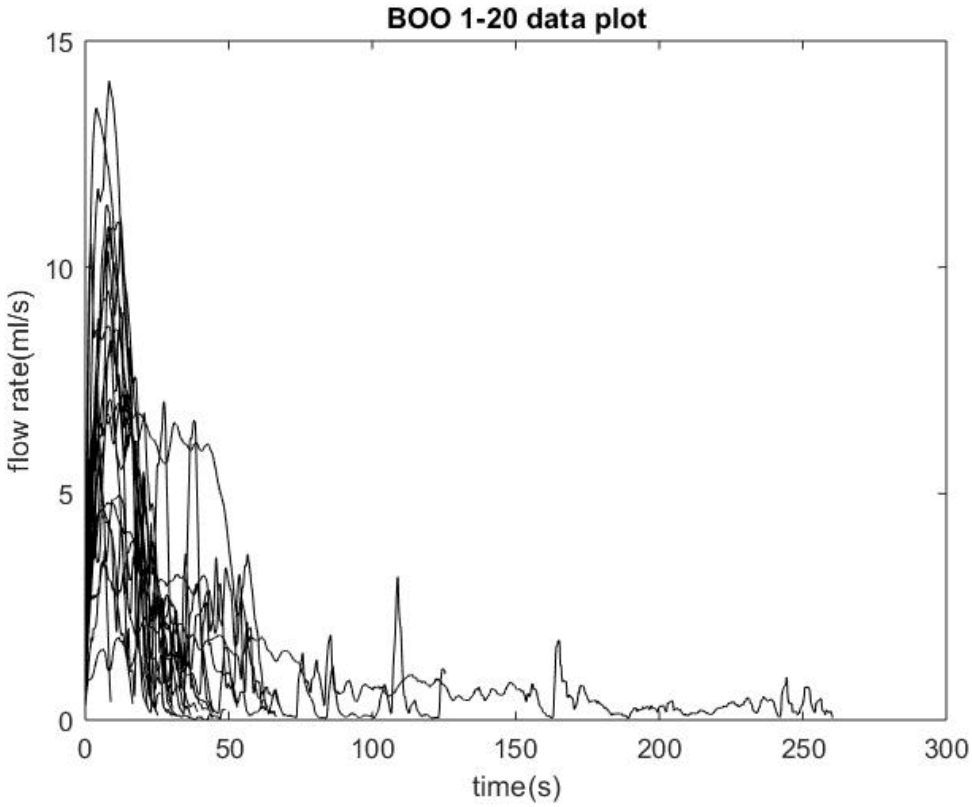

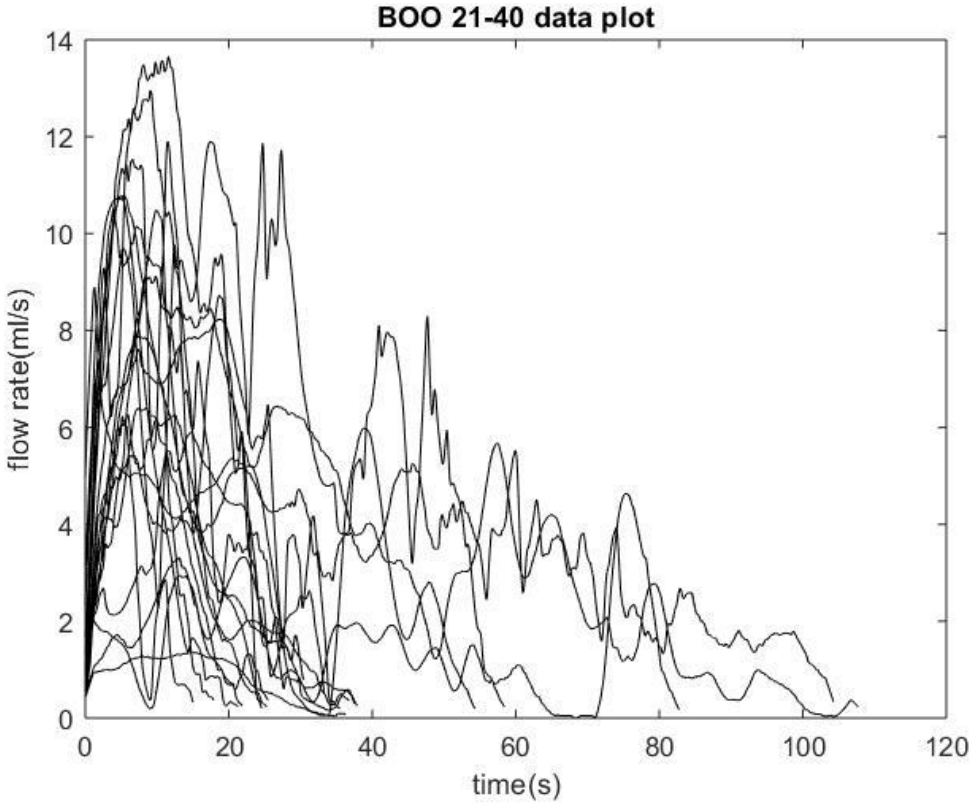

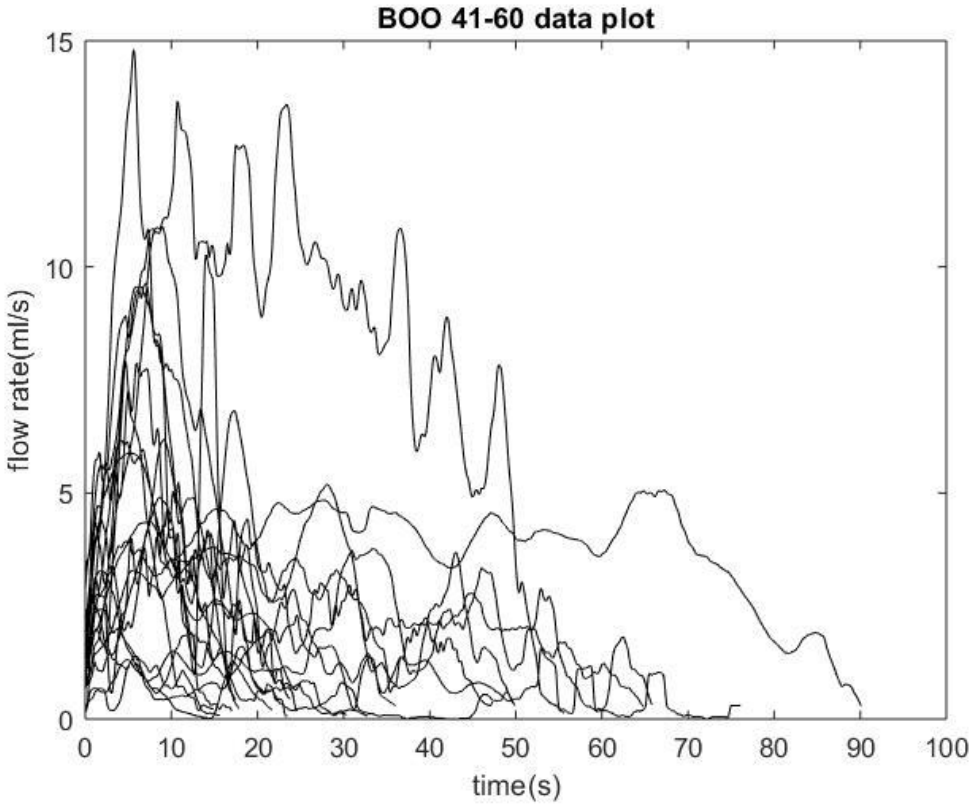
BOO 41-60 data plot
flow rate(ml/s)
time(s)
0
5
10
15
0
10
20
30
40
50
60
70
80
90
100

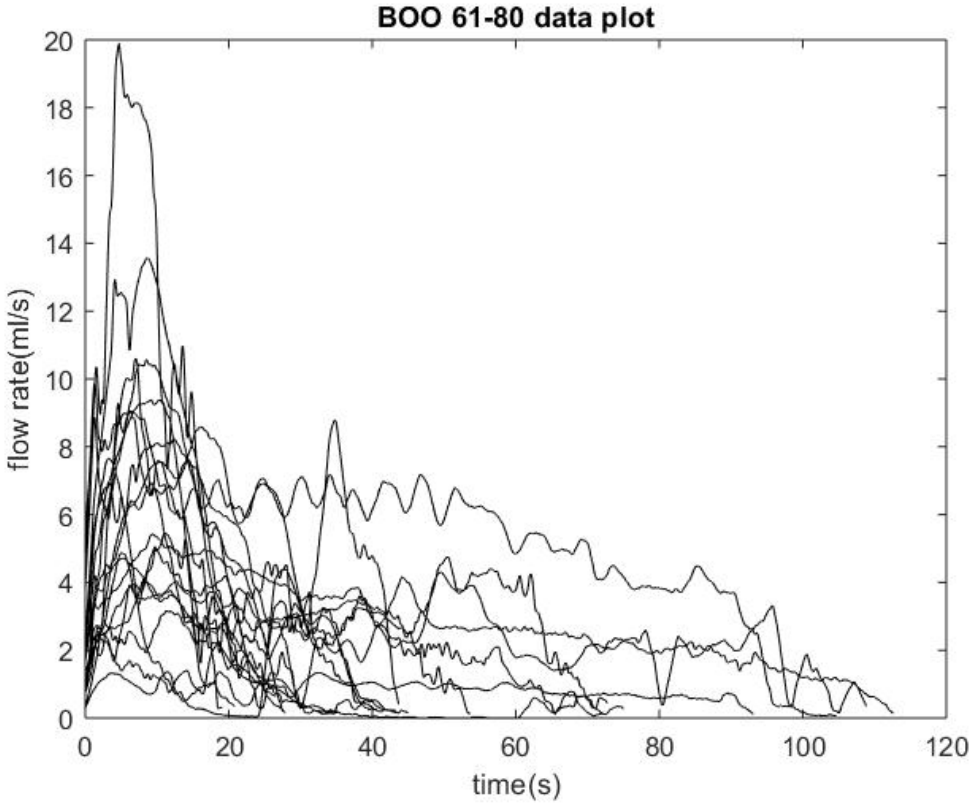
BOO 61-80 data plot
flow rate(ml/s)
time(s)
0
2
4
6
8
10
12
14
16
18
20
0
20
40
60
80
100
120

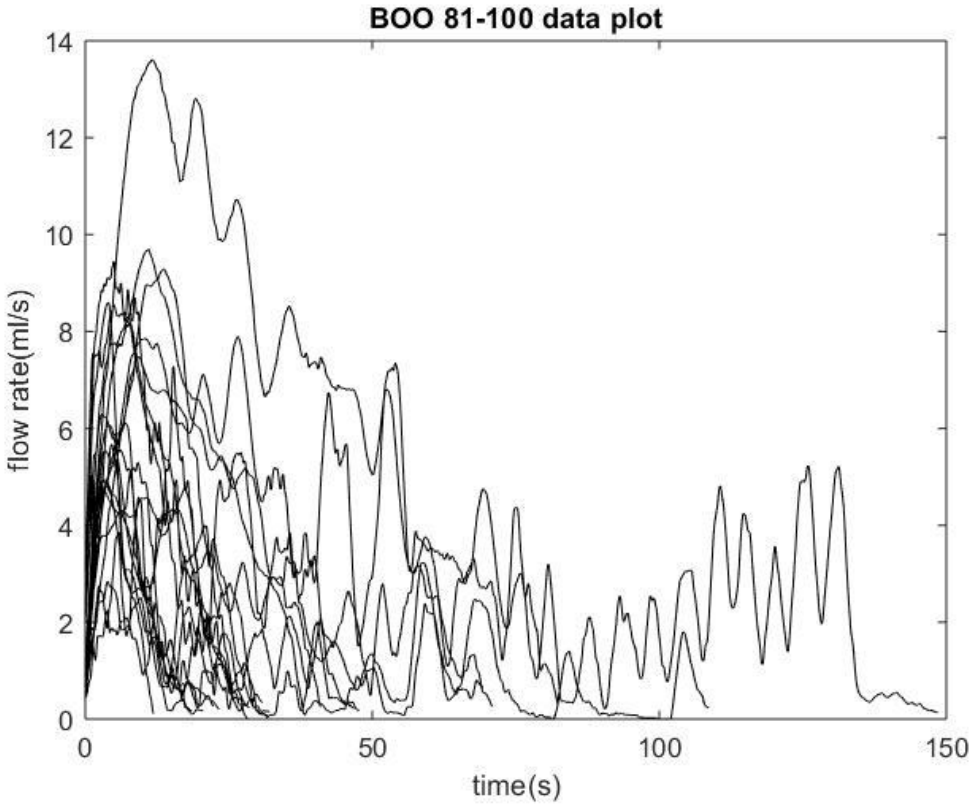
BOO 81-100 data plot
flow rate(ml/s)
time(s)
0
2
4
6
8
10
12
14
0
50
100
150

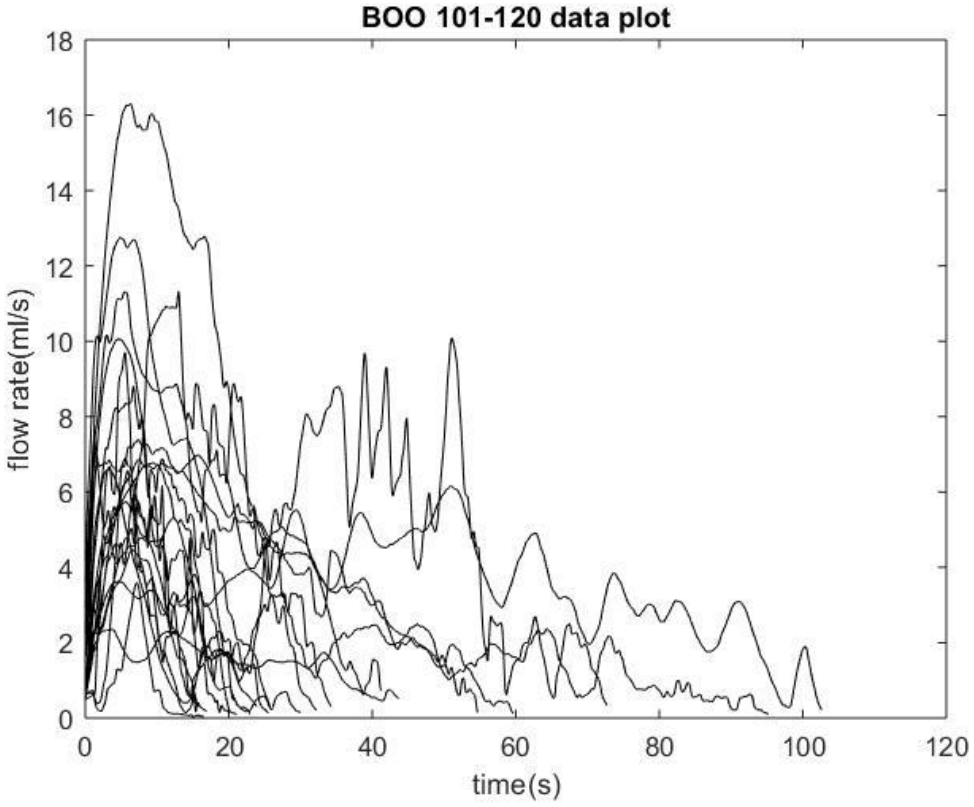
BOO 101-120 data plot
flow rate(ml/s)
time(s)
0
2
4
6
8
10
12
14
16
18
0
20
40
60
80
100
120

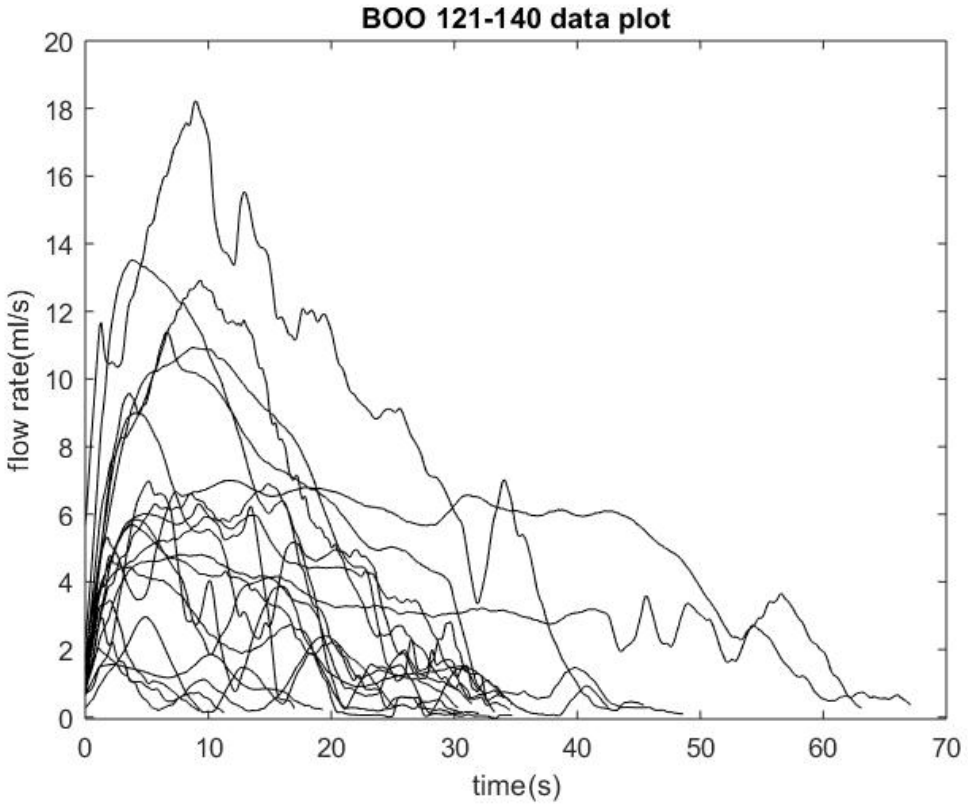

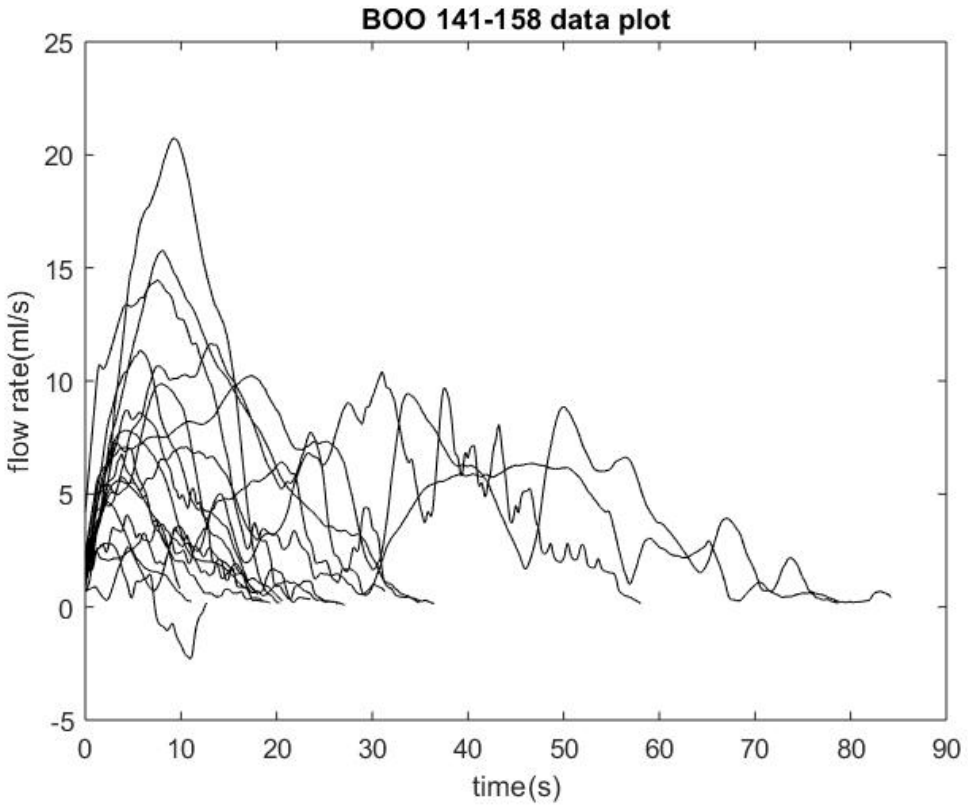

IX) Journal publications

How can we maximise the diagnostic utility of uroflow? : ICI-RS 2017
Andrew Gammie, Peter Rosier, Rui Li, Chris Harding

Neurourology and Urodynamics. 37 (supplement 4), pp. 20-24.

Introduction

The assessment of urine flow rate dates back to the 1950's and uroflowmetry is to date the most widely-used urodynamic assessment. This is in part due to its non-invasive nature, practical simplicity and low cost. The test is recommended as an initial objective evaluation for patients with signs and symptoms of lower urinary tract dysfunction by the UK National Institute for Health and Care Excellence (NICE)[1], European Association of Urology (EAU)[2], International Consultation on Incontinence (ICI)[3] and American Urological Association (AUA)[4]. Although the recommendation for uroflowmetry is relatively undisputed, the evidence with regard to the predictive value of the test is not very well established. Moreover, much of the potential information that a flowrate measurement contains is not very well studied and the evidence about the most studied parameter, maximum flowrate (Q_{max}), is not unambiguous. There is for example discrepancy in practice guidelines regarding recommendations for the use of specific cut-off values for Q_{max} in the assessment of men with lower urinary tract symptoms (LUTS). In a systematic review published recently only 30 studies could be included from a literature search dating back to 1970, confirming a dearth of high-level evidence regarding the diagnostic value of uroflowmetry[5]. The specific aim of this 2017 International Consultation on Incontinence Research Society (ICI-RS) think tank was to explore the question "How can we maximise the diagnostic utility of uroflow?". The areas of current knowledge are discussed with summaries of gaps in that knowledge. Recommendations are then made for studies to address those gaps.

Maximum flow rates

One of the main problems with uroflowmetry is lack of diagnostic specificity associated with the test. The majority of existing work has centred on the ability of urine flow tests to provide an estimation of the likelihood of bladder outflow obstruction (BOO) in male patients. Outflow diameter (flow controlling zone) is directly related to flow rate, but also depends on intravesical pressure, and the parameter that has been most researched is maximum urine flowrate (Q_{max}). The EAU LUTS guidelines comment that "The diagnostic accuracy of uroflowmetry for detecting BOO varies considerably, and is substantially influenced by threshold values"[2]. The evidence for this statement comes from large scale studies such as the ICS BPH study[6]. The study comprised 1271 men aged between 45 and 88 years recruited from 12 centres in Europe, Australia, Canada, Taiwan and Japan. They reported that a threshold Q_{max} of 10 mL/s has a specificity of 70%, a PPV of 70% and a sensitivity of 47% for BOO as defined by invasive urodynamics. Using a higher threshold for Q_{max} of 15 mL/s, the specificity was reduced to 38%, the PPV to 67% and the sensitivity increased to 82%. Thus, as in all diagnostic tests, there is a trade-off between sensitivity and specificity as different (flow rate in this case) thresholds are considered. Lower Q_{max} thresholds are more specific to diagnose BOO but less sensitive and as the threshold is raised the sensitivity increases but specificity decreases.

In women the relevance of maximum flowrate as a cut off is .even more difficult to establish. The prevalence of female BOO is much lower than in males, but may nowadays be increasing, perhaps because of more interventions that can cause outflow obstruction[7,8]**.** Though for most women, flow rates are high (above 15 – 20 mL/s)[9]**, t**he specificity of a low maximum flow rate towards the cause of dysfunction is not fully reported in the literature. Another group not extensively studied is healthy young men, who void with generally lower maximum flow rates than their female counterparts, which was observed especially when the voided volume is relatively low[10]. For women and for younger men, and to a lesser extent elderly men, therefore, very little conclusion can be drawn from uroflowmetry alone. As a starting point, volume correction for interpretation of the maximum flow rate is recently published.[11]

It is well known that maximum flow rate alone is insufficient for a specific diagnosis of LUT function, but there is not yet much evidence that other signs and symptoms, apart from age and gender , can be combined with this measurement to enhance diagnostic power.

Multiple uroflow measurements

Uroflowmetry is a clinical test that is performed by the patient. Inevitably, within-patient variability of the measurements made plays a role in the result. The AUA have noted in their recent guideline that "Clinicians should be aware that uroflow studies can be affected by the volume voided and the circumstances of the test" and advise that "Serial uroflowmetry measurements which are consistent, similar and comparable provide the most valuable information for the clinician."[4] This has led to a general recommendation that uroflowmetry parameters should preferably be evaluated with voided volume >150 mL and that serial measurements are most informative. This is supported by a study from Reynard et al. who concluded that the maximum Q_{max} of three clinic flow measurements provides a valuable improvement in diagnostic power over a single measurement to estimate the likelihood of BOO in elderly males with prostate enlargement[12].

A logical follow-on from these data has been the development of home uroflowmetry devices which can capture multiple voids under "usual" circumstances and thus theoretically reduce single observation inaccuracy. In a systematic review on the subject of home uroflowmetry recently published it was concluded that "the statistical benefit of averaging multiple measurements of Q_{max}, made feasible by home uroflowmetry, should translate to improved diagnostic accuracy and assessment of treatment outcome"[13]. However at the moment further studies are necessary to confirm this benefit, particularly to examine both the diagnostic and predictive value of flow variables derived from multiple recordings.

Flow-volume nomograms

Nomograms that allow for correction of flow rate for either the volume voided or the volume in the bladder are frequently presented and are produced from all urodynamic equipment. However, the utility of these for diagnosis varies greatly and is never strong. These nomograms are unable to provide a urodynamic diagnosis but can indicate the probability of normality of maximum flow rate. The premise that inter-patient volume correction with these nomograms helps to establish better evaluation of treatment effect (on Q_{max}) has not been confirmed.

Siroky[14] produced a flow-volume nomogram from 80 male patients of unreported age, with bladder volume (not voided volume) on the vertical axis. Later, Kadow[15] selected 123 older (between 50 and 80 years) male patients, and formed a nomogram with slower flow rates than Siroky, but using voided volume alone. The most comprehensive set of nomograms came from Haylen's Liverpool study[16], which produced nomograms from 331 male and 249 female patients of a wide age range. The Liverpool nomograms include, as did Siroky, graphs for both maximum and average flow rates, but also included a factor for age in the male equations and used voided volume. More recently, male[17] (bladder volume) and female[18] (voided volume) 'PGIMER' nomograms have been proposed for Indian populations, with factoring for the age of female patients. Additional proposals for male assessment have been made for individualised nomograms based on multiple flows[19] and the D index from within the VBN modelling system[20].

The clinical perspective is that flow rate is a screening test and that normal flow rate can be used to exclude voiding abnormalities. Since the nomograms are all proposed for indicative, rather than diagnostic, use, they are limited in application to initial screening and indication of treatment outcome. Nevertheless the sensitivity, specificity, type of volume measured and influence of age and population type for each nomogram could be more clearly described and understood, otherwise unmerited diagnostic capacity may be assumed.

Flow rate curve shape

The terms used to describe the shape of the urine flow rate curve over time vary considerably. In paediatric urology the analysis of uroflow pattern is standardized to a certain extent[21], although anomalies exist, and shape can serve as a guide to the existence of a specific

condition[3,21, 22]. Since patient inhibition can occur during uroflowmetry, good technical performance of the test is critical, or dysfunction may be erroneously diagnosed on the basis of procedure faults or technical artefacts.

Some of the terms to describe abnormally shaped flow curves may be regarded as confusing. For instance 'staccato-shaped' is used to describe an irregular, fluctuating curve and 'interrupted-shaped' to describe a curve with segments with zero flow[21], yet 'staccato' truly means 'separated, detached'. Standard descriptions of uroflow curve in adults have other difficulties, for instance the descriptions 'constrictive' and 'compressive' are used for different uroflow shapes[23],. Those labels are, however, describing the cause of the shape rather than the shapes themselves. Consistency and clarity in description is therefore required, in order that a full analysis of the diagnostic utility of uroflow shape can be undertaken.

Two research teams have used Q_{max} and Q_{ave} to diagnose urodynamic abnormality, and suggest relevance and applicability.[24, 25] However the accuracy varies when trialled on different databases and the limitations have been discussed[26]. A recent study[27] has presented some mathematical analysis of uroflow curve shape, counting multiple peaks within filtered curves and considering the frequency content of the curve shape, but this has so far analysed only small numbers of patients and the specificity does not yet exceed that of the simple Q_{max} cut-off of 10 ml/s to select symptomatic men with a high likelihood of BOO.

The current definition of dysfunctional voiding[22] is confusing, referring as it does to irregular flowrate caused by inability to void and or by underactivity of the detrusor and / or by outlet smooth or striated muscle activity. A container term as this is not helpful to ensure either optimum management or research to improve treatment for voiding difficulties.

Uroflow time measurements

ICS GUP defines flow time as "the time over which measurable flow actually occurs"[23]. However, the threshold above which flow is considered "measurable" is not defined, and the equipment sensitivity will therefore affect the time value recorded. The end of micturition is presumably considered to be at the end of measurable flow, but most urodynamic pressure flow studies will end with the patient giving a final cough, possibly resulting in measurable leakage which should not be regarded as part of the normal void. A recent study proposed that 0.5 ml/s be used as the standard threshold for registering flow and that post-void leaks be ignored for the purpose of time recording[28]. Rollema[29] reported that diagnosis of bladder outflow obstruction in men could be improved by considering the time from Q_{max} to the point where 95% of voided volume had been voided, but this parameter has never been confirmed and has not become standard.

Other measurements alongside uroflow

Flow lag time, defined as the time between pelvic muscle EMG decrease and urine flow beginning has been reported either to increase or to decrease as an effect of management of a variety of dysfunctional voiding types in children.[30] However, standardisation of meatus to flowmeter distance (or of intravesical or voided volume) has not been carried out in these studies. Pelvic floor dysfunction as a cause for irregular voiding can be expected to be present in adults, although the evidence, e.g. from studies that report pelvic muscle EMG, is lacking[3].

Given that abdominal straining has variable effects on flow rate, it is reasonable to suggest that non-invasive synchronous recording of abdominal pressure be investigated in different groups of patients. One study found that patients with detrusor underactivity are more likely to strain on voiding[31], while another found that men with bladder outlet obstruction strained less[32] which is understandable since a prostate receives just as much pressure increment as the bladder, as a consequence of its intraabdominal position, during abdominal pressure rises.

Areas for research

In view of the gaps in current knowledge detailed above, we recommend that studies be carried out to address the following research questions:

- Can maximum flow rate be improved as a diagnostic criterion for adult women and young adult men?
- Which definition of voiding dysfunction would be best applicable in clinical practice?
- What signs and symptoms can be combined with uroflowmetry to enhance its diagnostic power?
- Should an adult EMG – uroflowmetry test be designed?
- Should an abdominal pressure – uroflowmetry test be designed?
- How can the normalisation of flow rate to volume be improved, and nomograms consequently standardised?
- How can urine flow curve shape analysis be standardized and quantified?
- How can multiple flows and home uroflowmetry be applied to increase diagnostic accuracy?
- How can thresholds and protocols for measuring urine flow time be more clearly defined?

Conclusions

The ICI-RS 2017 meeting has proposed a number of research questions that should be addressed to increase the diagnostic utility of non-invasive uroflowmetry. There is scope for combining uroflowmetry with other non-invasive indicators, and for better standardisation of the test technique, flow-volume nomograms, uroflow shape descriptions and time measurements. Given the ubiquity of the test, and its vulnerability to misunderstanding, there is a need for a consensus document on Good Practice for Uroflowmetry.

REFERENCES

1. Lower urinary tract symptoms in men: management. NICE 2015 Update https://www.nice.org.uk/guidance/cg97
2. EAU Non-neurogenic Male LUTS Guideline 2017. http://uroweb.org/wp-content/uploads/13-Non-Neurogenic-Male-LUTS_2017_web.pdf
3. Abrams P, Cardozo L, Wagg A, Wein AJ. Incontinence: 6th International Consultation on Incontinence, Tokyo, September 2016. ICUD-ICS 2017.
4. American Urological Association Guidelines 2010. Benign Prostatic Hyperplasia. https://www.auanet.org/guidelines/benign-prostatic-hyperplasia-(2010-reviewed-and-validity-confirmed-2014)
5. R Veeratterapillay, RS Pickard, C Harding. The role of uroflowmetry in the assessment and management of men with lower urinary tract symptoms – revisiting the evidence. J Clin Urol 2013; 7(3):154–158
6. Reynard, J.M., et al. The ICS-'BPH' Study: uroflowmetry, lower urinary tract symptoms and bladder outlet obstruction. Br J Urol 1998; 82:619
7. Choi YS, Kim JC, Lee KS, Seo JT, Kim HJ, Yoo TK, Lee JB, Choo MS, Lee JG, Lee JY. Analysis of female voiding dysfunction: a prospective, multi-center study. Int Urol Nephrol. 2013; 45(4):989-94.
8. Salin A, Conquy S, Elie C, Touboul C, Parra J, Zerbib M, Debré B, Amsellem-Ouazana D. Identification of risk factors for voiding dysfunction following TVT placement. Eur Urol. 2007; 51(3):782-7; discussion 787.
9. Sorel MR, Reitsma HJB, Rosier PFWM, Bosch RJLHR, de Kort LMO. Uroflowmetry in healthy women: A systematic review. Neurourol Urodyn 2017; 36(4):953-959.
10. Kaynar M, Kucur M, Kiliç O, Akand M, Gul M, Goktas S. The effect of bladder sensation on uroflowmetry parameters in healthy young men. Neurourol Urodyn 2016; 35(5):622-4.
11. Agarwal MM, Patil S, Roy K, Bandawar M, Choudhury S, Mavuduru R, Sharma SK, Mandal AK, Singh SK. Rationalization of interpretation of uroflowmetry for a non-caucasian (Indian) population: conceptual development and validation of volume-normalized flow rate index. Neurourol Urodyn 2014; 33(1):135-41.
12. Reynard JM, Peters TJ, Lim C, et al. The value of multiple free-flow studies in men with lower urinary tract symptoms. Br J Urol 1996; 77:813–8.
13. Bray A, Griffiths C, Drinnan M, Pickard R. Methods and value of home uroflowmetry in the assessment of men with lower urinary tract symptoms: A literature review. Neurourol Urodyn 2012; 31:7–12.
14. Siroky MB, Olsson CA, Krane RJ. The flow rate nomogram: I. Development. J Urol 1979; 122:665-8.
15. Kadow C, Howells S, Lewis P, Abrams P. A flow rate nomogram for normal males over the age of 50. Proceedings of the 15th Annual Meeting of the International Continence Society, London, 1985:138-9.
16. Haylen BT, Ashby D, Sutherst JR, et al. Maximum and average urine flow rates in normal male and female populations-the Liverpool nomograms. Br J Urol 1989; 64:30.
17. Agarwal MM, Patil S, Roy K, Bandawar M, Choudhury S, Mavuduru R, Sharma S K, Mandal AK, Singh SK. Rationalization of interpretation of uroflowmetry for a non-caucasian (Indian) population: conceptual development and validation of volume-normalized flow rate index. Neurourol Urodyn 2014; 33:135–141.
18. Barapatre Y, Agarwal MM, Singh SK, et al. Uroflowmetry in healthy women: Development and validation of flow-volume and corrected flow-age nomograms. Neurourol Urodyn 2009; 28:1003-1009.
19. Bray A, Harding C, Pickard R, Drinnan M. Individualized volume-corrected maximum flow rate correlates with outcome from bladder outlet surgery in men with lower urinary tract symptoms. Int J Urol 2016; 23:587–592.

20. Valentini FA, Nelson PP, Zimmern PE. Non-Invasive Evaluation of Bladder Outlet Obstruction in Men Suspected of Benign Prostatic Hyperplasia: Usefulness of the D Index. Curr Urol 2012; 6:124–128.
21. Austin PF, Bauer SB, Bower W et al. The standardization of terminology of lower urinary tract function in children and adolescents: Update report from the standardization committee of the International Children's Continence Society. Neurourol Urodyn 2016; 35: 471–481.
22. Artibani W, Cerruto MA. Dysfunctional voiding. Curr Opin Urol 2014; 24(4):330-5.
23. Schaefer W, Abrams P, Liao L, Mattiasson A, Pesce F, Spangberg A, Sterling AM, Zinner NR, van Kerrebroeck P, International Continence S. Good Urodynamic Practices: Uroflowmetry, Filling Cystometry, and Pressure-Flow Studies". Neurourol Urodyn 2002; 21:261-274.
24. Futyma K, Nowakowski Ł, Bogusiewicz M, Ziętek A, Wieczorek AP, Rechberger T. Use of uroflow parameters in diagnosing an overactive bladder—Back to the drawing board. Neurourol Urodyn 2015; 36:198–202.
25. Kwon SL, Phil HS, Young HK. Does uroflowmetry parameter facilitate discrimination between detrusor underactivity and bladder outlet obstruction? Investig Clin Urol 2016; 57(6):437–441
26. Schaefer W. RE: Futyma et al. use of uroflow parameters in diagnosing an overactive bladder — Back to the drawing board and ICS News 613. Neurourol Urodyn 2017;
27. Li R, Gammie A, Zhu Q, and Nibouche M. Mathematical modelling analysis of male urine flow trace. International Continence Society 2016 conference, Japan. Poster 144.
28. Gammie A, Yoshida S, Steup A et al. Flow time and voiding time – definitions and clinical usefulness. N&U in preparation.
29. Rollema HJ. Uroflowmetry in males. PhD thesis, University of Groningen, 1981.
30. Van Batavia JP, Combs AJ, Fast AM, Glassberg KI. Use of non-invasive uroflowmetry with simultaneous electromyography to monitor patient response to treatment for lower urinary tract conditions. J Pediatr Urol 2014; 10(3):532-7.
31. Gammie A, Kaper M, Dorrepaal C, Kos T, Abrams P. Signs and Symptoms of Detrusor Underactivity: An Analysis of Clinical Presentation and Urodynamic Tests From a Large Group of Patients Undergoing Pressure Flow Studies. Eur Urol. 2016; 69:361-9.
32. Reynard JM, Peters TJ, Lamond E, Abrams P. The significance of abdominal straining in men with lower urinary tract symptoms. Br J Urol. 1995; 75(2):148-53.

Urine flow rate curve shapes and their descriptors

Rui Li, Andrew Gammie, Quan Zhu, Mokhtar Nibouche
Neurourology and Urodynamics. 37(8), pp. 2289-2989

Abstract

Aims: To review the descriptors and definitions of urine flow rate curve shape with a view to promoting greater clarity and to propose standard terms

Methods: A search was made in the PubMed and ICS standardization documents on urine flow rate curve shape.

Results: The flow shape descriptors and their definitions are summarised and presented. 'Normal' was widely used for describing a bell-shaped flow curve, and 'plateau' was mostly used where the ICS describe 'constrictive' flow shape. The use of shape descriptors 'fluctuating', 'compressive', 'tower-shaped' and 'intermittent' varied in the literature.

Conclusion: This survey provides an overview of flow shape descriptors and their definitions. We suggest it is clearer to use only descriptors that describe shape alone, i.e. normal, fluctuating, intermittent and plateau, with comments on symmetry and Q_{max}.

Introduction

Uroflowmetry serves as a preliminary urodynamic test for physicians to indicate the possible cause of lower urinary tract symptoms (LUTS). Alongside the most researched parameter maximum flow rate (Q_{max}), the shape of urine flow rate curve is also reported to associate with one or more voiding abnormalities.[1]

The International Continence Society (ICS) defines a normal flow shape as 'arc-shaped with high maximum flowrate'.[2] However, the definition did not quantitatively specify the parameter range for normal shape. More quantitative definitions have therefore been proposed. For example, Nishimoto et al.[3] use three parameters, the ratio of maximum flow rate (Q_{max}) and the voiding time (T_v), the ratio of time to peak flow (TQ_{max}) and T_v, and the ratio of the average flow rate (Q_{ave}) and Q_{max}, to differentiate normal and abnormal shape, but this has not become standard.

As suggested by Gammie et al.[4] from the ICI-RS 2017 meeting, the present study investigates the shape of urine flow curve described in the literature and highlights the problems with these descriptors. Proposals for standardised use are suggested.

Methods

A literature search was made in PubMed and ICS standardisation documents, for titles and abstracts of papers including 'shape' or 'pattern', and additionally including 'urodynamic' or 'uroflow' or 'urine flow' or 'uroflowmetry' or 'urinary flow' dated to 5 January 2018. The search resulted in a total of 680 articles. After the selection procedure (Figure 1), 22 articles

were included in this survey.[2,3,5-24]

Results

The flow shape descriptors in the literature were summarised first under the shape name that the ICS has defined,[5,6] namely 'normal', 'constrictive', 'compressive', 'fluctuating' and 'intermittent'. Further definitions, such as 'tower' used by the International Children's Continence Society (ICCS), were included and where possible listed under the relevant ICS definition. A detailed summary of shape definitions is presented as in table 1.

1. Normal

The definitions of normal flow curve are similar in most articles, which are bell-shaped or arc-shaped, approximately symmetrical, uninterrupted and with no rapid amplitude changes.[3-18,20-23] ICCS specifies in children the bell-shaped curve should be regardless of volume voided.[5] Nishimoto et al. suggest quantitative definition using values for the parameters noted above[3] ($Q_{max}/T_v \geq 0.78$, $0.32 \leq TQ_{max}/T_v \leq 0.54$, $Q_{ave}/Q_{max} < 1.59$). Four other articles specifically define normal flow shape: Wyndaele suggests $Q_{max} > 15$ml/s,[8] Abrams indicates Q_{max} appears in first 30% of curve and within 5 seconds from start,[9] Mostafavi et al. use flow within 5% to 90% range of the Iranian nomogram and $Q_{max}^2 >$ volume voided for normal shape,[13] and Ghobish uses time ratio ($T_r = TQ_{max}$/flow time) of 25%-60% and flow ratio ($Q_r = Q_{ave}/Q_{max}$) of 25%-75% to define normal shape.[18]

2. Constrictive

Schaefer et al. in the ICS Good Urodynamic Practices document define constrictive shape as a smooth, flat and plateau-like curve with lower flow rate.[2] It is named as plateau in 10 articles,[5,7,12-17,20,21] and in other articles as 'long flow + low max flow',[8] long and low Q_{max},[11] box-shaped,[18] and prolonged.[19] It is agreed in most articles that constrictive flow shape has a relatively longer flow time, flattened shape with a constant Q_{max} almost the same as Q_{ave}. In addition, five articles have given a more specific definition: variations less than 1ml/s,[12,14] variation<1ml/s for at least 4 seconds,[20] Q_{max}/flow time<0.5,[13] Q_r>80% and T_r<10%.[18]

3. Compressive

ICS defines the compressive flow shape as a flattened asymmetric low curve with a slowly declining end part.[2] Additionally Ghobish defines it by 30%-60% Q_r and 10-25% T_r[18], and van der Vis-Melsen et al. name it 'low flat' with definition of flat flow with low average and maximum index of urine transport (IUT, the ratio of flow rate and square root of bladder volume).[23] Other researchers have mostly the same definition as ICS, but use different terms: slow start,[8] flattened,[16] low flow,[17] long-tail,[18] approximately normal,[19] and prostatic.[21]

4. Fluctuating

Fluctuating flow shape is described by the ICS as a continuous urine flow having multiple peaks.[5]. The ICCS[7], and also Mostafavi et al.[13] call it staccato, and define it as an irregular fluctuating curve without flow reaching zero, where fluctuations are greater than root of Q_{max}. The shape is named as fluctuating in five other articles with the same definition as in ICS.[8,13,16,17,21] Two articles name this flow pattern as intermittent, defined as a wavy curve not reaching the baseline with a duration of at least 15 seconds,[20] and variations in flow rate of at least 5ml/s.[22] Fantl calls it multiple peak, and specifies that the 2nd peak amplitude should be higher or equal to 20% of Q_{max}[10]. Pauwels names this flow shape undulating, and defines it as asymmetric curve with steep slope, with a long and flattened foothill.[10] van der Vis-Melsen et al. call this shape sawtooth and define with low average IUT and normal maximum IUT.[23]

5. Intermittent

The intermittent flow shape is defined as flow stopping and starting during a single void in an ICS standardisation document.[6] Other defined names are: interrupted,[7,10,13,18] fractioned, [21] void 2x,[8] fractionated[11,17,20,22] and sawtooth.[15] Even though the name of this shape varies, the definition is generally the same as the ICS standardisation. Three articles give additional definitions for this shape. Fantl considers intermittent as flow less than 2ml/s instead of completely stopping,[10] Ghobish further subdivided intermittency into two patterns by interruption duration threshold of ≤ 2 second, named type A, and repeated interruptions due to abdominal straining as type B,[18] and Jensen et al. define intermittent flow as lasting for at least 15 seconds of flow time with one or more interruptions.[20]

6. Tower-shaped

This shape has not been defined in any ICS document, but ICCS defines it as sudden, high-amplitude flow with short duration.[6] Abrams calls it supranormal and gives the more specific definition of a sharply increase flow to a very high Q_{max} in the first 1-3 seconds, and followed by a sudden reduction.[9] Chou et al.[16] and Jorgensen et al.[17] call this shape 'tall and peaked' and 'high flow' respectively, but the definition is similar to ICCS. Using Q_{max}>95% on the Iranian nomogram, Mostafavi et al. also call this pattern 'tower'.[13]

7. Other shape definitions

Ghobish defines two extra shapes: 'high start' as 20%-60% Q_r and 0-10% T_r to describe a sudden rise to Q_{max} then steep steady fall shape, and 'inverted long-tail' as 30%-60% Q_r with T_r>60% to describe a steady rise then sudden fall down shape.[18]

Shih investigates flow shape by using a geometric approach and divides flow patterns into three groups by quantitative classification rules. An almost normal to mildly obstructive shape is defined as Q_{max}≥15ml/s when volume voided ≥200ml or Q_{max} ≥10ml/s when volume voided <200ml, and time to Q_{max} is in the range of 5 seconds to 5/12 flow time, and Q_{max}/Q_{ave} >4/3. A moderately to severely obstructive pattern is defined as Q_{ave} ≤4ml/s or flow time ≥90 seconds

when volume voided is less than 400ml. The remaining patterns are recognised as mildly to moderately obstructive.[24]

Discussion

The urine flow curve shape contains relevant and interpretable information on a patient's urinary conditions, and it is suggested it could serve as a guide to identify LUT dysfunction.[2,5,7] However, the definitions found in the literature are not consistent and it is not possible to uncover pathophysiology when terms are not consistently used. In ICS Good Urodynamic Practices, the shape definitions of constrictive and compressive are describing the presumed cause of the shape, not the shape itself.[2,4] Since the musical definition of staccato follows the Italian meaning 'detached', the use of this phrase for fluctuating yet continuous flow is misleading.

The start and end point for a flow curve is not properly defined. For instance, an early or end dribble is normally included in the flow curve, as it is a part of voiding, but the shape could therefore be classified as intermittent even the rest of flow is bell-shaped. Jensen et al. exclude 'bubbles', i.e. small separate flows, less than 2ml/s at the start and end of micturition for pre-processing of the flow data.[20] A recent study proposed that 0.5ml/s could be used as the threshold point for the starting and ending point of micturition,[25] which may help avoid erroneous classification of urine flow shape, but this has not become standard.

The present survey summarises the descriptors used for flow shape and their definitions, compared with current ICS/ICCS standardization. We found that the descriptor and definition for normal flow shape was consistently used, while plateau was mostly used for describing ICS's 'constrictive' shape. The descriptors of compressive, fluctuating, intermittent and tower-shaped varied in the literature, with some researchers giving more quantitative definitions for these shapes.

There is no strong correlation between any shape to specified symptoms or diagnosis reported in these articles. Furthermore, Pauwels et al. demonstrates that a bell-shaped curve could not be an exclusion criterion of voiding dysfunction in women,[11] and Chou et al. noted that the flow pattern could not be used as a screening test for urinary dysfunctions.[16]

We therefore propose that only shape descriptors that refer to actual shape, easily defined, are the ones considered for standard use. We suggest using normal, fluctuating, intermittent as defined by the ICS, and plateau instead of the ICS's 'constrictive', for describing flow shape, with additional comment on symmetry and Q_{max}. This removes from use descriptors that are misleading, e.g. 'staccato' and 'biphasic'. A complex flow shape could be described as a combination of descriptors or with specified Q_{max} detail. For example, 'compressive' could be expressed as an asymmetric shape with low Q_{max} in the first half, and 'tower' described as a normal shape with a very high Q_{max}.

Any definitions that refer to possible cause are not recommended, such as prostatic, constrictive and compressive, as it may be taken by inexpert observers to imply diagnosis. Other definitions requiring detailed mathematical analysis are not readily usable, and could therefore only be recommended if diagnostic specificity could be proven. As yet, no shape definition fulfils these criteria.

Conclusion

The varying descriptors of urine flow curve shape cause confusion and may result in inaccurate clinical screening. Consistency and clarity in description are required, and development of standardisation of shape descriptors is recommended. We suggest that only 'normal', 'fluctuating', 'intermittent' and 'plateau' descriptions, with additional comment on symmetry and Q_{max}, be used to describe urine flow rate curve shape, and the definitions for these descriptors should follow the terms in the ICS standardization documents

REFERENCES

1. Abrams P, Cardozo L, Wagg A, Wein AJ. Incontinence: 6th International Consultation on Incontinence, Tokyo, September 2016. ICUD-ICS 2017.
2. Schäfer W, Abrams P, Liao L, Mattiasson A, Pesce F, Spangberg A, Sterling AM, Zinner NR, Kerrebroeck PV, International Continence Society. Good urodynamic practices: Uroflowmetry, filling cystometry, and pressure - flow studies. *Neurourol Urodyn*. 2002;21(3):261-274.
3. Nishimoto K, Iimori H, Ikemoto S, Hayahara N. Criteria for differentiation of normal and abnormal uroflowmetrograms in adult men. *British Journal of Urology*. 1994;73(5):494-497
4. Gammie A, Rosier P, Li R, Harding C. How can we maximize the diagnostic utility of uroflow?: ICI-RS 2017. *Neurourol Urodyn.* Early view. DOI: 10.1002/nau.23472. Published online: 9 JAN 2018
5. Abrams P, Cardozo L, Fall M, Griffiths D, Rosier P, Ulmsten U, van Kerrebroeck P, Victor A, Wein A. The Standardisation of Terminology of Lower Urinary Tract Function. *Neurourol Urodyn.* 2002;21(2):167-178
6. Haylen BT, de Ridder D, Freeman RM, Swift SE, Berghmans B, Lee J, Monga A, Petri E, Rizk DE, Sand PK, Schaer GN. An International Urogynecological Association (IUGA)/International Continence Society (ICS) joint report on the terminology for female pelvic floor dysfunction. *Int Urogynecol J*. 2010 Jan;21(1):5-26.
7. Austin PF, Bauer SB, Bower W, Chase J, Franco I, Hoebeke P, Rittig S, Vande Walle J, von Gontard A, Wright A, Yang SS, Nevéus T. The standardization of terminology of lower urinary tract function in children and adolescents: update report from the Standardization Committee of the International Children's Continence Society. *J Urol.* 2014;191(6):1863-1865
8. Wyndaele JJ. Normality in urodynamics studied in healthy adults. *J Urol*. 1999;161(3):899-902.
9. Abrams, P. Urodynamics. 2006; 3rd edition. Springer-Verlag London
10. Fantl JA, Smith PJ, Schneider V, Hurt WG, Dunn LJ. Fluid weight uroflowmetry in women. *Am J Obstet Gynecol*. 1983;145(8):1017-24.
11. Pauwels E, De Wachter S, Wyndaele JJ. A normal flow pattern in women does not exclude voiding pathology. *Int Urogynecol J Pelvic Floor Dysfunct*. 2005;16(2):104-8;
12. Gutierrez SC. Urine flow in childhood: a study of flow chart parameters based on 1,361 uroflowmetry tests. *J Urol*. 1997;157(4):1426-8.
13. Mostafavi SH, Hooman N, Hallaji F, Emami M, Aghelnezhad R, Moradi-Lakeh M, Otukesh H. The correlation between bladder volume wall index and the pattern of uroflowmetry/external sphincter electromyography in children with lower urinary tract malfunction. *J Pediatr Urol*. 2012;8(4):367-74.
14. Babu R, Harrison SK, Hutton KA. Ballooning of the foreskin and physiological phimosis: is there any objective evidence of obstructed voiding? *BJU Int*. 2004;94(3):384-7.

15. Boothroyd AE, Dixon PJ, Christmas TJ, Chapple CR, Rickards D. The ultrasound cystodynamogram--a new radiological technique. *Br J Radiol*. 1990;63(749):331-2.
16. Chou TP, Gorton E, Stanton SL, Atherton M, Baessler K, Rienhardt G. Can uroflowmetry patterns in women be reliably interpreted? *Int Urogynecol J Pelvic Floor Dysfunct*. 2000;11(3):142-7.
17. Jørgensen JB, Colstrup H, Frimodt-Møller C. Uroflow in women: an overview and suggestions for the future. I*nt Urogynecol J Pelvic Floor Dysfunct*. 1998;9(1):33-6.
18. Ghobish AA. Quantitative and qualitative assessment of flowmetrograms in patients with prostatodynia. *Eur Urol.* 2000;38(5):576-83.
19. Kinahan TJ, Churchill BM, McLorie GA, Gilmour RF, Khoury AE. The efficiency of bladder emptying in the prune belly syndrome. *J Urol*. 1992; 148:600-3.
20. Jensen KM, Nielsen KK, Jensen H, Pedersen OS, Krarup T. Urinary flow studies in normal kindergarten--and schoolchildren. *Scand J Urol Nephrol.* 1983;17(1):11-21.
21. Jørgensen, J. Balslev and Jensen, K. M.-E. and Klarskov, P. and Bernstein, Inge and Abel, Ivan, Mogensen, P. Intra- and inter- observer variations in classification of urinary flow curve patterns. *Neurourol Urodyn*. 1990;9(5):535-539.
22. Mattsson S, Spångberg A. Urinary flow in healthy schoolchildren. *Neurourol Urodyn*. 1994;13(3):281-96.
23. van der Vis-Melsen MJ, Baert RJ, Rajnherc JR, Groen JM, Bemelmans LM, De Nef JJ. Scintigraphic assessment of lower urinary tract function in children with and without outflow tract obstruction. *Br J Urol*. 1989;64(3):263-9.
24. Shih WJ. A geometric approach to the analysis of physiological flow data. *Stat Med*. 1994;13(3):261-73.
25. Gammie A, Yoshida S, Steup A, Kaper M, Dorrepaal C, Kos T, Abrams P. Flow time and voiding time – definitions and use in identifying detrusor underactivity. *Neurourol Urodyn*. 2016;35:s68.

Mathematical analysis on Urine Flow Traces for Non-invasive Diagnosis of Detrusor Underactivity in Men

Rui Li, Andrew Gammie, Quan Zhu, Mokhtar Nibouche

Neurourology and Urodynamics. 36 (supplement 3), pp. 87-88.

Hypothesis / aims of study

Detrusor underactivity (DU) is still largely under researched and can only be diagnosed by invasive pressure flow studies (PFS). Theoretically, the flow shape of DU is different from bladder outlet obstruction (BOO), but in practice PFS is the only gold standard for diagnosing DU. It is suggested that detrusor muscle contraction and abdominal squeezing act in total different frequencies, 0.1Hz and 1Hz respectively, which could be an indicator for differentiating DU and BOO [1]. However, this hypothesis has not been quantitatively validated. Therefore, continuing last year's research [2], we have conducted a novel study on validating frequencies of abdominal and detrusor muscle activity as reflected in urine flow, and propose a potential indicator for diagnosing DU.

Study design, materials and methods

Urine flow data of 114 adult male patients who had undergone PFS were analysed. Based on their PFS record, these patients were divided into three groups: 46 BOO, 44 DU, and 24 normal (DU and BOO disease free). A free urine flow rate was performed before each PFS, and the shape of those flows analysed. The starting and ending voiding point was selected by the threshold value of 0.5ml/s. Then a third order Butterworth filter was applied on the urine flow rate curve with different cut-off frequencies (1Hz, 0.8Hz, 0.6Hz, 0.5Hz, 0.3Hz and 0.1Hz), to count the peak numbers in each raw curve and filtered curve. The ratio of the number of peaks in the raw curve and the filtered curves was calculated for statistical analysis to find the best sensitivity/specificity for diagnosing DU. An example plot of raw curve and 1Hz filtered curve is presented in figure 1.

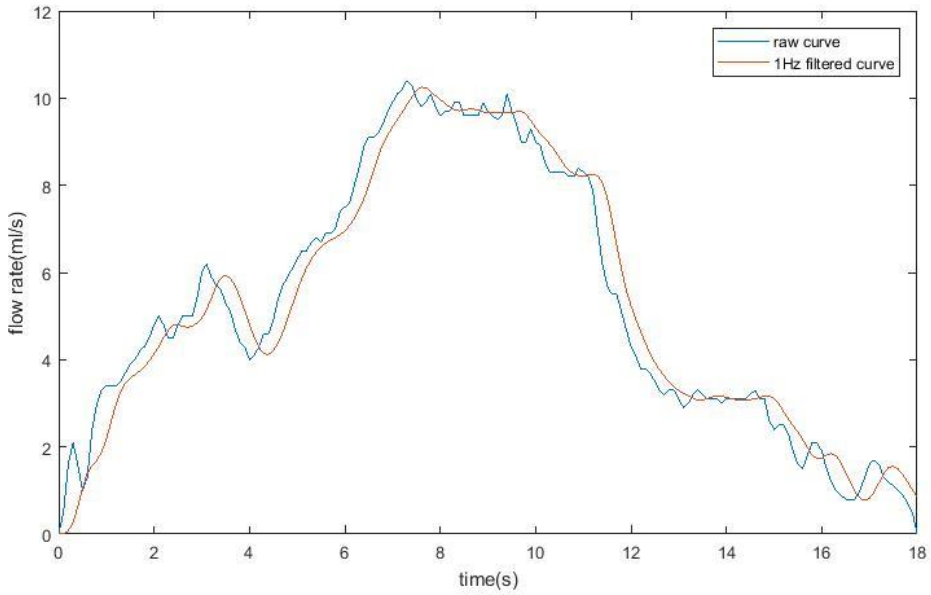

Figure 1 Raw urine flow rate curve and 1Hz filtered curve

All statistical analysis was performed in SPSS version 23, Mann-Whitney U test and T-student test were performed as appropriate. A statistically significant difference was considered as *P* value<0.05.

Results

We found the best statistically significant difference (*P*<0.002) on DU/BOO in ratio of peak numbers of 1Hz filtered curve against 0.1Hz filtered curve, followed by raw curve against 0.1Hz filtered curve with *P* value of 0.002 and 0.8Hz against 0.1Hz with *P* value of 0.002. Further receiver operating characteristic (ROC) analysis was performed on these three peak ratios in DU against with BOO and disease free group. The plot of ROC is presented as in figure 2.

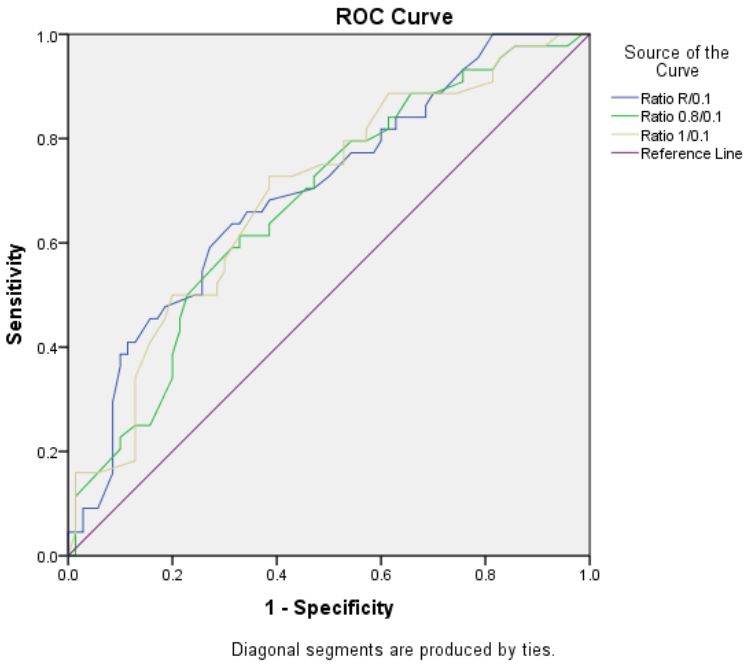

Figure 2 ROC analysis on ratio of peak numbers in raw curve/0.1Hz filtered curve, 0.8Hz/0.1Hz filtered curve and 1Hz/0.1Hz filtered curve

The ratio of peak numbers in 1Hz filtered curve against 0.1Hz filtered curve has the largest area under the curve of 0.691. With cut-off value of 8.37, the best sensitivity and specificity for diagnosing DU are 73% and 61% respectively.

Interpretation of results

It is suggested in urine flow rate data, an averaging should be taken in a 2 second window for reducing drops and artefacts [3], which equates to a 1Hz filter for a 10Hz sampling rate urodynamic equipment. In this research, we found the best diagnosing power for DU is the ratio of peak numbers in 1Hz filtered against 0.1Hz filtered curve. As DU patients have relativity lower detrusor contractility than BOO patients, they may have more abdominal straining for voiding out the urine. Therefore, we found the ratio of peak numbers in before and after filtering abdominal squeezing curve has significant statistical difference between DU group and BOO group. This result also verifies the hypothesis of frequencies for abdominal and detrusor squeezing are around 1Hz and 0.1Hz respectively.

Concluding message

This study shows promising non-invasive indicator for diagnosing DU in men by comparing the number of peaks in 1Hz filtered curve against the 0.1Hz filtered curve. It has also made suggestions on possible frequencies of abdominal squeezing and detrusor straining. Further research will follow on more frequency analytical methods, such as Fourier analysis and wavelet theory, to achieve a decent diagnosing power on non-invasively diagnosing DU and by combining multiple clinical parameters.

Median frequency and sum of amplitude changes in rising slope: two potential non-invasive indicators for differentiating DU from BOO in males

Rui Li, Andrew Gammie, Quan Zhu, Mokhtar Nibouche

Neurourology and Urodynamics. 37 (supplement 5), pp. 248-249

Hypothesis / aims of study

It remains a challenge to non-invasively differentiate detrusor underactivity (DU) from bladder outlet obstruction (BOO) in males, and the gold standard is pressure flow studies, which is invasive, relatively expensive and may cause bleeding and infection. This novel study aims to non-invasively differentiate DU from BOO in males by analysing urine flow rate curves in the frequency domain. The hypothesis is that underactive patients may perform more abdominal straining than obstructed patients during micturition due to their underactive detrusor. Thus, it is possible to analyse the urine flow rate in frequency domain and derive non-invasive parameters for differentiating these two groups, as abdominal muscle strains in a different frequency range comparing with detrusor contraction [1].

Study design, materials and methods

Free-flow data of 273 adult male patients who had also undergone PFS were analysed in this research. Based on their PFS record, these patients are divided into three groups: 104 BOO, 93 DU, and 76 normal (DU and BOO disease free) for reference. All free flow data has pre-processed by threshold value of 0.5ml/s for the start and end micturition point [2].

To leave only the fluctuations in the flow curve for analysis in frequency domain, a bandpass Kaiser window filter has been designed and applied on the pre-processed flow data. The selection criteria and specifications for the filter are listed as below:

- The passband of filter should be flat and ideally without ripples, for the accuracy frequency analysis result.
- The roll-off should be sharp, for a better filter performance.
- The group delay response should be a constant value, for shifting back filtered curve with same data sequence length as raw curve.
- The bandpass range is set to 0.1-1Hz, for maximise reducing fluctuation by detrusor contraction with frequency under 0.1Hz and artefact noise such as coughing.
- The attenuation is set to -40dB, for reducing artefact fluctuations up to 50ml/s to 0.5ml/s.

Then the sum of amplitude changes is calculated in the filtered flow curve, which is presented as in figure 1. Meanwhile, the frequency spectra of filtered flow curves are generated by fast Fourier transform, and median frequency values are calculated as the frequency value dividing power spectrum into two regions with equal amplitude, which are as presented in figure 2. The filtered flow curve is also divided into two parts by maximum flow rate (Q_{max}), half of voiding time (Tv), and the location where half of volume is voided, to calculate median frequency in each part.

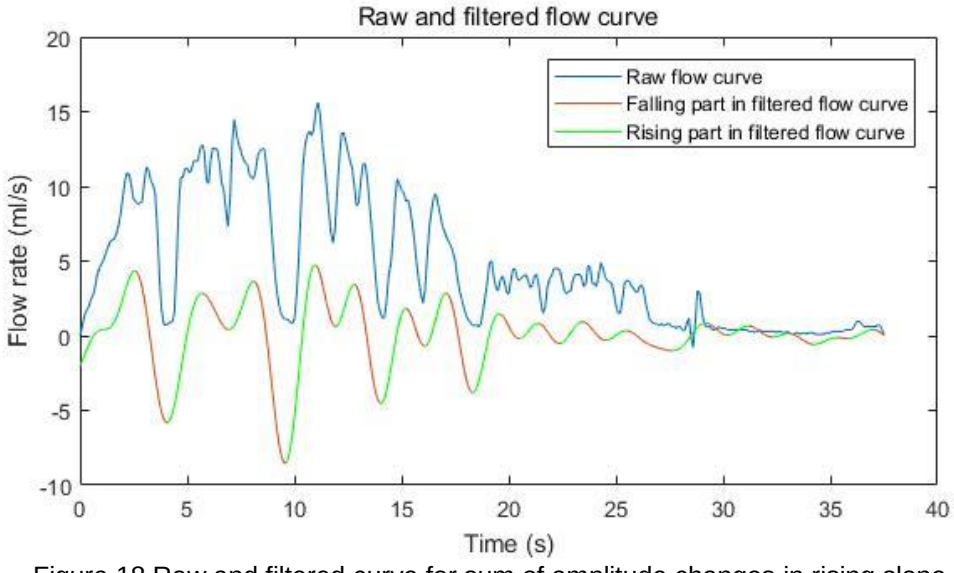

Figure 18 Raw and filtered curve for sum of amplitude changes in rising slope

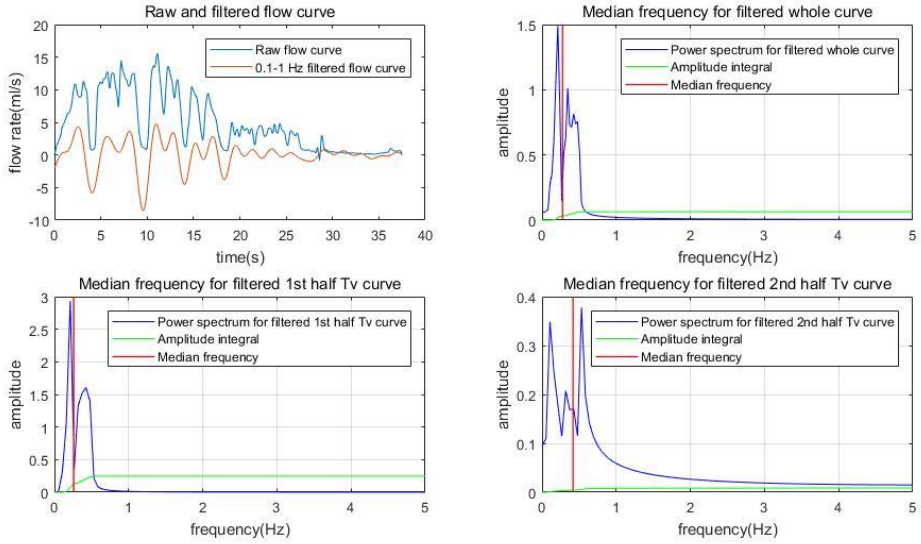

Figure 19 Median frequency in whole, 1st and 2nd half Tv filtered curve

All statistical analysis was performed in SPSS version 24, Mann-Whitney U test and T-student test were performed as appropriate. A statistically significant difference was considered as P value<0.05.

Results

We found the significantly statistical difference in sum of amplitude changes in rising slope with P value<0.001, between DU group (mean±SD, 27.4±20.2) and BOO group (mean±SD, 18.3±14.2). Area under the curve (AUC) value is 0.651 in receiver operating characteristic (ROC) analysis, with 63.4% sensitivity and 65.4% specificity. However, no statistical difference is found for differentiating DU from BOO when this parameter takes a ratio to Q_{max} or volume voided.

In median frequency analysis, the significantly statistical difference for differentiating DU with BOO appear in the filtered whole flow curve (DU vs BOO=0.42±0.10 vs 0.48±0.10) with P value of 0.0001, followed by in the first half volume voided part (P<0.001), ratio of median frequency in 1st to 2nd half part divided by Q_{max}, (P=0.002), ratio of median frequency in whole filtered curve to 2nd half part divided by Q_{max} (P=0.003) and median frequency in 1st half part divided by Tv (P=0.004). The AUC value is 0.665 for median frequency in filtered whole flow curve, with 43% sensitivity and 86.5% specificity.

Interpretation of results

In this study, we found the flow rate curve fluctuations during micturition in DU patients group have higher amplitude changes than BOO group, and the frequency difference in the whole filtered flow curve. Currently the sensitivity and specificity of these two indicators could not yet exceed those of the simple Q_{max} cut-off of 10ml/s to select symptomatic men with a high likelihood of BOO, but it still shows promise that these may serve as additional indicator for preliminary screening of DU before invasive pressure flow studies. Furthermore, these indicators could be combined with other non-invasive parameters to enhance current diagnosing accuracy.

Concluding message

This study shows promising non-invasive indicators for diagnosing DU in men by analysing urine flow curves in the frequency domain. Further research will explore other possible non-invasive parameters, and mathematically combined with existing indicators for achieving more promising diagnostic accuracy of DU in male.

Multivariate analysis of variance for maximising the diagnosing accuracy in differentiating DU from BOO in males

Rui Li, Andrew Gammie, Quan Zhu, Mokhtar Nibouche

Neurourology and Urodynamics. 37 (supplement 5), pp. 327-328.

Hypothesis / aims of study

Detrusor underactivity (DU) and bladder outlet obstruction (BOO) bother almost half of elder men. Although the treatment is different for these two lower urinary tract symptoms, invasive pressure flow studies remains the only gold standard for diagnosing both. To non-invasively differentiate DU from BOO, a few studies have mathematically analysed urine flow rate curve and proposed promising parameters [1,2], but each proposed parameter is not strong enough for diagnostic usage. Therefore, in this study we aim to use multivariate analysis of variance on parameters derived from free flow data to assess the possibility of non-invasive differentiating DU from BOO in males.

Study design, materials and methods

Free-flow data of 273 adult male patients who had also undergone PFS were analysed in this research. Based on their PFS record, these patients are divided into three groups: 104 BOO, 93 DU, and 76 normal (DU and BOO disease free) for reference. All free flow data has pre-processed by threshold value of 0.5ml/s for the start and end micturition point [3].

The multivariate analysis is performed by bundling multiple dependent variables into a weighted linear combination variable to achieve the best statistically significant between two groups. The following non-invasive variables which have significant statistical difference between two groups, are employed for multivariate analysis:

- Parameters obtained from 2 seconds averaging window filtered urine flow rate data, including Q_{max} (P<0.0001), Q_{ave} by voiding time (P<0.01), Q_{ave} by flow time (P<0.0001) and ratio of Q_{max} time to voiding time (P=0.05).
- Parameters mathematically derived from 2 seconds averaging window filtered urine flow rate data, including mean flow rate in rising part and falling part (P<0.01 and P=0.01 respectively), and ratio of flow time to voiding time.
- Parameters required complex mathematically calculation of raw flow data, including median frequency values in different bandpass filtered curve (statistical difference varies from P=0.0001 to P<0.05), ratio values of peak numbers in different lowpass filtered curve (P<0.0001), time constant value in falling part of 2 seconds averaging window filtered curve (P=0.01), and sum of amplitude changes in rising slope in 0.1Hz to 1Hz filtered flow curve (P<0.001).

Then the inputted parameters are assigned with coefficients each and summed to create a variable which has the best diagnosing accuracy on differentiating DU with BOO.

Non-invasive parameters were derived in Matlab 2017a. All statistical analysis was performed in SPSS version 24, Mann-Whitney U test and T-student test were performed as appropriate. A statistically significant difference was considered as P value<0.05.

Results

The variable calculated in multivariate analysis has significantly statistical difference between DU with BOO groups, with P value less than 10^{-22}. The area under the curve in receiver operation characteristic analysis is 0.872, which is presented as in figure 1, the most balanced sensitivity and specificity for the new variable are 73.1% and 84.6% respectively on differentiating DU from BOO.

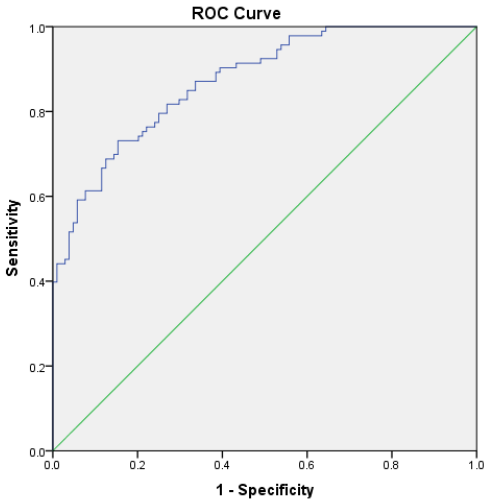

Figure 20 Area under curve for new variable on differentiating DU with BOO

Interpretation of results

The result shows that multivariate analysis could improve the diagnosing accuracy, by mathematical linear combining the inputted parameters. While the single variable could have limited diagnosing power, such as Q_{max} with $P<0.0001$ only having area under curve value of 0.634, the combination of these non-invasive parameters shows promise on differentiating DU from BOO. Moreover, the diagnosing accuracy could possibly be further improved if any other non-invasive parameter is employed. However, it should be noted that the current result is only valid in training procedure, and a larger data number is needed for validation before diagnostic use.

Concluding message

In this study, we found the multivariate analysis could improve the diagnosing accuracy by combining parameters which have statistical difference between DU and BOO groups, and presented the possibility to non-invasively differentiate DU with BOO only by analysing the flow rate data alone. Further research will focus on explore other parameters which could serve as additional indicators for differentiating two symptoms, and other classification methods such as neural network and classification/regression tree analysis.

Urine flow rate shape template and intermittent flow in males

Rui Li, Andrew Gammie, Quan Zhu, Mokhtar Nibouche

Neurourology and Urodynamics. 37 (supplement 5), pp. 128-129

Hypothesis / aims of study

Uroflowmetry serves as a preliminary urodynamic test for physicians to indicate the possible cause of lower urinary tract symptoms. Alongside the most researched parameter maximum flow rate (Q_{max}), the shape of urine flow rate curve is also reported to associate with one or more voiding abnormalities [1]. Therefore, this novel study aims at by mathematically generating free-flow shape template in specified diagnostic groups, bladder outlet obstruction (BOO) and detrusor underactivity (DU), to assess its possibility for non-invasive diagnostic use.

Study design, materials and methods

Free-flow data of 273 adult male patients who had also undergone PFS were analysed in this research. Based on their PFS record, these patients are divided into three groups: 104 BOO, 93 DU, and 76 normal (DU and BOO disease free) for reference. For each flow data, the starting and ending point has been selected by the threshold value of 0.5ml/s, then 2 seconds averaging window filter has been applied as suggested by ICS good urodynamic practice [2].

For the accuracy of the shape template, the intermittent flow data is not considered in template generating. ICS defines intermittent flow shape as flow stopping and starting during a single void [3]. However, an early or end dribble is normally included in the flow curve, as it is a part of voiding, the shape could therefore be classified as intermittent even the rest of flow is bell-shaped. We therefore detect intermittent flow on criteria of flow rate<0.5ml/s in the 0.5% to 98% volume void part, and generate flow shape template on non-intermittency data in the same area following the steps listed below:

1. Normalise flow curve into amplitude of 1 and samples of 1000, by dividing whole flow curve by Q_{max} and resampling of 1000 samples.
2. Calculate the mean values on each sample point in normalised flow curves in both diagnostic groups
3. Divide the whole generated data sequence by the maximum value in both diagnostic groups

Then the calculated data sequences are the shape template for BOO and DU. To assess the diagnostic usage of the template, all BOO and DU non-intermittent flow data in 0.5%-98% volume voided area are normalised and calculated the ratio of sum square errors (Res) on each re-sample point comparing with BOO template and comparing with DU template.

Intermittency detection and template generation were calculated in Matlab 2017a. Statistical analysis was performed in SPSS version 24, Mann-Whitney U test and T-student test were performed as appropriate. A statistically significant difference was considered as P value<0.05.

Results

In total of 197 DU and BOO data, 75 data has been detected as intermittent, the rest 71 BOO and 51 DU non-intermittent data are employed for the template generating. The templates for each diagnostic group are presented as in figure 1.

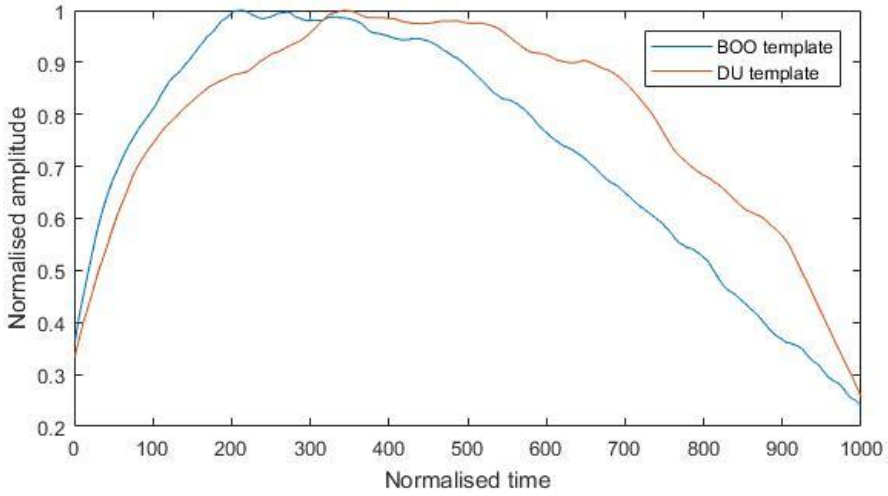

Figure 21 BOO and DU flow shape template

The Res value is found having significant statistical difference between DU and BOO groups, with *P*=0.005. In receiver operating characteristic (ROC) analysis, area under curve (AUC) is 0.676 with 71% sensitivity and 63% specificity.

Interpretation of results

In this study, we found the flow shape template, generated by normalised flow curves, has a shape difference between two diagnostic groups. As presented in figure 1, the BOO template shows an asymmetric shape with maximum amplitude value appears in the first half and prolonged falling slope, while the DU template is almost a bell shape with maximum amplitude value located nearly at centre. The main differences between two templates are the maximum value location and the descending speed in falling slope.

The ICS definition on intermittency did not specify the starting and ending point to count stopping flow, and this could result in categorising flow curve with very small volume of starting or ending dibbles as an intermittent curve. In our study, we found it would be more accurate to only count in 0.5% to 98% volume voided area for intermittency detection.

The parameter Res generated in our study could serve as an additional non-invasive indicator for differentiating non-intermittency DU and BOO flow in male. Although the diagnosing power could not be compared with simple Q_{max}<10ml/s for selecting male with BOO, the diagnosing accuracy for this new proposed parameter could be enhanced with other non-invasive indicators. It also shows the promise to explore the shape difference in other symptomatic groups, and its further application on diagnostic usage.

Concluding message

This study finds the shape difference between DU and BOO in males and proposes a novel non-invasive indicator for differentiating DU from BOO if the flow is non-intermittent. Further research will analyse the shape template difference in other diagnostic groups, and explore the possibility of non-invasively diagnosing DU by combining other non-invasive parameters.